NSF-RA-E-75-317
PB 294022

The John A. Blume Earthquake Engineering Center
Department of Civil Engineering
Stanford University

AMBIENT VIBRATION STUDY OF SIX SIMILAR HIGH-RISE APARTMENT BUILDINGS

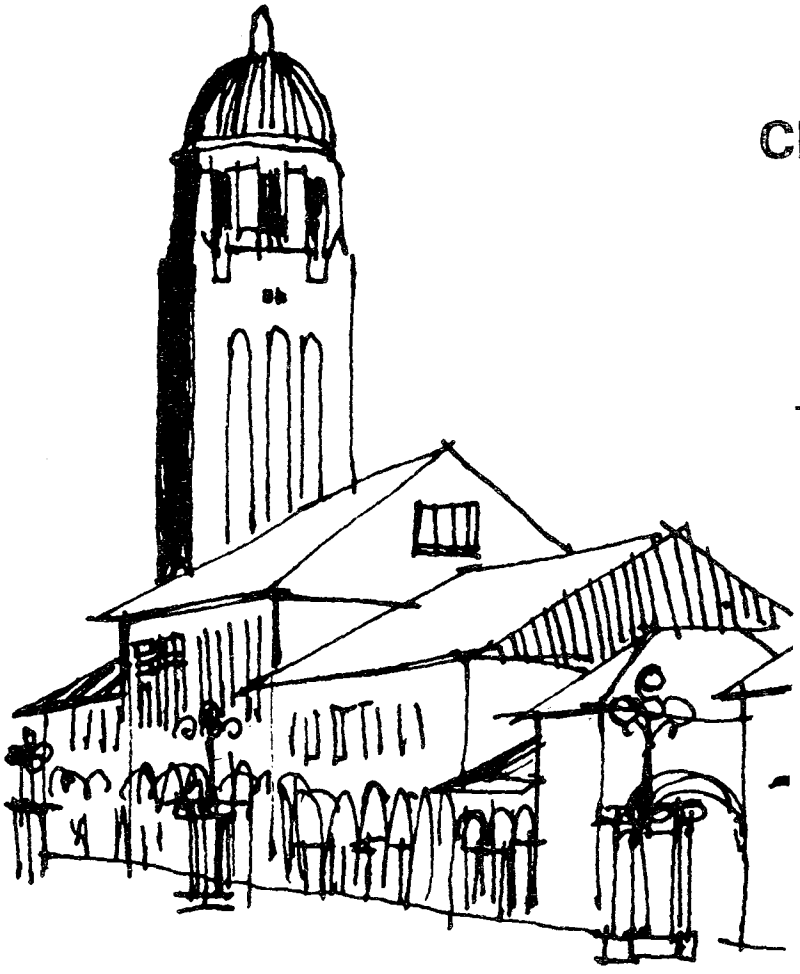

by
Charles Alan Kircher
and
Haresh C. Shah

This research was supported by the
National Science Foundation
Grant GI-34967

Report No. 14
January 1975

REPRODUCED BY
NATIONAL TECHNICAL INFORMATION SERVICE
U.S. DEPARTMENT OF COMMERCE
)URCES
DATION

50272-101

REPORT DOCUMENTATION PAGE	1. REPORT NO. NSF-RA-E-75-317	2.	3. Recipient's Accession No. PB294022

4. Title and Subtitle Ambient Vibration Study of Six Similar High-Rise Apartment Buildings	5. Report Date January 1975
	6.
7. Author(s) C.A. Kircher, H.C. Shah	8. Performing Organization Rept. No. 14
9. Performing Organization Name and Address Stanford University The John A. Blume Earthquake Engineering Center Department of Civil Engineering Stanford, California 94305	10. Project/Task/Work Unit No.
	11. Contract(C) or Grant(G) No. (C) (G) GI34967
12. Sponsoring Organization Name and Address Applied Science and Research Applications (ASRA) National Science Foundation 1800 G Street, N.W. Washington, D.C. 20550	13. Type of Report & Period Covered
	14.

15. Supplementary Notes

16. Abstract (Limit: 200 words)

Two 12-story high-rise apartment buildings and four 8-story high-rise apartment buildings in Escondido Village on the Stanford University Campus were analyzed to determine their dynamic characteristics. The ambient vibration analyses performed on the buildings produced a collection of power spectral density functions for each building. Although higher modes were undoubtedly present in the power spectral density plots, in general, only the fundamental mode could be consistently identified. An estimate of the percent of critical damping associated with the fundamental mode was calculated for the four 8-story buildings. A mathematical method for comparison of two power spectral densities based on the definition of the correlation coefficient was developed. Pairs of power spectral density plots, as displayed in both the linear magnitude scale and logarithmic magnitude scale, were then compared using this mathematical method. Comparison results conclude that: (1) the method of ambient vibration analysis used produces accurate and reliable results; (2) after enough individually measured and calculated power spectral density functions are averaged together, the resulting power spectral density function is representative of a stationary process; (3) power spectral density plots obtained at different floor levels for the same accelerometer direction may not appear similar unless the overall modal vibrations are sufficiently stronger than any local points of energy transfer; and (4) the buildings analyzed of identical design may often be slightly different in their natural frequencies, and that this slight difference can be accurately determined by this method of ambient vibration analysis.

17. Document Analysis a. Descriptors

Buildings	Vibration	Spectrum analysis
Dynamic structural analysis	Vibration tests	
Structural analysis	Spectral energy distribution	

b. Identifiers/Open-Ended Terms

Ambient vibration analysis

Power spectral density functions

c. COSATI Field/Group

18. Availability Statement	19. Security Class (This Report)	21. No. of Pages
NTIS		92
	20. Security Class (This Page)	22. Price PC A05/MF A01

(See ANSI-Z39.18) See Instructions on Reverse OPTIONAL FORM 272 (4-77) (Formerly NTIS-35) Department of Commerce

CAPITAL SYSTEMS GROUP, INC.
6110 EXECUTIVE BOULEVARD
SUITE 250
ROCKVILLE, MARYLAND 20852

AMBIENT VIBRATION STUDY OF SIX SIMILAR HIGH-RISE APARTMENT BUILDINGS

by

Charles Alan Kircher

Haresh C. Shah

This research was supported by the
National Science Foundation
Grant GI-34967

Any opinions, findings, conclusions or recommendations expressed in this publication are those of the author(s) and do not necessarily reflect the views of the National Science Foundation.

PREFACE

It is of continuing interest to the field of Structural Engineering to examine the nature of structural vibrations. Today, there are numerous needs for such examinations but probably none so important as those associated with the determination of a structure's natural frequencies and associated modal damping values. It is precisely these quantities which are so critical in the prediction of a structure's response due to either strong ground motion or excessive wind loads. It is to this objective, the better understanding of dynamic structural response, that this work is directed.

The material presented herein is concerned with the results of the ambient vibration analyses performed and not with the method of analysis itself. The interested reader will find a detailed description of the method of analysis in the Engineer thesis, "Determination of the Dynamic Characteristics of Full Scale Structures by the Application of Fourier Analysis," (Kircher [1]). The result of an individual on-site analysis is simply the power spectral density function. The power spectral density function (function of frequency) is the magnitude squared of the Fourier transform of the given vibration record (function of time). The vibration records measured on the subject buildings located on Stanford Campus were all produced by means of a small accelerometer. Such acceleration vs time vibration records represent the building's characteristics as excited by random forces and as sensed by the accelerometer's particular position and orientation within the building. The power spectral density function may then be considered a "fingerprint" of any particular building for the given accelerometer orientation.

Preceding page blank

For those readers interested in a random vibration reference, Crandall and Mark [2] is suggested. Bracewell [3] is an excellent source of information about the Fourier transform and its properties, while Blackman and Tukey [4] probably provide the most sophisticated reference on power spectrum measurement and analysis. Many other investigators have been interested in the application of Fourier analysis for the determination of the dynamic characteristics of buildings [5,7,8]. All the available references on this topic are not included in the list of references of this report.

The material presented in this report is a result of research, conducted by C. A. Kircher and supervised by H. C. Shah, toward the completion of a doctoral thesis. The essence of this work will provide a chapter of that dissertation to be published later this year. Additional research toward a Ph.D. degree being currently performed by C. A. Kircher and supported by the National Science Foundation Grant GI-34967 and the Department of Water Resources, State of California, Grants DWR B51254 and B51454, includes the following:

(1) The ambient and nonambient analyses of air blast circuit breakers and the accompanying support structures located at the A. D. Edmonston Pumping Plant, California. The purpose of this work is to examine the relationship between the nonlinear dynamic characteristics of the structure and the r.m.s. level of excitation.

(2) The ambient and nonambient analysis of two suspended-floor high-rise buildings located in Mountain View and San Jose, California. The purpose of this work is to compare two identical buildings of unique design and to compare the measured dynamic characteristics with the analytical results calculated by B. Goodno [6] using a combined normal mode and finite element method of analysis.

CONTENTS

		Page
1.	INTRODUCTION	1
	1.1 Purpose of Work	1
	1.2 Power Spectral Density Plots	2
2.	A METHOD FOR THE COMPARISON OF TWO POWER SPECTRAL DENSITY PLOTS	7
	2.1 Introduction	7
	2.2 Description of Correlation Method	7
	2.3 An Example	9
3.	COMPARISON OF POWER SPECTRAL DENSITY PLOTS OBTAINED FOR THE SAME BUILDING, ACCELEROMETER LOCATION, AND DIRECTION	13
	3.1 Purpose and Procedure	13
	3.2 Results and Conclusions	15
4.	COMPARISON OF POWER SPECTRAL DENSITY PLOTS OBTAINED IN THE SAME BUILDING FOR DIFFERENT ACCELEROMETER ORIENTATIONS	17
	4.1 Purpose and Procedure	17
	4.2 Results for Different Floor Levels, Same Accelerometer Position and Direction	17
	4.3 Results for Different Accelerometer Position, Same Floor Level and Direction	21
	4.4 Results for Different Accelerometer Directions, Same Floor Level and Location	23
5.	COMPARISON OF FOUR 8-STORY BUILDINGS OF IDENTICAL DESIGN	25
	5.1 Purpose and Procedure	25
	5.2 Results and Conclusions	26
6.	COMPARISON OF TWO 12-STORY BUILDINGS OF IDENTICAL DESIGN	31
	6.1 Purpose and Procedure	31
	6.2 Results and Conclusions	31
7.	GENERAL CONCLUSIONS	33

CONTENTS (Cont)

		Page
REFERENCES		35
Appendix A.	POWER SPECTRAL DENSITY PLOTS FOR THE BLACKWELDER BUILDING AND A SUMMARY OF THE RESULTS	37
Appendix B.	POWER SPECTRAL DENSITY PLOTS FOR THE QUILLEN BUILDING AND A SUMMARY OF THE RESULTS	45
Appendix C.	POWER SPECTRAL DENSITY PLOTS FOR THE McFARLAND BUILDING AND A SUMMARY OF THE RESULTS	53
Appendix D.	POWER SPECTRAL DENSITY PLOTS FOR THE HOSKINS BUILDING AND A SUMMARY OF THE RESULTS	61
Appendix E.	POWER SPECTRAL DENSITY PLOTS FOR THE HULME BUILDING AND A SUMMARY OF THE RESULTS	69
Appendix F.	POWER SPECTRAL DENSITY PLOTS FOR THE BARNES BUILDING AND A SUMMARY OF THE RESULTS	77
Appendix G.	LIST OF EQUIPMENT USED ON SITE IN THE AMBIENT VIBRATION STUDY PERFORMED ON SIX HIGH-RISE APARTMENT HOUSES IN ESCONDIDO VILLAGE	85
Appendix H.	LIST OF EQUIPMENT, ADDITIONAL TO APPENDIX G, USED FOR AMBIENT AND NON-AMBIENT VIBRATION STUDIES OF FULL-SCALE STRUCTURES	87
Appendix I.	A COLLECTION OF SITES OF STRUCTURES WHICH HAVE BEEN USED IN AMBIENT AND NONAMBIENT VIBRATION STUDIES	89

ILLUSTRATIONS

Figure		Page
2.1	Results of correlation of Fig. A.1 and Fig. A.5	10
2.2	Results of correlation of Fig. A.2 and Fig. A.6	10
3.1	Results of correlation of Fig. B.1 and Fig. B.3	14
3.2	Results of correlation of Fig. B.2 and Fig. B.4	14
4.1	Results of correlation of Fig. A.7 and Fig. A.9	18
4.2	Results of correlation of Fig. A.8 and Fig. A.10	18
4.3	Results of correlation of Fig. A.3 and Fig. A.5	19
4.4	Results of correlation of Fig. A.4 and Fig. A.6	19
4.5	Results of correlation of Fig. A.7 and Fig. A.1	22
4.6	Results of correlation of Fig. A.8 and Fig. A.2	22
4.7	Results of correlation of Fig. A.3 and Fig. A.1	24
4.8	Results of correlation of Fig. A.4 and Fig. A.2	24
6.1	Results of correlation of Fig. A.1 and Fig. B.3	32
6.2	Results of correlation of Fig. A.2 and Fig. B.4	32
A.1	Power spectral density plot, Blackwelder Building	38
A.2	Power spectral density plot, Blackwelder Building	38
A.3	Power spectral density plot, Blackwelder Building	39
A.4	Power spectral density plot, Blackwelder Building	39
A.5	Power spectral density plot, Blackwelder Building	40
A.6	Power spectral density plot, Blackwelder Building	40
A.7	Power spectral density plot, Blackwelder Building	41
A.8	Power spectral density plot, Blackwelder Building	41
A.9	Power spectral density plot, Blackwelder Building	42
A.10	Power spectral density plot, Blackwelder Building	42

ILLUSTRATIONS (Cont)

Figure		Page
A.11	Power spectral density plot, Blackwelder Building	43
A.12	Power spectral density plot, Blackwelder Building	43
A.13	Power spectral density plot, Blackwelder Building	44
A.14	Power spectral density plot, Blackwelder Building	44
B.1	Power spectral density plot, Quillen Building	46
B.2	Power spectral density plot, Quillen Building	46
B.3	Power spectral density plot, Quillen Building	47
B.4	Power spectral density plot, Quillen Building	47
B.5	Power spectral density plot, Quillen Building	48
B.6	Power spectral density plot, Quillen Building	48
B.7	Power spectral density plot, Quillen Building	49
B.8	Power spectral density plot, Quillen Building	49
B.9	Power spectral density plot, Quillen Building	50
B.10	Power spectral density plot, Quillen Building	50
B.11	Power spectral density plot, Quillen Building	51
B.12	Power spectral density plot, Quillen Building	51
B.13	Power spectral density plot, Quillen Building	52
B.14	Power spectral density plot, Quillen Building	52
C.1	Power spectral density plot, McFarland Building	54
C.2	Power spectral density plot, McFarland Building	54
C.3	Power spectral density plot, McFarland Building	55
C.4	Power spectral density plot, McFarland Building	55
C.5	Power spectral density plot, McFarland Building	56
C.6	Power spectral density plot, McFarland Building	56

ILLUSTRATIONS (Cont)

Figure		Page
C.7	Power spectral density plot, McFarland Building	57
C.8	Power spectral density plot, McFarland Building	57
C.9	Power spectral density plot, McFarland Building	58
C.10	Power spectral density plot, McFarland Building	58
C.11	Power spectral density plot, McFarland Building	59
C.12	Power spectral density plot, McFarland Building	59
D.1	Power spectral density plot, Hoskins Building	62
D.2	Power spectral density plot, Hoskins Building	62
D.3	Power spectral density plot, Hoskins Building	63
D.4	Power spectral density plot, Hoskins Building	63
D.5	Power spectral density plot, Hoskins Building	64
D.6	Power spectral density plot, Hoskins Building	64
D.7	Power spectral density plot, Hoskins Building	65
D.8	Power spectral density plot, Hoskins Building	65
D.9	Power spectral density plot, Hoskins Building	66
D.10	Power spectral density plot, Hoskins Building	66
D.11	Power spectral density plot, Hoskins Building	67
D.12	Power spectral density plot, Hoskins Building	67
E.1	Power spectral density plot, Hulme Building	70
E.2	Power spectral density plot, Hulme Building	70
E.3	Power spectral density plot, Hulme Building	71
E.4	Power spectral density plot, Hulme Building	71
E.5	Power spectral density plot, Hulme Building	72
E.6	Power spectral density plot, Hulme Building	72

ILLUSTRATIONS (Cont)

Figure		Page
E.7	Power spectral density plot, Hulme Building	73
E.8	Power spectral density plot, Hulme Building	73
E.9	Power spectral density plot, Hulme Building	74
E.10	Power spectral density plot, Hulme Building	74
E.11	Power spectral density plot, Hulme Building	75
E.12	Power spectral density plot, Hulme Building	75
F.1	Power spectral density plot, Barnes Building	78
F.2	Power spectral density plot, Barnes Building	78
F.3	Power spectral density plot, Barnes Building	79
F.4	Power spectral density plot, Barnes Building	79
F.5	Power spectral density plot, Barnes Building	80
F.6	Power spectral density plot, Barnes Building	80
F.7	Power spectral density plot, Barnes Building	81
F.8	Power spectral density plot, Barnes Building	81
F.9	Power spectral density plot, Barnes Building	82
F.10	Power spectral density plot, Barnes Building	82
F.11	Power spectral density plot, Barnes Building	83
F.12	Power spectral density plot, Barnes Building	83

TABLES

Number		Page
1.1	Natural frequencies for the Blackwelder Building	3
1.2	Natural frequencies for the Quillen Building	3
1.3	First mode natural frequencies and corresponding damping values for four 8-story buildings of identical design	5
5.1	Peak correlation values between power spectral density plots for four 8-story buildings of identical design	27
5.2	Peak correlation values between power spectral density plots for four 8-story buildings of identical design	27
5.3	Peak correlation values between power spectral density plots for four 8-story buildings of identical design	27
5.4	Peak correlation values between power spectral density plots for four 8-story buildings of identical design	28
5.5	Peak correlation values between power spectral density plots for four 8-story buildings of identical design	28
5.6	Peak correlation values between power spectral density plots for four 8-story buildings of identical design	28
A.1	Summary of the predominant energy transfer points for the Blackwelder Building	37
B.1	Summary of the predominant energy transfer points for the Quillen Building	45
C.1	Summary of the predominant energy transfer points for the McFarland Building	53
D.1	Summary of the predominant energy transfer points for the Hoskins Building	61
E.1	Summary of the predominant energy transfer points for the Hulme Building	69
F.1	Summary of the predominant energy transfer points for the Barnes Building	77

Chapter 1

INTRODUCTION

1.1 Purpose of Work

Two 12-story high-rise apartment buildings and four 8-story high-rise apartment buildings located in Escondido Village on Stanford Campus were chosen for this study because of their "identical" designs. Having two or more buildings of "identical" design provides the opportunity to compare both the structural similarity of the buildings and the ambient level forces exciting the structures; as well as the method of analysis, itself. If two Power Spectrums are to be similar for two different buildings, it is necessary that three conditions be met. The first condition is that the method of analysis be the same for both analyses. The second condition is that the buildings be structurally similar. "Identical" is assumed to be an unrealistic description of anything but the original design. Third, the forces exciting the structures must be similar. In the case of ambient analysis, these forces are of two forms. First, there are the so-called "forced" vibrations of electrical motors and pumps within modern high-rise apartments. Second, there are the "random" forces of wind, ground motion, people moving within the building, etc.

The purpose of this work may be summarized as follows:

(1) Determine the natural frequencies and modal damping values, when possible, for the six buildings.

(2) Develop an accurate mathematical procedure for the systematic comparison of two power spectrums.

(3) Examine the reliability of the method of analysis, itself, by comparing the results of two power spectral density plots obtained for the same location and direction in the same building.

(4) Examine the similarities and differences of power spectral density plots obtained in the same building but for different locations or directions.

(5) Examine the similarities or differences of power spectral density plots obtained for the same position and direction in different buildings of identical design.

1.2 Power Spectral Density Plots

The actual work performed in the field encompassed a three week period of data gathering and on-site analysis in Escondido Village on the Stanford Campus. Power spectrums were obtained for the six buildings described at different floor levels, as well as different locations on each floor level. The method of analysis for a given floor level involved performing three measurements and corresponding analyses. The three measurements were taken at three different locations, longitudinal, transverse through the center of gravity, and transverse near the end of the building. Comparison of power spectral densities obtained from the locations, transverse in the center and transverse at the end of the building, made it possible to separate the transverse and torsional modes of vibration.

The six buildings analyzed include two 12-story buildings of identical design, Blackwelder and Quillen, and four 8-story buildings of identical design, McFarland, Hoskins, Hulme, and Barnes. The power spectral density plots obtained along with a table summarizing the results for each plot, may be found in Appendices A, B, C, D, E, and F. A summary taken from Table A.1 of the natural frequencies seen for the Blackwelder building is given in Table 1.1. It should be noted that, while the first mode can be seen very distinctly, the second and third

Table 1.1

NATURAL FREQUENCIES FOR THE BLACKWELDER BUILDING

Direction	Natural Frequency (Hz)		
	1st	2nd	3rd
Transverse	2.01	8.9-9.0	---
Longitudinal	2.89	---	---
Torsional	2.68	10.6	---

modes are not clearly defined and their frequencies can only be estimated. For the Blackwelder Building, it was impossible to identify any third mode component of frequency. This does not imply that the third mode component did not exist but that it could not be clearly differentiated from other nearby energy transfer points. The results taken from Table B.1 for the Quillen Building are given in Table 1.2. Again, it was difficult to interpret the power spectral density plots. The frequencies given for the third modes in Table 1.2 should only be considered as the most likely values. In general, the power spectral density plots were not suitable for the calculation of modal damping values for

Table 1.2

NATURAL FREQUENCIES FOR THE QUILLEN BUILDING

Direction	Natural Frequency (Hz)		
	1st	2nd	3rd
Transverse	1.93	8.8-9.0	(15.0-15.1)
Longitudinal	2.74	11.0	---
Torsional	2.58	9.7	(17.6-17.9)

the Blackwelder and Quillen Buildings. It may also be noted that the Quillen Building has a consistently lower fundamental frequency for all three directions than the Blackwelder Building.

Table 1.3 provides a summary of the fundamental natural frequencies and the associated damping terms for the four 8-story buildings of identical design. It was not possible to estimate the second or third modal frequencies for these buildings. The two values given correspond to measurements taken at different times at different locations, but in the same direction. The very small (1.6%-2.4%) but consistent discrepancy suggests a slightly nonlinear aspect of these four buildings. The damping values calculated range from 1.6% to 3.4% of critical. These are relatively large values for damping since the buildings were experiencing such a low level of ambient excitation (e.g., r.m.s. $\cong 10^{-5}$ g). What these relatively large values for damping might actually be describing is a nonlinear system whose slightly varying resonant frequency is "blurring" the resonance peak. The result would be a broadened resonance peak and, hence, a larger calculated value of the damping.

Table 1.3

FIRST MODE NATURAL FREQUENCIES AND CORRESPONDING DAMPING VALUES
FOR FOUR 8-STORY BUILDINGS OF IDENTICAL DESIGN

Direction / Building	Transverse			Longitudinal		Torsional	
	Natural Frequency (Hz)	% of Critical Damping	Position of Accelerometer	Natural Frequency (Hz)	% of Critical Damping	Natural Frequency (Hz)	% of Critical Damping
McFarland	2.60	1.8	center	2.54	1.8	3.83	1.6
	2.64	2.9	end				
Hoskins	2.58	3.4	center	2.54	1.9	3.85	1.9
	2.62	2.3	end				
Hulme	2.72	2.9	center	2.60	2.0	3.69	1.7
	2.66	2.7	end				
Barnes	2.60	2.2	center	2.58	2.1	3.59	1.8
	2.54	3.3	end				

Intentionally Blank

Chapter 2

A METHOD FOR THE COMPARISON OF TWO POWER SPECTRAL DENSITY PLOTS

2.1 Introduction

To facilitate an easy comparison of two power spectral density plots, a computer program was written to perform a point-by-point correlation of the two given functions. The power spectral density functions compared were all originally for a frequency range of 0-50 Hz. The range of comparison, however, was truncated to 0-25 Hz, since the frequency range 25-50 Hz was usually poorly defined and of marginal interest to practical engineering. The results of the correlations of two power spectral densities are numbers whose absolute value is always one or less. A value of 0.9 or greater would indicate very good correlation or, correspondingly, very similar power spectral densities. The results of the correlations of two power spectral densities were suitable for plotting, and the most interesting results may be found as plots in Chapters 2, 3, 4, and 6.

2.2 Description of Correlation Method

Essentially a power spectral density plot of frequency range 0-50 Hz, described by 512 data points, was truncated to the range of 0-25 Hz described by 256 data points. Two truncated power spectral density functions of 256 points each were then cross-correlated point-by-point to determine the correlation coefficient ρ, defined:

Preceding page blank

$$\rho = \frac{1}{256} \sum_{i,j=1}^{256} \left(\frac{S_{xx}(f_i) - \overline{S_{xx}}}{\sqrt{\frac{1}{256} \sum_{k=1}^{256} \left(S_{xx}(f_k) - \overline{S_{xx}} \right)^2}} \right) \left(\frac{S_{yy}(f_j) - \overline{S_{yy}}}{\sqrt{\frac{1}{256} \sum_{k=1}^{256} \left(S_{yy}(f_k) - \overline{S_{yy}} \right)^2}} \right) \tag{2.1}$$

where

$S_{xx}(f_i)$ = discrete power spectral density function X

$S_{yy}(f_i)$ = discrete power spectral density function Y

$$\overline{S_{xx}} = \frac{1}{256} \sum_{i=1}^{256} S_{xx}(f_i) = \text{mean value of } S_{xx}(f_i)$$

$$\overline{S_{yy}} = \frac{1}{256} \sum_{i=1}^{256} S_{yy}(f_i) = \text{mean value of } S_{yy}(f_i)$$

It is also of interest to correlate two power spectral density functions for values other than $i = j$ in Eq. (2.1). This is equivalent to performing the correlation of $S_{xx}(f_i)$ and $S_{yy}(f_j)$ where $S_{yy}(f_j)$ has been shifted some number of places $n = j - i$ with respect to $S_{xx}(f_i)$. The value n, the number of places shifted, could then be changed from $n = 0$ to $n = -1,-2,-3$, etc. and to $n = 1,2,3$, etc. At each shift, the correlation coefficient was calculated. The result is a set of correlation values for two power spectral density functions describing how well the two functions are correlated as one function is shifted with respect to the other. Since there are 256 data points describing a range 0-25 Hz, a shift of one place corresponds to approximately 0.1 Hz.

If two spectrums are to be similar, then one would expect to find the maximum correlation coefficient to be near a value of $n = 0$. For two identical power spectral densities, one would expect the maximum value of the calculated correlation coefficient to be unity and occur at $n = 0$. This method of comparison of two power spectral density functions was applied to functions as represented in both their logarithmic magnitude scales, as well as their linear magnitude scales. Since power spectral density functions usually contain values which vary by several orders of magnitude, the logarithmic magnitude scale is necessary to facilitate the comparison of the so-called "valleys" or smaller values of the power spectral density function. A correlation between two power spectral density functions, displayed in the linear magnitude scale, only compares the peaks of the functions.

2.3 An Example

As an example of this method of comparison, two power spectral density plots having essentially nothing in common were correlated. The power spectral density plots compared were for different accelerometer locations and directions in the Blackwelder Building. The results of the correlation may be seen in Fig. 2.1 for the comparison of the linear magnitudes and in Fig. 2.2 for the comparison of the logarithmic magnitudes. In the linear domain, the best correlation is 0.51279, occuring at a shift of 9 places from the center. The value at the center is only 0.05709, indicating almost no correlation. The value 0.51279 is most likely a result of the "overlap" of the two first mode resonance peaks, which may be seen in Figs. A.1 and A.5 in Appendix A.

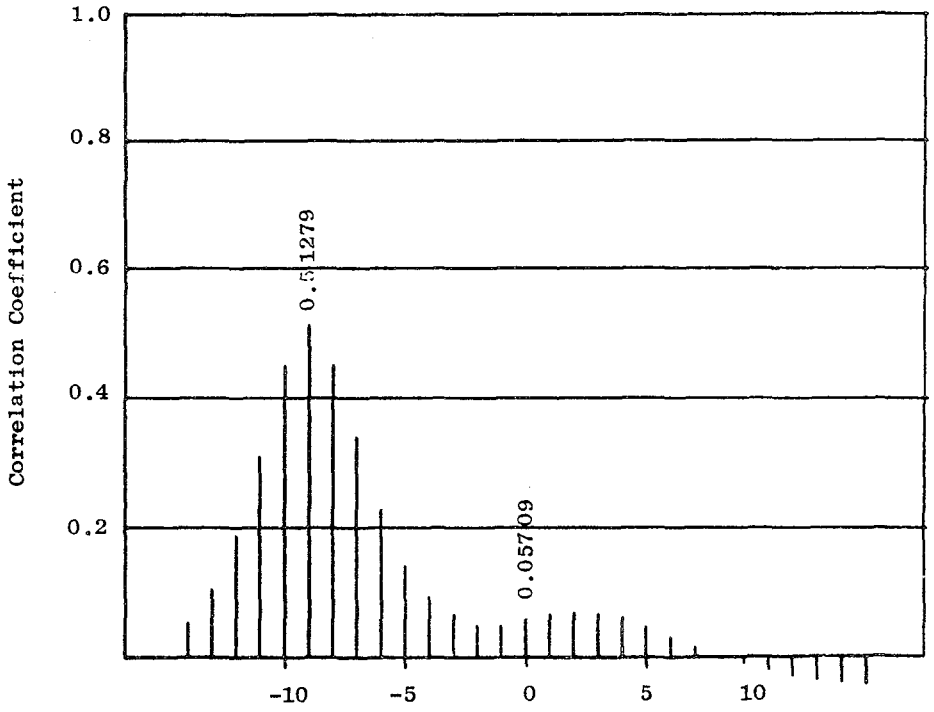

Fig. 2.1. RESULTS OF CORRELATION OF FIG. A.1 AND FIG. A.5.

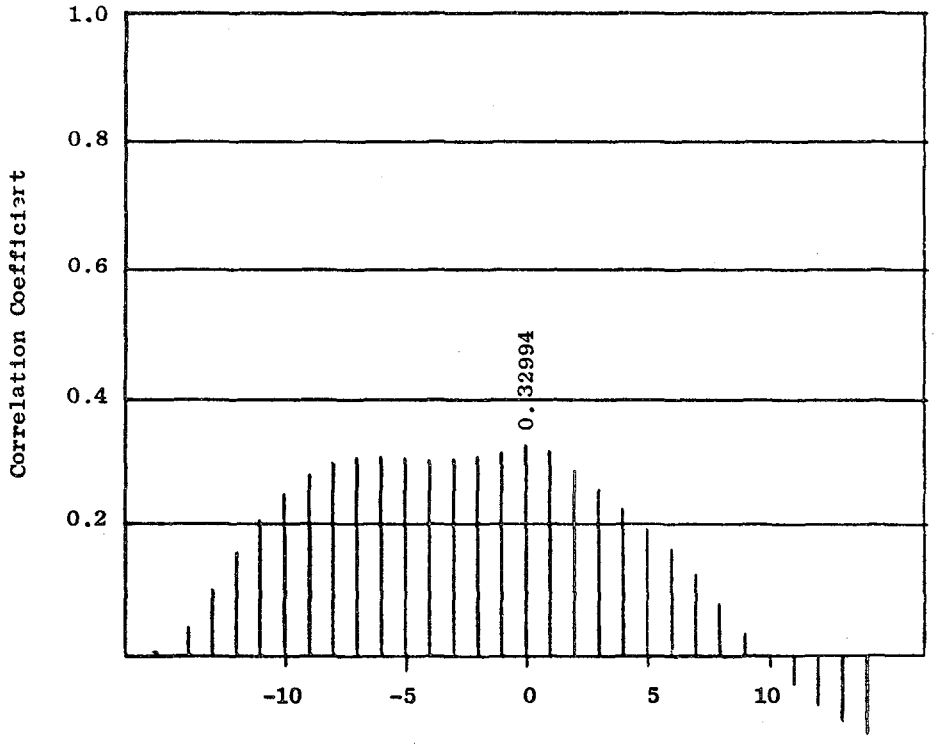

Fig. 2.2. RESULTS OF CORRELATION OF FIG. A.2 AND FIG. A.6.

The essence of Fig. 2.1 is that Figs. A.1 and A.5 have very little in common unless one is shifted a great deal with respect to the other. Figure 2.2, based on the logarithmic magnitude representations of the power spectral density plots, gives a somewhat different result. Here a value of 0.32994 is the maximum and occurs at the origin. Although very low in terms of correlation, the maximum at the origin indicates that there are similarities between the two spectrums. The similarities are most likely a result of being in the same building (i.e., Blackwelder Building). There is also an effect due to the nature of discrete Fourier analysis which causes the power spectral density plots to have a bias in the "noise" near the origin (i.e., 0.0 Hz). That is, the analysis of very weak noisy signals causes a build-up in magnitude of the Fourier coefficients very near 0.0 Hz. In some cases, this build-up is significant, especially when the power spectral densities are viewed in the logarithmic magnitude scale.

Chapter 3

COMPARISON OF POWER SPECTRAL DENSITY PLOTS OBTAINED FOR THE SAME BUILDING, ACCELEROMETER LOCATION, AND DIRECTION

3.1 Purpose and Procedure

To provide information about the accuracy and reliability of this method of ambient vibration analysis, a correlation was made of two power spectral densities obtained at the same location and direction in the same building. The results of this correlation are displayed in Fig. 3.1 for the comparison of the linear magnitude display of the power spectral densities and in Fig. 3.2 for corresponding logarithmic magnitude display. The only difference between the two calculated power spectral densities is that one power spectral density plot represents 100 averaged calculations, while the other represents 200 averaged calculations. It must be remembered that the nature of ambient vibration analysis employs the technique of spectrum averaging. Spectrum averaging is the method of data measurement and power spectral density calculation repeated over and over until the sum of these individual power spectral densities becomes representative of the building's vibrations. Since the wind is the major exciting force of the structure under ambient conditions and is certainly not stationary for any single measurement, it is apparent that any two individual measurements will vary in their frequency content. Hence, even for the same location, direction, and building, any two individual power spectral densities should vary in their shape.

Preceding page blank

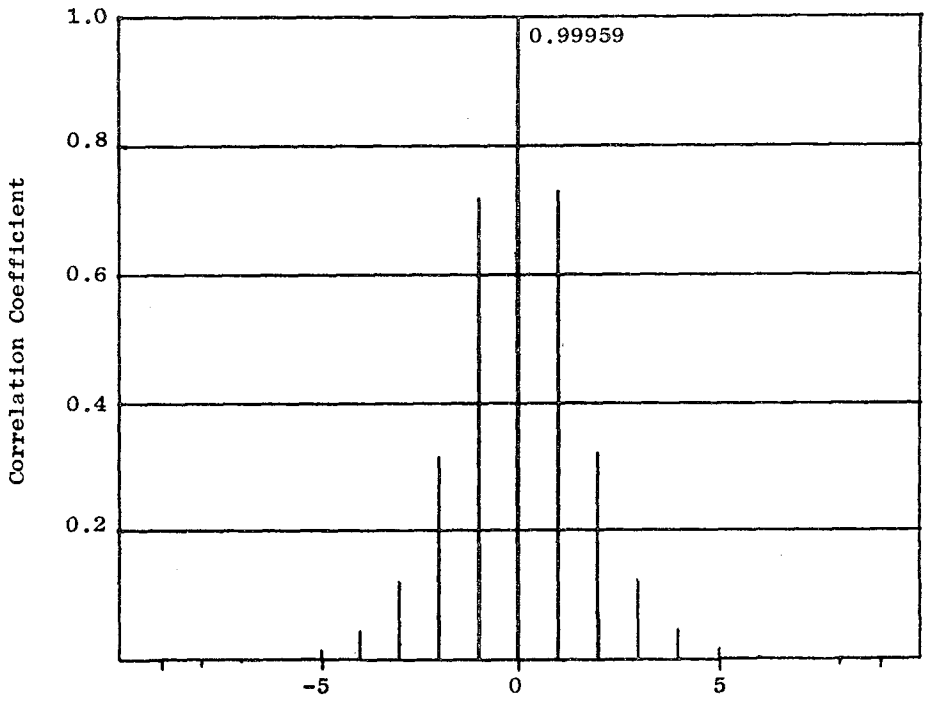

Fig. 3.1. RESULTS OF CORRELATION OF FIG. B.1 AND FIG. B.3.

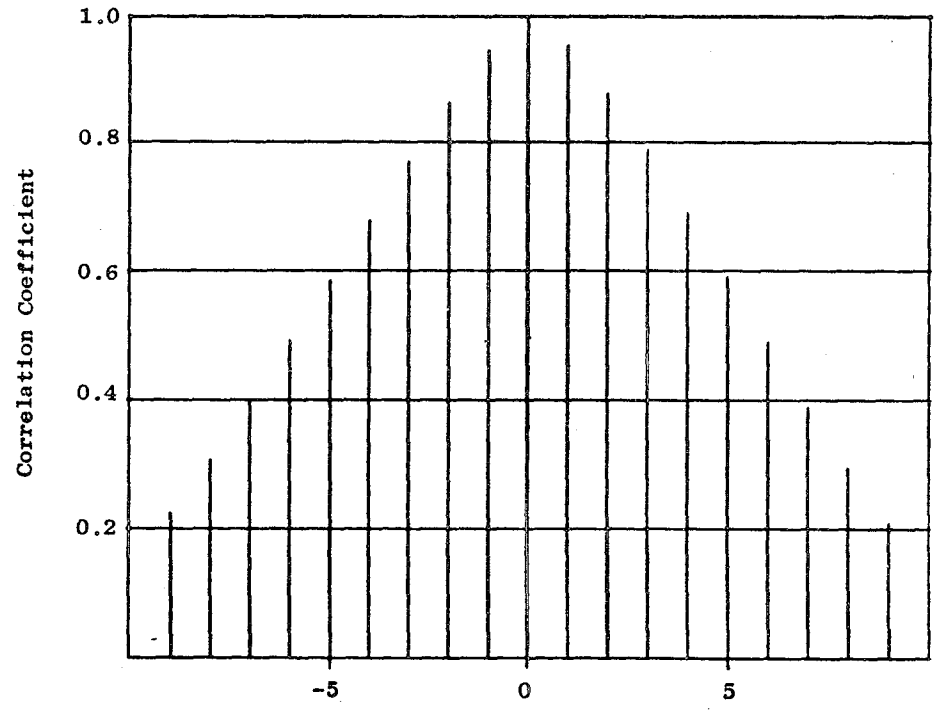

Fig. 3.2. RESULTS OF CORRELATION OF FIG. B.2 AND FIG. B.4.

3.2 Results and Conclusions

In light of the preceding argument, the results displayed in Figs. 3.1 and 3.2 are remarkable. The correlation coefficient between 100 averaged spectrums and 200 averaged spectrums is 0.99959 for the linear magnitude display and 0.99441 for the logarithmic magnitude display. In essence, these spectrums are identical. The conclusions reached on the basis of this result is, first, that the method of measurement, analysis, and spectrum averaging is reliable and accurate to a very precise degree. Second, the total data analyzed to produce the 100 and 200 averaged spectrums must be considered stationary in nature. Stationarity implies both a linear time-invariant structure, as well as a stationary forcing function. It is not surprising that the building should appear linear and time invariant at such a low level of excitation applied continuously by the wind. However, it is somewhat remarkable that the wind itself appears stationary after 100 individual spectrums have been averaged. 100 spectrums correspond to 1024 seconds or 17.67 minutes of data. It is quite likely that a considerably shorter length of data would also produce stationary results; in fact, after 10 averages, the averaged power spectral density function becomes quite representative of the stationary goal. This is certainly true for the major peaks. However, 50 to 100 individual power spectral densities must be averaged together to insure that energy transferred at all r.m.s. levels (as displayed in the log format) is representative of stationary data.

Intentionally Blank

Chapter 4

COMPARISON OF POWER SPECTRAL DENSITY PLOTS OBTAINED IN THE SAME BUILDING FOR DIFFERENT ACCELEROMETER ORIENTATIONS

4.1 Purpose and Procedure

Comparisons of sets of power spectral densities obtained from the same building but at different accelerometer locations or directions have been made. The results of these comparisons describe the similarity, or lack thereof, of two power spectral density plots which should have some common energy transfer points. Three distinct comparisons were performed. First, a comparison was made of sets of power spectral densities obtained in the same direction but at different floor levels. Second, power spectral densities obtained at the same accelerometer floor level and direction but at different locations (i.e., transverse, center vs end) were compared. Third, power spectral densities were compared for the same accelerometer floor level and location, but for different directions.

4.2 Results for Different Floor Levels, Same Accelerometer Position and Direction

The results of the correlations of power spectral densities obtained by accelerometers at different floor levels in the same building, same direction are presented in Figs. 4.1, 4.2, 4.3, and 4.4. These results are for the Blackwelder Building, comparing the 6th and 12th floor power spectral density plots. A strong similarity between a power spectral density obtained on the 6th floor and one obtained on the 12th, is expected since both spectrums should contain the same natural frequencies.

Preceding page blank

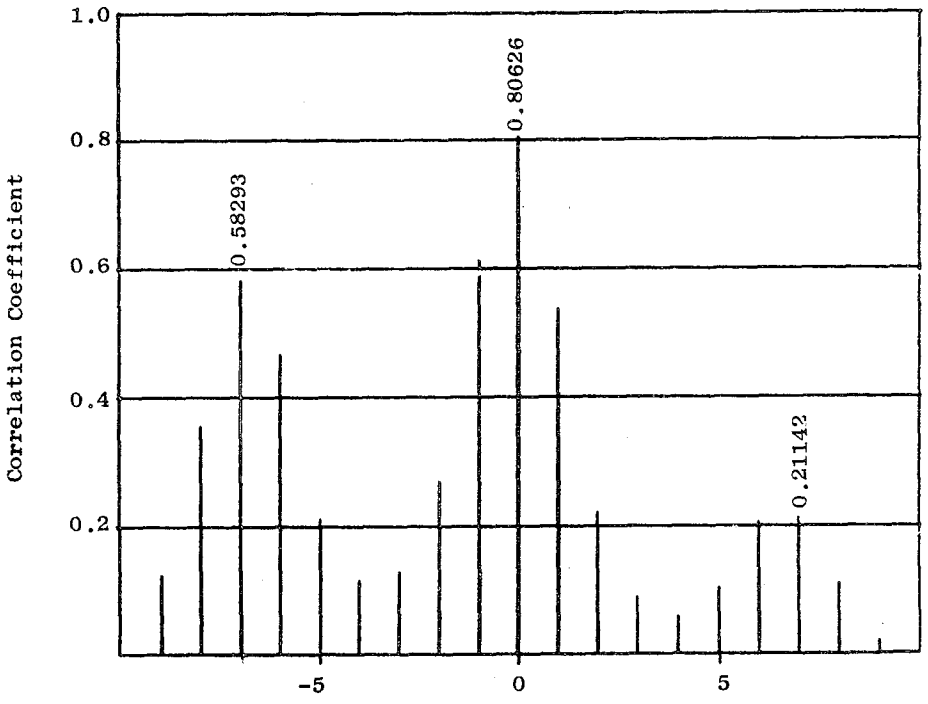

Fig. 4.1. RESULTS OF CORRELATION OF FIG. A.7 AND FIG. A.9.

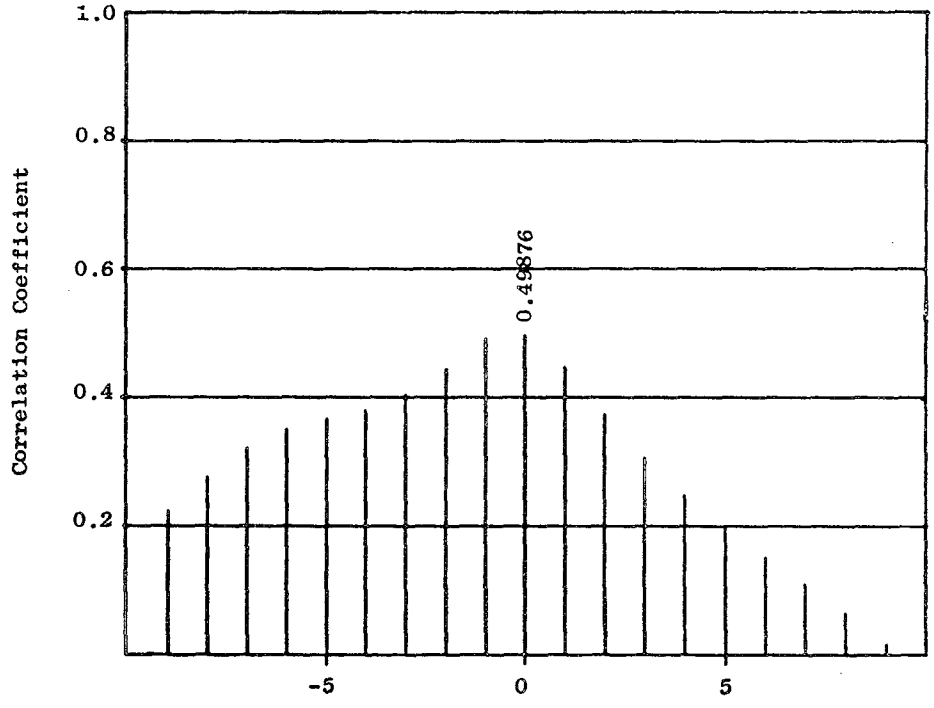

Fig. 4.2. RESULTS OF CORRELATION OF FIG. A.8 AND FIG. A.10.

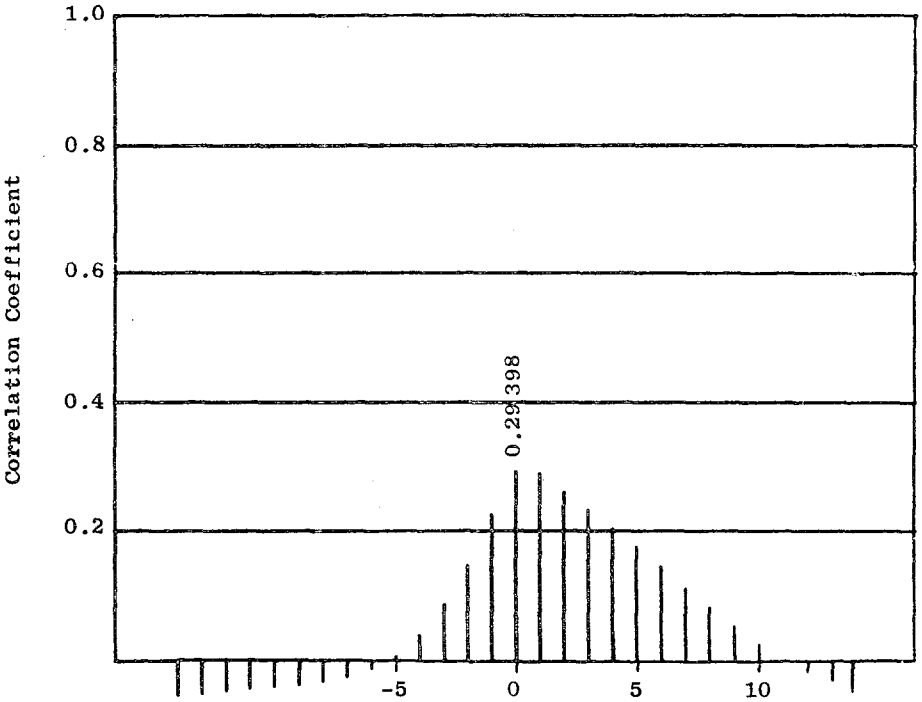

Fig. 4.3. RESULTS OF CORRELATION OF FIG. A.3 AND FIG. A.5.

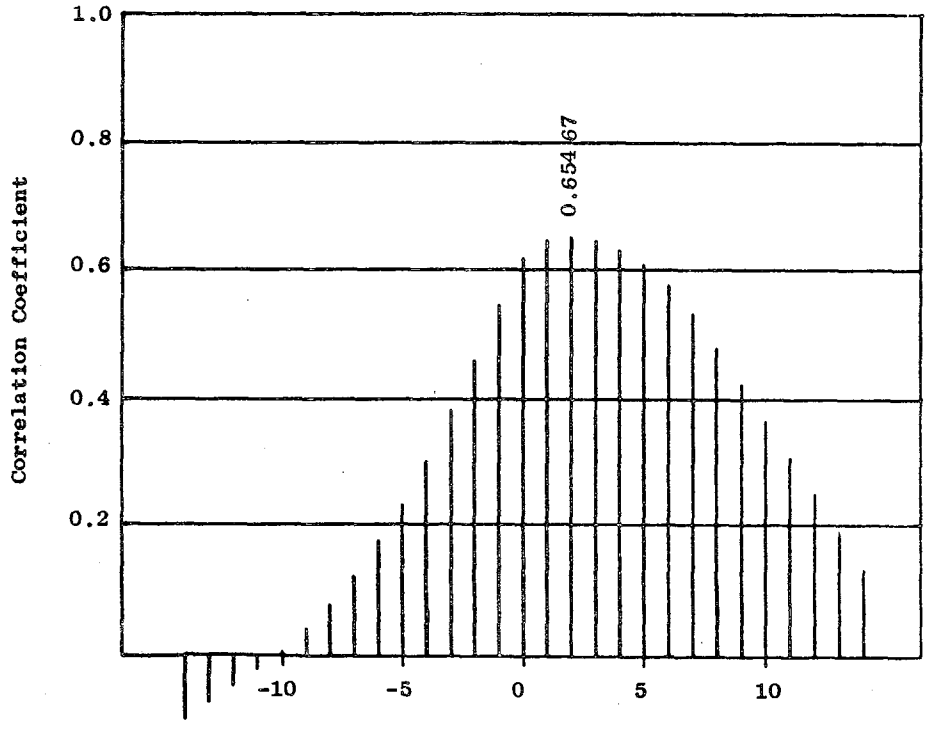

Fig. 4.4. RESULTS OF CORRELATION OF FIG. A.4 AND FIG. A.6.

However, the degree to which each natural frequency is represented is not expected to be similar since the magnitude of each modal vibration is a function of elevation within the structure.

On the basis of Fig. 4.1 (linear magnitudes) and Fig. 4.2 (logarithmic magnitudes), a strong similarity is seen to exist between power spectral densities obtained in the transverse direction at the end of the building for the 6th floor and in the same accelerometer location and direction on the 12th floor. In Fig. 4.1, the peak correlation coefficient value 0.80626 occurred at the origin (i.e., $n = 0$ shifts). The two other peaks, 0.58293 and 0.21142, are a result of shifts of seven places and the corresponding overlapping of the torsional and translational first mode natural frequencies. In Fig. 4.3 (linear magnitudes) and Fig. 4.4 (logarithmic magnitudes), representing a comparison of measurements in the Blackwelder Building, longitudinal direction, 12th and 6th floors, a somewhat less convincing correlation is seen. On the basis of Fig. 4.3, a very poor correlation of 0.29398 does occur at the origin. This low correlation value indicates that the strongest energy transfer points on the power spectral densities compared are not all indicative of the building's natural frequencies. Figure 4.4 shows that the best correlation occurs at a shift of two points from the origin. While such a small shift (e.g., 2 shofts approximately equals 0.2 Hz) might indicate a change in the common natural frequencies from one measurement to the next, it most likely indicates that the source of the largest energy transfer points seen on the two power spectral densities (above the 1st mode) are not common. This is probably a result of resonances which occur only at particular locations or floor levels (e.g., wall panel vibrations). Such local vibrations would not be expected to

be identical between the 12th and 6th floors. Forced vibrations resulting from electrical equipment are also expected to be stronger at different floor levels.

4.3 Results for Different Accelerometer Position, Same Floor Level and Direction

Several comparisons were made of power spectral densities obtained by accelerometers on the same floor in the transverse direction in the center of the building and at the end of the building. Figure 4.5 (linear magnitudes) and Fig. 4.6 (logarithmic magnitudes) represent results typical of such correlations. The correlation value of 0.86427, which occurs at the origin (i.e., $n = 0$ shifts) in Fig. 4.5, indicates a very strong similarity for these two power spectral densities. Such good correlation is, again, a result of the presence of a well defined first mode resonance. The other peak, 0.41901, in Fig. 4.5 is a result of the overlapping of the first mode in torsion and the first mode for the transverse direction when Fig. A.1 (center) has been shifted seven places to the left with respect to Fig. A.7 (end). In Fig. 4.6, the comparison of the logarithmic magnitudes of the two power spectral densities obtained at the end and in the middle of the Blackwelder Building, a peak correlation value of 0.61038 is again seen to occur at the origin. Although not as large as the peak correlation value for the linear magnitude display, the value 0.61038 and its location at the origin are strong supporters of the definite correlation of the two logarithmic magnitude power spectral densities. It is expected that the correlation for the logarithmic magnitude spectrums will never be as good as the correlations for the linear magnitude spectrums since they, by the nature of the

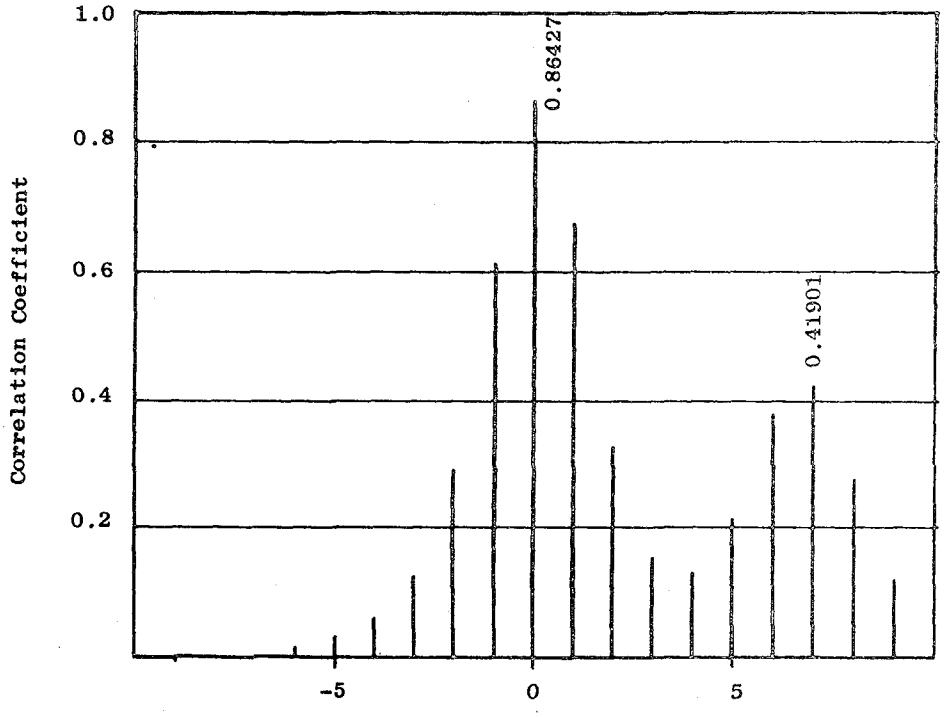

Fig. 4.5. RESULTS OF CORRELATION OF FIG. A.7 AND FIG. A.1.

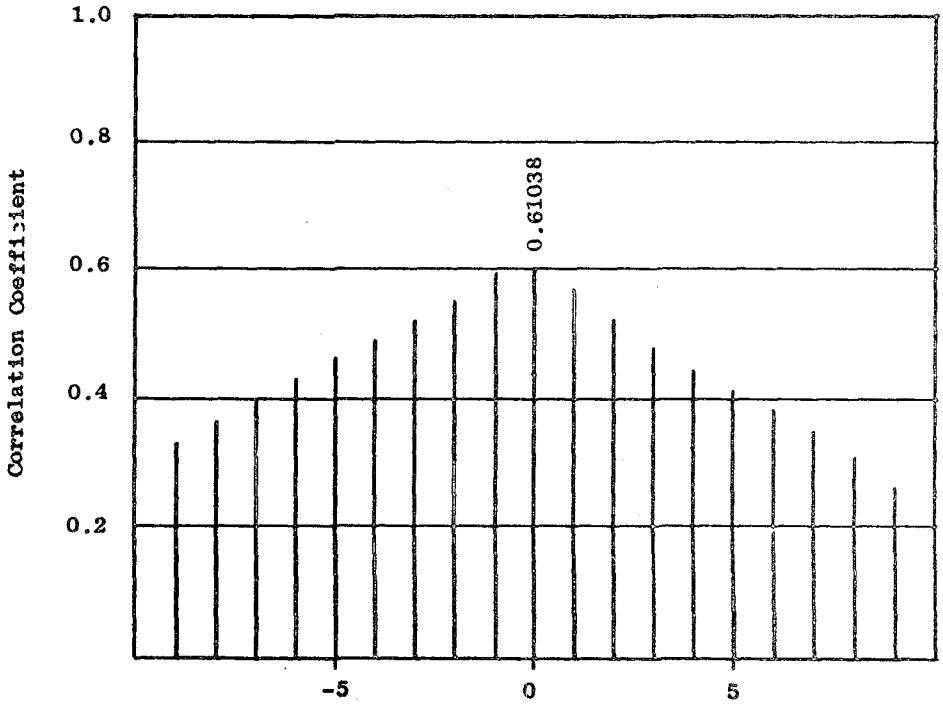

Fig. 4.6. RESULTS OF CORRELATION OF FIG. A.8 AND FIG. A.2.

logarithmic magnitude, force the comparison of all energy transfer points contained in the power spectral density, whether large or small. The comparisons of the linear displays of the power spectrums are biased toward large numbers and therefore really only compare the peaks of the power spectral densities.

4.4 Results for Different Accelerometer Directions, Same Floor Level and Location

The third and last comparison performed within the same building was for an accelerometer orientation with a common floor level and location but for different directions. The goal of such a comparison was to discover if there existed a significant correlation to suggest that common energy transfer points exist for power spectral densities obtained at a common accelerometer location, but different directions. Excitation sources such as eccentric motors could create local vibrations which would not necessarily be uniaxially orientated and, hence, create common energy transfer points for different directions. The results of such comparisons are presented in Fig. 4.7 (linear magnitudes) and Fig. 4.8 (logarithmic magnitudes). On the basis of Fig. 4.7 it can be concluded that essentially no correlation exists unless the two power spectral densities are shifted enough to facilitate the overlapping of the two unrelated first modes. Likewise, in Fig. 4.8, the best correlation, 0.61590, occurs sufficiently far from the origin (i.e., $n = 8$ shifts) to permit the same conclusion. On the basis of Figs. 4.7 and 4.8, it is apparent that power spectral densities obtained in different directions, although common location, can not be expected to have common energy transfer points.

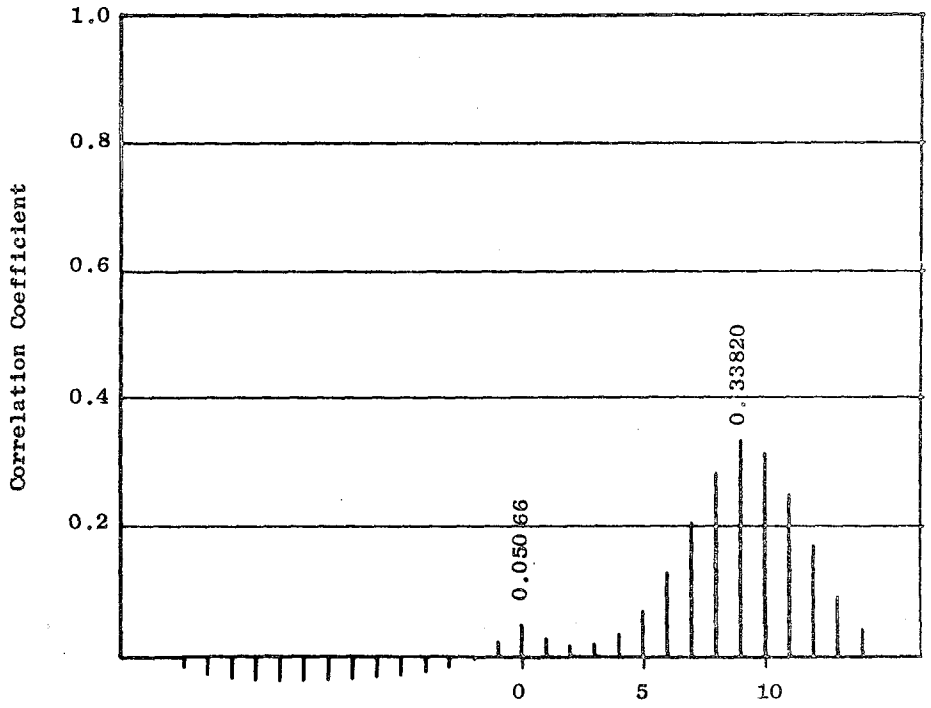

Fig. 4.7. RESULTS OF CORRELATION OF FIG. A.3 AND FIG. A.1.

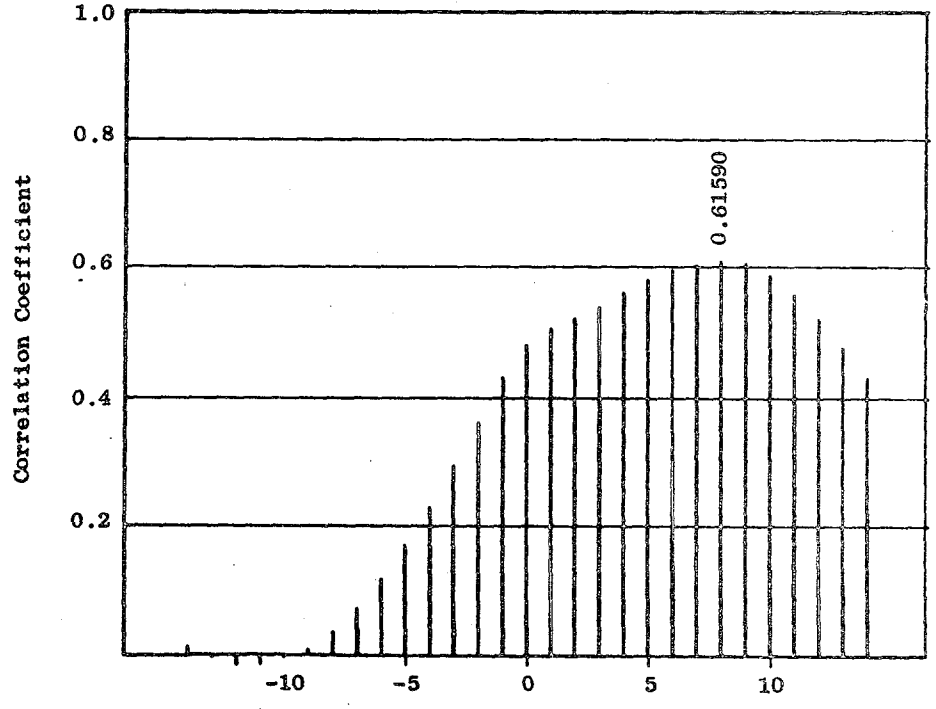

Fig. 4.8. RESULTS OF CORRELATION OF FIG. A.4 AND FIG. A.2.

Chapter 5

COMPARISON OF FOUR 8-STORY BUILDINGS OF IDENTICAL DESIGN

5.1 Purpose and Procedure

Escondido Village, on the Stanford Campus, proved to be an excellent site for this ambient vibration analysis study, since it provided a number of buildings of identical design. Four such buildings, McFarland Building, Hoskins Building, Hulme Building, and Barnes Building, are all 8-story reinforced concrete apartment buildings of identical design. These four buildings provided the information necessary to compare their power spectral density plots for both accelerometer directions transverse in the center and transverse at the end, as well as the longitudinal direction. All measurements were taken on the same floor level (i.e., 8th floor) and the same location in each building. Table 1.3 has already given a summary of the first mode natural frequencies. The results given in Table 1.3 are taken from figures where 512 frequency data points are used to describe a frequency range 0-10 Hz. The resolution of such graphs is thus approximately 0.02 Hz for the width between any two points. It may be seen, however, that the first mode natural frequency may appear different by as much as 3 points or 0.06 Hz for two different measurements. The two measurements correspond to the transverse fundamental frequency as seen in the center of the building and as seen at the end of the building. An explanation for this is not obvious, but it does appear that at ambient force levels the natural frequencies of buildings are not constant when calculated to an accuracy greater than 0.1 Hz. This apparent nonlinearity does not appear, in the case of these four buildings, to be a result of different levels of excitation.

While the values given in Table 1.3 are not constant to two decimal places, they still may be used to indicate very slight but noticeable differences in first mode natural frequencies for the four buildings. Comparisons of the power spectral densities for the four buildings should also reflect this difference. In the comparison of the power spectrums, however, the frequency range is 0-25 Hz described by 256 frequency data points. This reduced resolution makes the first modes appear more alike for different buildings. However, the 0-25 Hz frequency range permits a comparison of all natural frequencies if their presence is noticeable in the power spectrums correlated.

5.2 Results and Conclusions

The results of the comparisons of the four buildings, McFarland, Hoskins, Hulme, and Barnes, are presented in a matrix format in Tables 5.1 and 5.2 for the longitudinal accelerometer direction, Tables 5.3 and 5.4 for the transverse (center) accelerometer direction, and Tables 5.5 and 5.6 for the transverse (end) accelerometer direction. The values given in the tables are the peak correlation values, with them are also given, in parentheses, the number of places shifted for the occurrence of the peak correlation values. As would be expected when a spectrum is correlated with itself, the peak correlation value is unity, occurring at the origin (i.e., $n = 0$ shifts). The results presented in this matrix are obviously of a symmetrical matrix form.

The results presented in Table 5.1, longitudinal and linear magnitude display, show a very good correlation between all four buildings. However, on the basis of the results in two cases, Hulmes correlations indicate that its frequencies are slightly (i.e., $n = 1$ shift) higher.

Table 5.1

PEAK CORRELATION VALUES BETWEEN POWER SPECTRAL DENSITY PLOTS FOR FOUR 8-STORY BUILDINGS OF IDENTICAL DESIGN. Measurements taken in longitudinal direction; linear magnitude scale; (Figs. C.3, D.3, E.3, F.3).

	*Value in parentheses is the number of places (n) shifted for best correlation.			
	McFarland	Hoskins	Hulme	Barnes
McF.	1.00000 (0)	0.90873 (0)	0.51301 (-1)	0.97326 (0)
Hos.	0.90873 (0)	1.00000 (0)	0.43355 (0)	0.84617 (0)
Hul.	0.51301 (+1)	0.43355 (0)	1.00000 (0)	0.52927 (+1)
Bar.	0.97326 (0)	0.84617 (0)	0.52927 (-1)	1.00000 (0)

Table 5.2

PEAK CORRELATION VALUES BETWEEN POWER SPECTRAL DENSITY PLOTS FOR FOUR 8-STORY BUILDINGS OF IDENTICAL DESIGN. Measurements taken in longitudinal direction; logarithmic magnitude scale; (Figs. C.4, D.4, E.4, F.4).

McF.	1.00000 (0)	0.73115 (0)	0.64986 (0)	0.68332 (0)
Hos.	0.73115 (0)	1.00000 (0)	0.35760 (0)	0.49801 (0)
Hul.	0.64988 (0)	0.35760 (0)	1.00000 (0)	0.80645 (0)
Bar.	0.68333 (0)	0.49801 (0)	0.80645 (0)	1.00000 (0)

Table 5.3

PEAK CORRELATION VALUES BETWEEN POWER SPECTRAL DENSITY PLOTS FOR FOUR 8-STORY BUILDINGS OF IDENTICAL DESIGN. Measurements taken in transverse (center) direction; linear magnitude scale; (Figs. C.1, D.1, E.1, F.1).

McF.	1.00000 (0)	0.94777 (0)	0.89427 (-1)	0.61148 (0)
Hos.	0.94777 (0)	1.00000 (0)	0.87357 (-1)	0.59056 (0)
Hul.	0.89427 (+1)	0.87357 (+1)	1.00000 (0)	0.64982 (+1)
Bar.	0.61148 (0)	0.59056 (0)	0.64982 (-1)	1.00000 (0)

Table 5.4

PEAK CORRELATION VALUES BETWEEN POWER SPECTRAL DENSITY PLOTS FOR FOUR 8-STORY BUILDINGS OF IDENTICAL DESIGN. Measurements taken in transverse (center) direction; logarithmic magnitude scale; (Figs. C.2, D.2, E.2, F.2).

	*Value in parentheses is the number of places (n) shifted for best correlation.			
	McFarland	Hoskins	Hulme	Barnes
McF.	1.00000 (0)	0.84112 (0)	0.66064 (0)	0.61081 (0)
Hos.	0.84112 (0)	1.00000 (0)	0.69845 (0)	0.57269 (0)
Hul.	0.66064 (0)	0.69845 (0)	1.00000 (0)	0.75699 (0)
Bar.	0.61081 (0)	0.57269 (0)	0.75699 (0)	1.00000 (0)

Table 5.5

PEAK CORRELATION VALUES BETWEEN POWER SPECTRAL DENSITY PLOTS FOR FOUR 8-STORY BUILDINGS OF IDENTICAL DESIGN. Measurements taken in transverse (end) direction; linear magnitude scale; (Figs. C.5, D.5, E.5, F.5).

McF.	1.00000 (0)	0.80527 (0)	0.80644 (+1)	0.69637 (+3)
Hos.	0.80527 (0)	1.00000 (0)	0.66823 (+1)	0.61703 (+3)
Hul.	0.80644 (-1)	0.66823 (-1)	1.00000 (0)	0.84547 (+1)
Bar.	0.69637 (-3)	0.61703 (-3)	0.84547 (-1)	1.00000 (0)

Table 5.6

PEAK CORRELATION VALUES BETWEEN POWER SPECTRAL DENSITY PLOTS FOR FOUR 8-STORY BUILDINGS OF IDENTICAL DESIGN. Measurements taken in transverse (end) direction; logarithmic magnitude scale; (Figs. C.6, D.6, E.6, F.6).

McF.	1.00000 (0)	0.81021 (+1)	0.71066 (0)	0.72073 (0)
Hos.	0.81021 (-1)	1.00000 (0)	0.52474 (-2)	0.55496 (0)
Hul.	0.71066 (0)	0.52474 (+2)	1.00000 (0)	0.86482 (0)
Bar.	0.72073 (0)	0.55496 (0)	0.86482 (0)	1.00000 (0)

This corresponds to the fact that Hulme had the highest (2.60 Hz) first mode natural frequency, and that comparisons of linear representations of the power spectrums emphasize the correlation of the high energy transfer, first mode frequencies. Likewise, in Table 5.3, transverse (center) and linear magnitude display, Hulme again appears to have slightly (i.e., $n = 1$ shift) higher frequencies. This is again compatible with the results given in Table 1.3. The results of the comparisons of the logarithmic magnitude displays for the longitudinal direction and the transverse (center) direction presented in Tables 5.2 and 5.4, respectively, indicate excellent correlation values also. Remarkably, in all cases, the best correlation between any two buildings occurs at the origin (i.e., $n = 0$ shifts). This result is indicative of the fact that all four buildings are very similar in the manner in which they are transferring energy for the range 0-25 Hz. Even though it is virtually impossible to identify any modal frequencies above the first, the magnitudes of the energy transfer points for the range 0-25 Hz are quite similar for all four buildings.

Tables 5.5 and 5.6 are for the correlations of power spectral density plots obtained at the end of the building in the transverse direction. Such power spectral densities contain both transverse and torsion modal frequencies. Once again, for the linear display comparisons, the slight difference in first mode torsional frequencies as listed in Table 1.3 are represented in shift values of $n = 1$ for Hulme and $n = 3$ for Barnes for the location of the peak correlation values. The logarithmic magnitude display comparisons, Table 5.6, also yield good correlation values. In essence, while small differences in these four buildings may be determined, these four buildings are, in terms of practical engineering work, identical in the manner in which they transfer energy.

Intentionally Blank

Chapter 6

COMPARISON OF TWO 12-STORY BUILDINGS OF IDENTICAL DESIGN

6.1 Purpose and Procedure

As a final demonstration of the remarkable similarity that power spectral density plots obtained from two different buildings may have, two 12-story buildings, Quillen and Blackwelder, are compared in the transverse (center) direction. The results are presented in Fig. 6.1 for the comparison of the linear magnitude display of the power spectrums, and Fig. 6.2 for the comparison of the logarithmic magnitude display.

6.2 Results and Conclusions

The shape of the correlation values in Fig. 6.1, as well as a peak value of 0.98887, indicates that the power spectral densities are virtually identical. However, the peak correlation value of 0.98887 occurs at a shift of $n = 1$ places from the origin. It appears that although the power spectral density plot's shape for the Blackwelder Building is extremely similar with power spectral density plot's shape for the Quillen Building in the linear magnitude display, the frequencies for the Blackwelder Building are slightly higher. This result is supported by the earlier results for the natural frequencies of these two buildings listed in Tables 1.1 and 1.2. The results of Fig. 6.2, the comparison of the logarithmic magnitude displays, yield a peak correlation value of 0.70438 at a shift of $n = 2$ places from the origin. This suggests that the natural frequencies above the first mode are also larger in the Blackwelder Building than in the Quillen Building, but that both are still quite similar in the nature of the points of energy transfer.

Preceding page blank

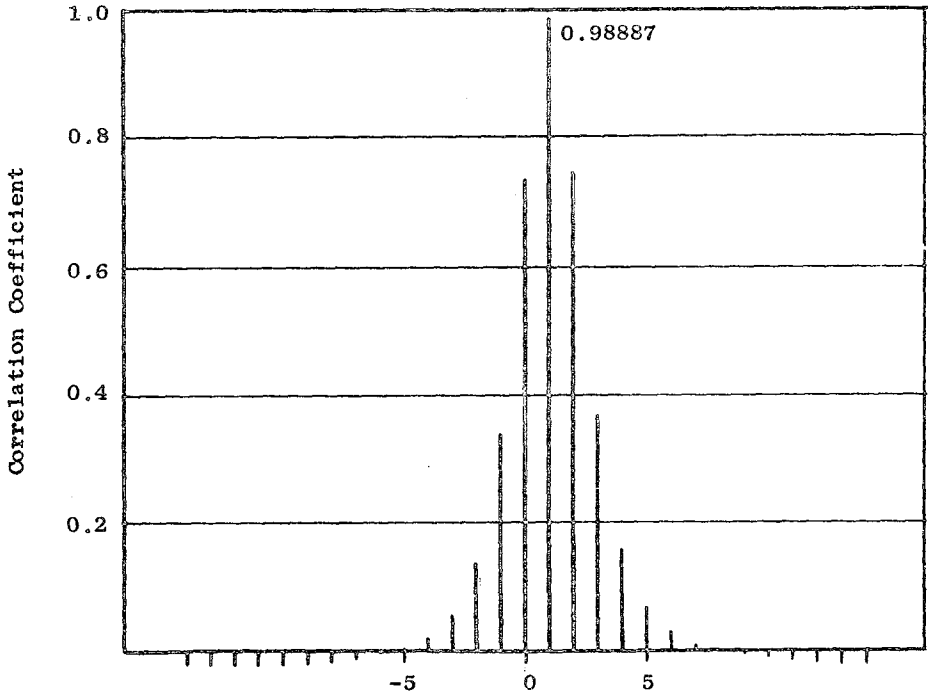

Fig. 6.1. RESULTS OF CORRELATION OF FIG. A.1 AND FIG. B.3.

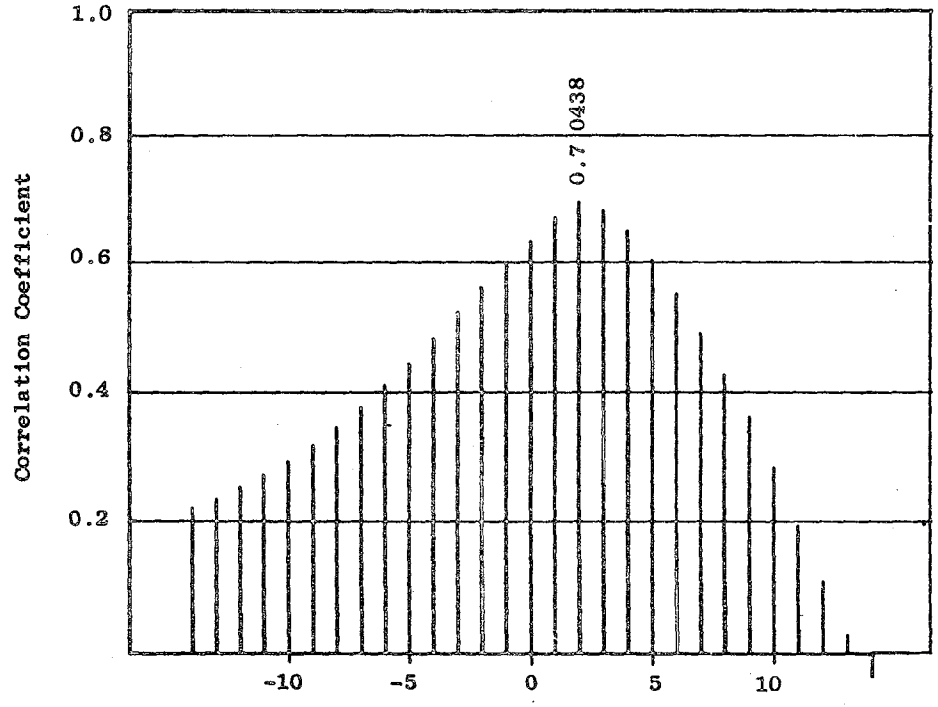

Fig. 6.2. RESULTS OF CORRELATION OF FIG. A.2 AND FIG. B.4.

Chapter 7

GENERAL CONCLUSIONS

Two 12-story high-rise apartment buildings, Blackwelder and Quillen, and four 8-story high-rise apartment buildings, McFarland, Hoskins, Hulme, and Barnes, located in Escondido Village on the Stanford University Campus, were analyzed to determine their dynamic characteristics. The ambient vibration analyses performed on the buildings produced a collection of power spectral density functions for each building. Although higher modes were undoubtedly present in the power spectral density plots, in general, only the fundamental mode could be consistently identified. An estimate of the percent of critical damping associated with the fundamental mode was calculated for the four 8-story buildings.

A mathematical method for comparison of two power spectral densities based on the definition of the correlation coefficient was developed. Pairs of power spectral density plots, as displayed in both the linear magnitude scale and logarithmic magnitude scale, were then compared using this mathematical method. On the basis of the results of these comparisons, the following conclusions may be made.

(1) The method of ambient vibration analysis used, involving Fourier analysis and the technique of "spectrum averaging," produces accurate and reliable results.

(2) After enough individually measured and calculated power spectral density functions are averaged together, the resulting power spectral density function is representative of a stationary process. This implies that the building appears as a linear time-invariant structure, and that the wind, the principle random excitation source, is a stationary process.

(3) Power spectral density plots obtained at different floor levels for the same accelerometer direction may not appear very similar unless the overall modal vibrations are sufficiently stronger than any local points of energy transfer.

(4) Power spectral density plots obtained for the same accelerometer direction and floor level but at different positions (i.e., center vs end) have strong similarities.

(5) Power spectral density plots obtained for the same accelerometer position and floor level, but different directions, have essentially nothing in common. This implies that most of the energy transfer is uniaxially orientated.

(6) The buildings analyzed of identical design may often be slightly different in their natural frequencies, and that this slight difference (e.g., less than 4%) can be accurately determined by this method of ambient vibration analysis. However, for most engineering purposes, the buildings of identical design may be assumed to have "identical" dynamic characteristics.

REFERENCES

1. Charles Alan Kircher, "Determination of the Dynamic Characteristics of Full-Scale Structures by the Application of Fourier Analysis," Technical Report No. 177, Stanford University, June 1973.

2. S. H. Crandall and W. D. Mark, Random Vibrations, Academic Press, Inc., New York, 1963.

3. Ron Bracewell, The Fourier Transform and Its Applications, McGraw-Hill Book Co., New York, 1965.

4. R. B. Blackman and J. W. Tukey, The Measurement of Power Spectra, Dover Publications, Inc., New York, 1958.

5. Gary C. Hart, Marshall Lew, and Roger DiJulio, "High-Rise Building Response: Damping and Period Non-Linearities," Fifth World Conference on Earthquake Engineering, Rome, 1973.

6. B. Goodno, "Dynamic Analysis of Suspended-Floor Highrise Buildings Using Super-Elements," Ph.D. Thesis, Stanford University, September 1974.

7. P. C. Jennings, R. Matthiesen, and J. Hoerner, "Forced Vibration of a 22-Story Steel Frame Building," California Institute of Technology and UCLA School of Engineering and Applied Science, EERL 71-01, February 1971.

8. J. Ray Stagner and Gary G. Hart, "Damping Estimation and Digital Filtering Applied to Structural Motion Studies," UCLA-ENG 7181, December 1971.

Appendix A

POWER SPECTRAL DENSITY PLOTS FOR THE BLACKWELDER BUILDING AND A SUMMARY OF THE RESULTS

Table A.1

SUMMARY OF THE PREDOMINANT ENERGY TRANSFER POINTS FOR THE BLACKWELDER BUILDING

Figure	Accelerometer Orientation			Number of Spectrums Averaged	Natural Frequencies (Hz)		Other Points (Hz)
	Direction	Position in Bldg.	Floor Level		1st	2nd	
A.1 A.2	transverse	center	12th	100	2.0	8.9	15.6 21.3
A.3 A.4	longitudinal	center	12th	100	2.9		15.8 25.8
A.5 A.6	longitudinal	center	6th	125	2.9		15.3 26.5
A.7 A.8	transverse	end	12th	100	2.0 2.7	9.0 10.6	13.0 14.6 21.3
A.9 A.10	transverse	end	6th	150	2.0 2.7	10.6	15.0 21.2 26.2
A.11 A.12	longitudinal	center	12th	50	2.89	---	---
A.13 A.14	transverse	end	12th	20	2.01 2.68	---	---

Preceding page blank

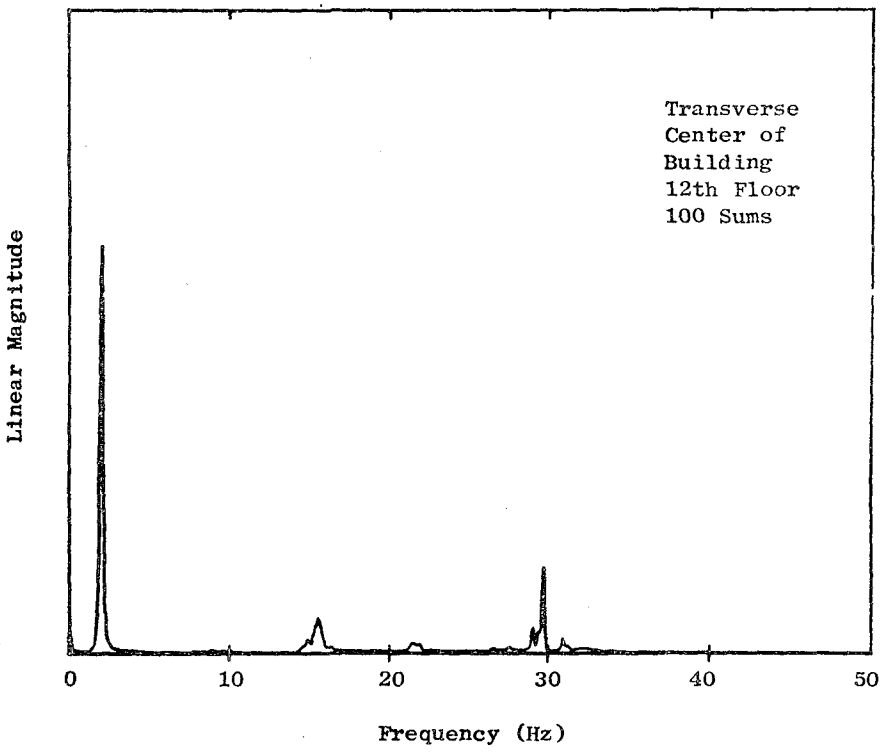

Fig. A.1. POWER SPECTRAL DENSITY PLOT, BLACKWELDER BUILDING.

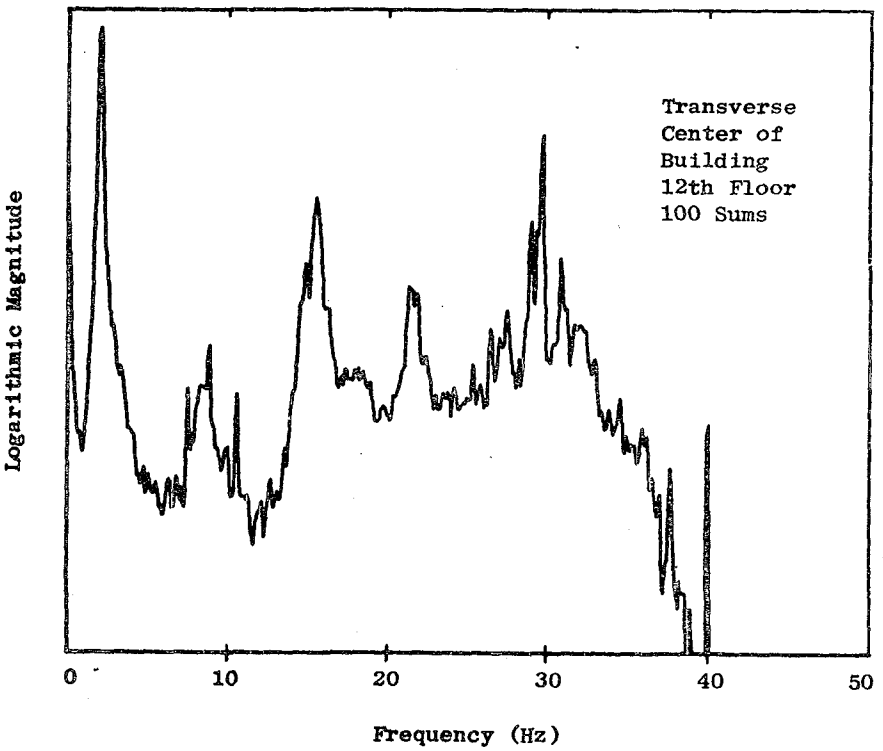

Fig. A.2. POWER SPECTRAL DENSITY PLOT, BLACKWELDER BUILDING.

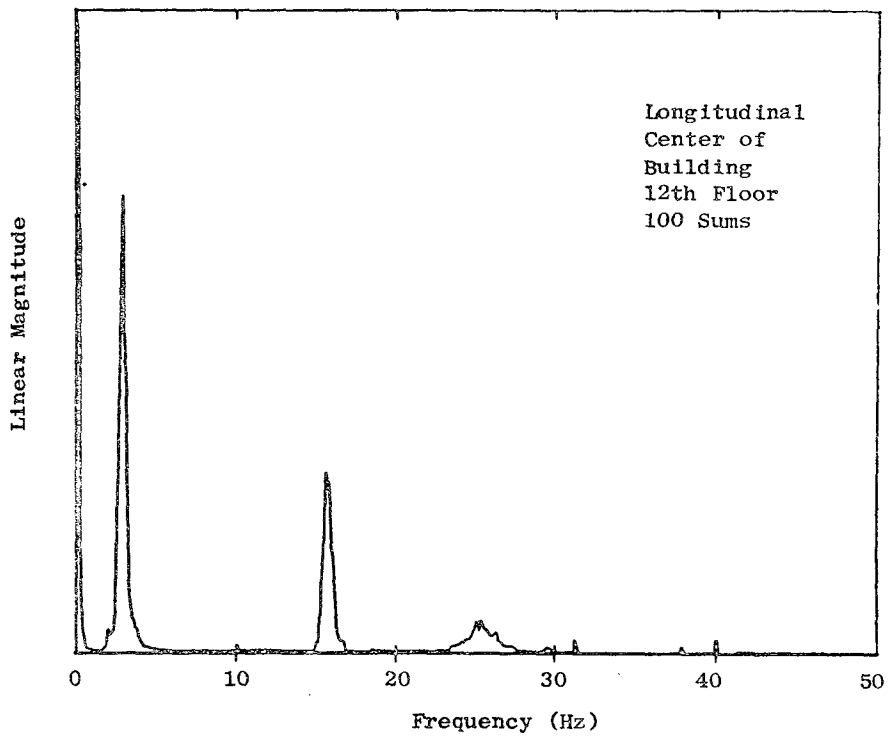

Fig. A.3. POWER SPECTRAL DENSITY PLOT, BLACKWELDER BUILDING.

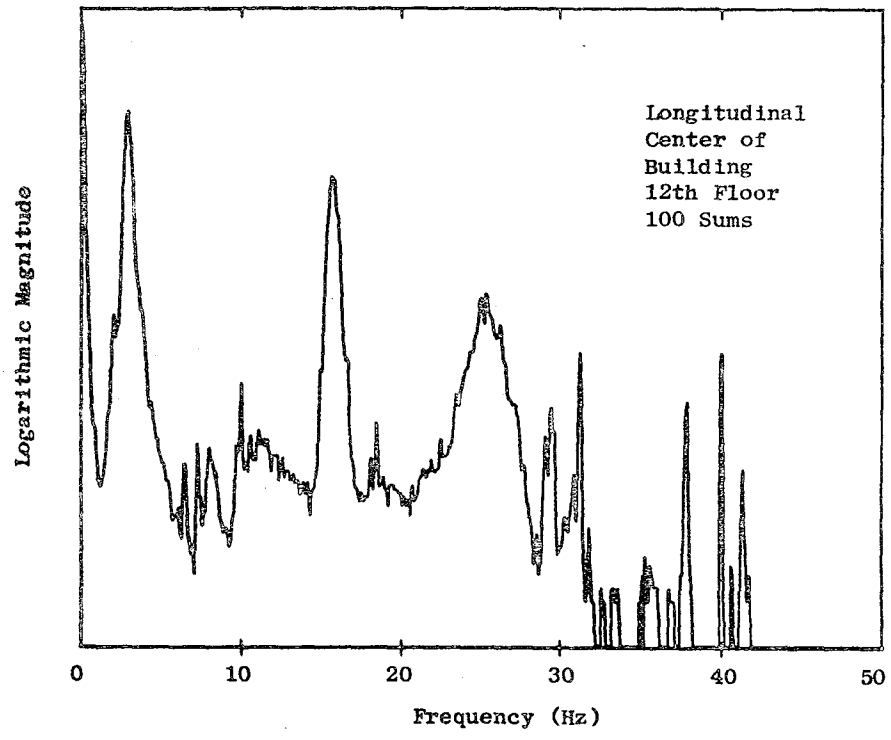

Fig. A.4. POWER SPECTRAL DENSITY PLOT, BLACKWELDER BUILDING.

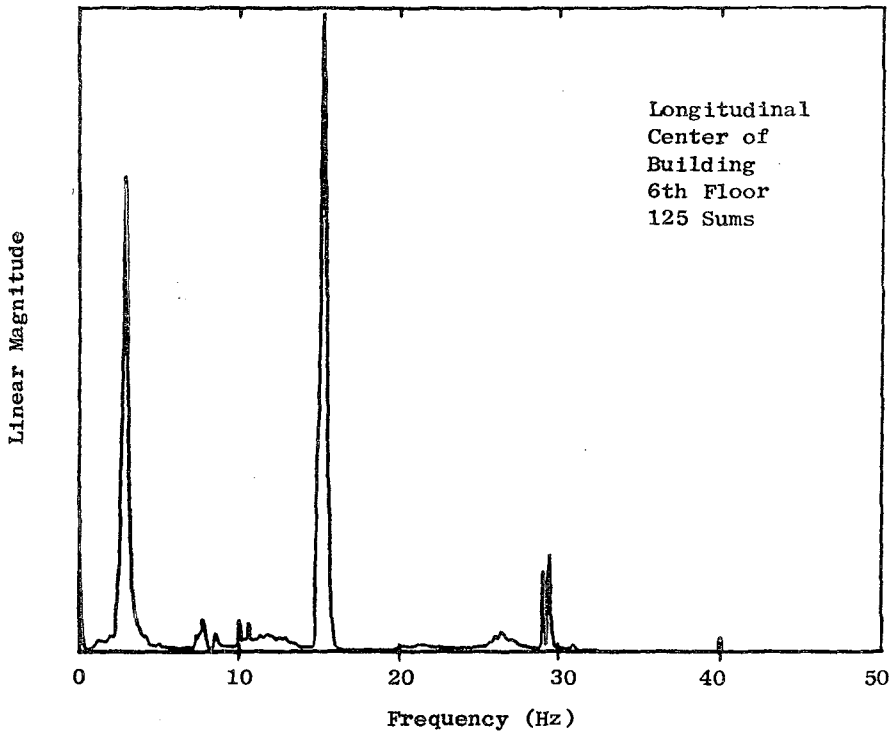

Fig. A.5. POWER SPECTRAL DENSITY PLOT, BLACKWELDER BUILDING.

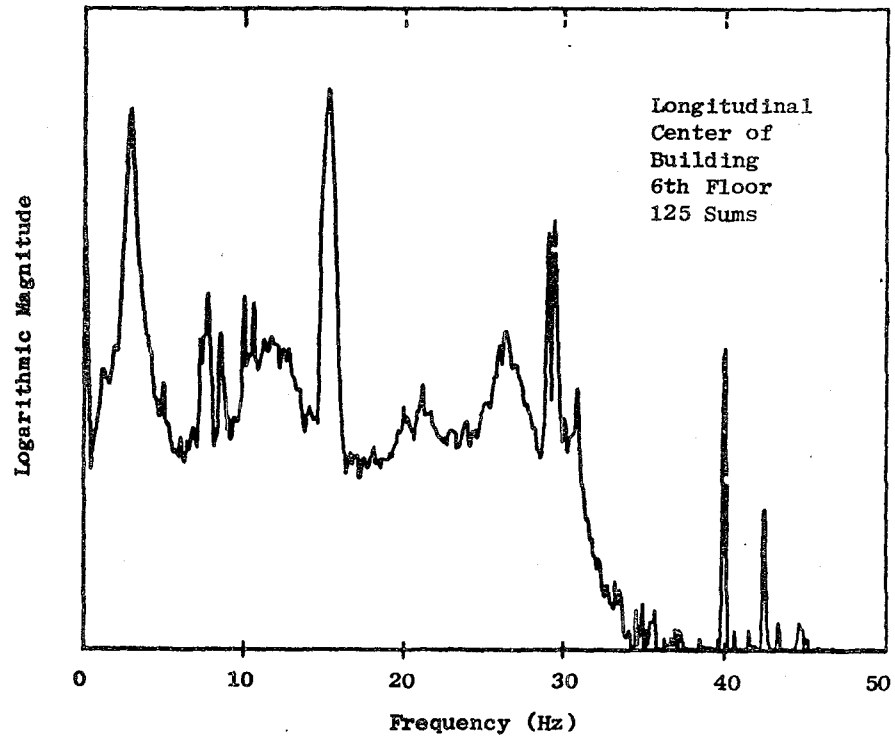

Fig. A.6. POWER SPECTRAL DENSITY PLOT, BLACKWELDER BUILDING.

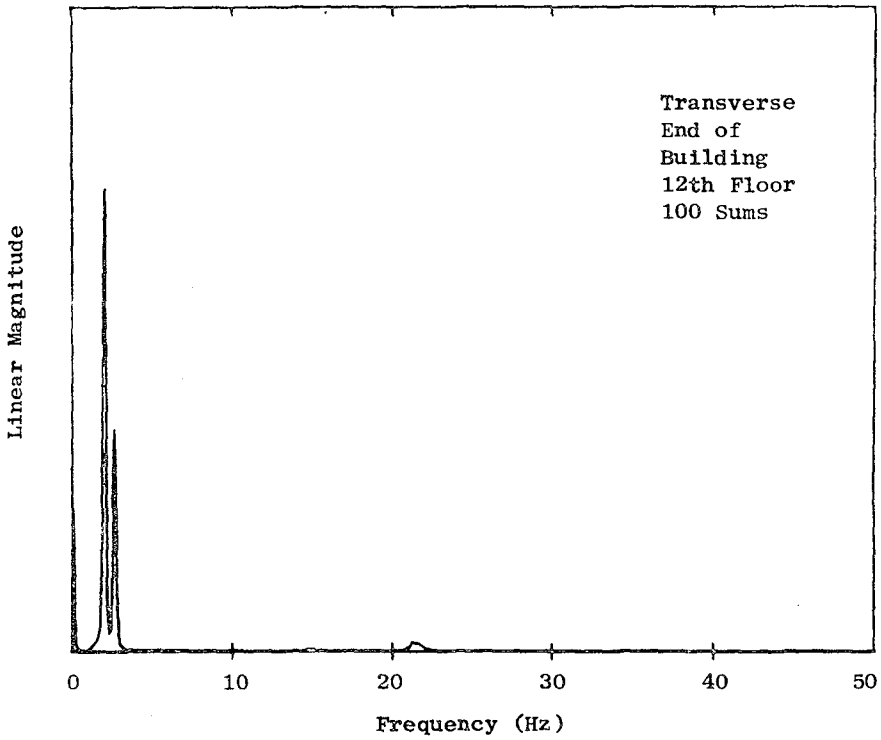

Fig. A.7. POWER SPECTRAL DENSITY PLOT, BLACKWELDER BUILDING.

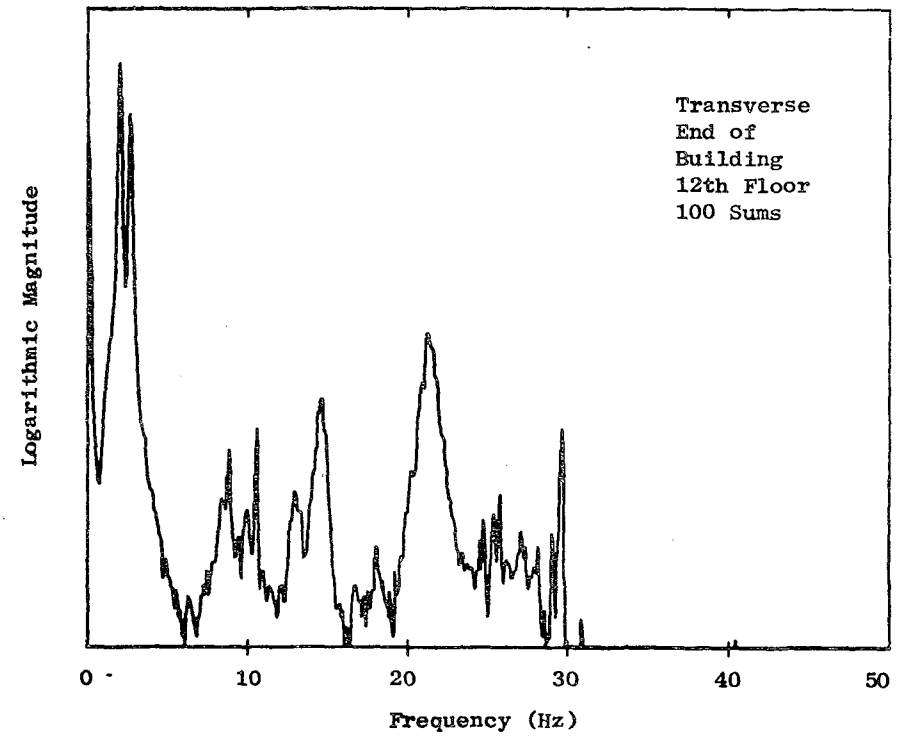

Fig. A.8. POWER SPECTRAL DENSITY PLOT, BLACKWELDER BUILDING.

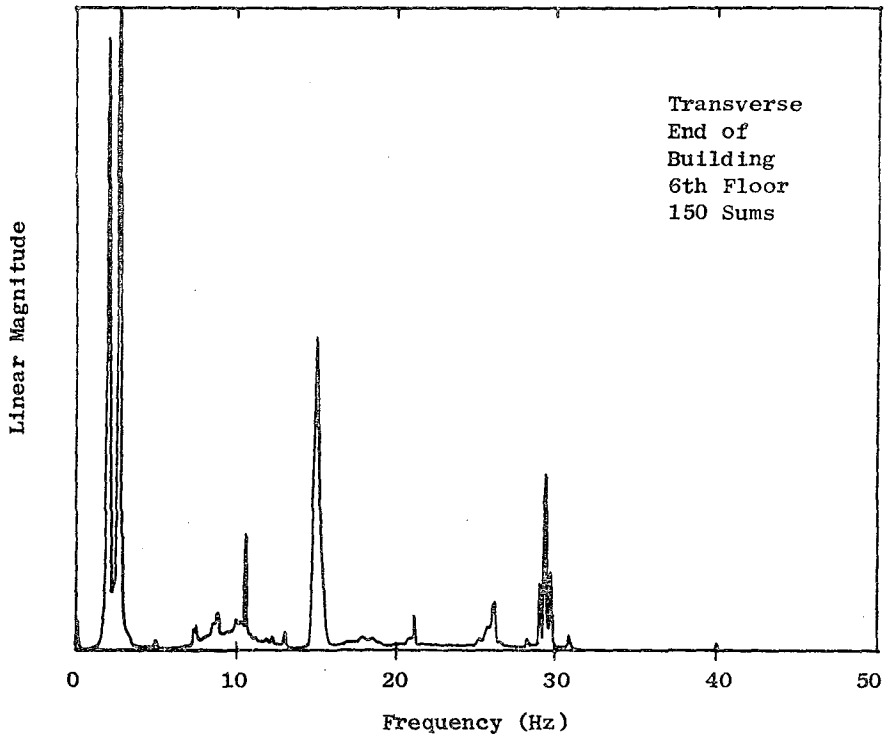

Fig. A.9. POWER SPECTRAL DENSITY PLOT, BLACKWELDER BUILDING.

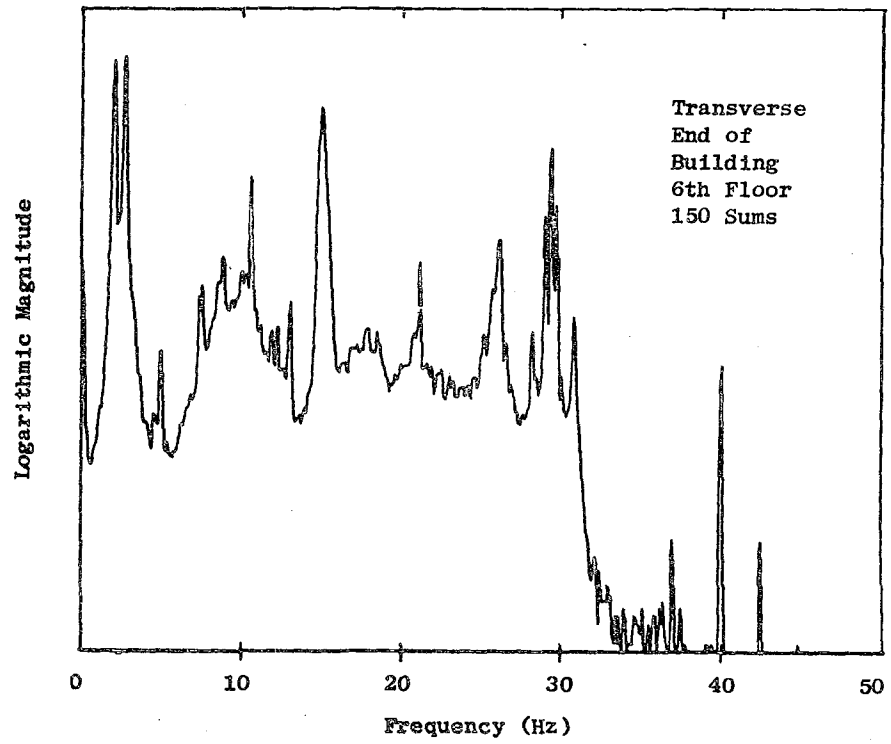

Fig. A.10. POWER SPECTRAL DENSITY PLOT, BLACKWELDER BUILDING.

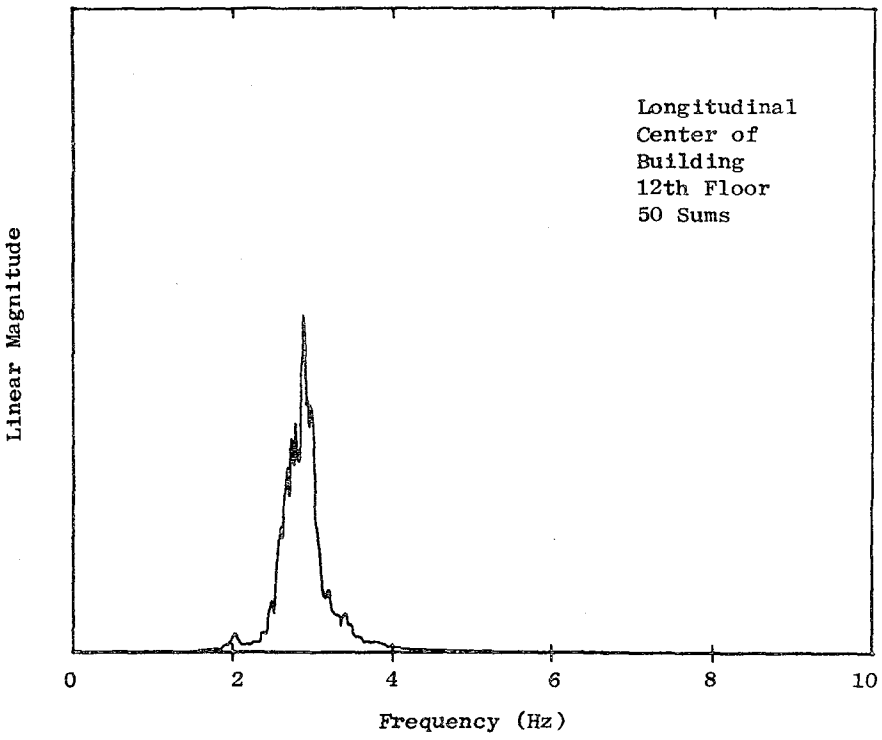

Fig. A.11. POWER SPECTRAL DENSITY PLOT, BLACKWELDER BUILDING.

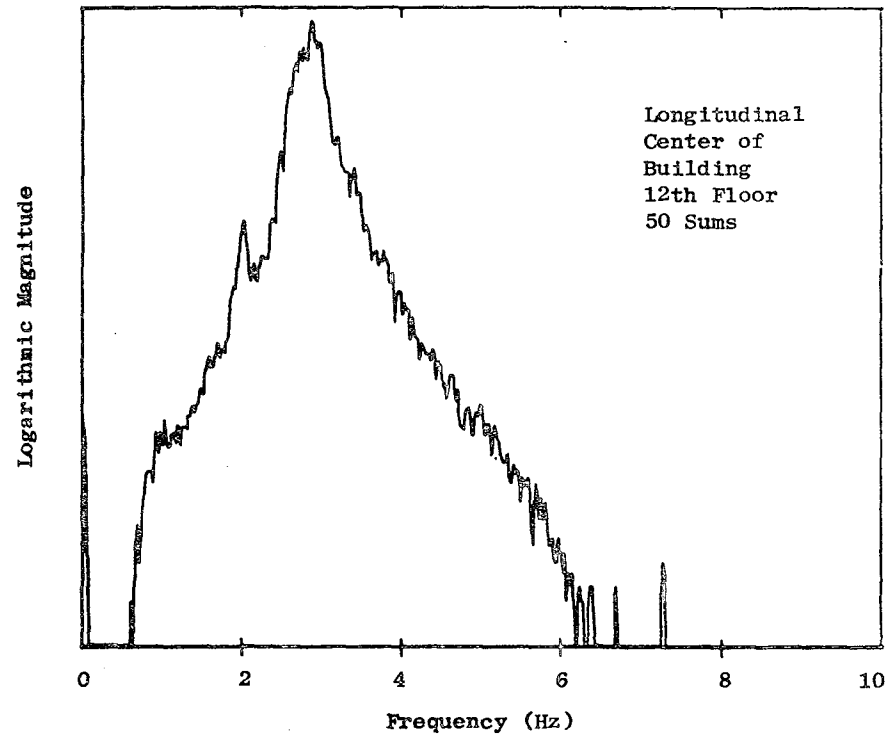

Fig. A.12. POWER SPECTRAL DENSITY PLOT, BLACKWELDER BUILDING.

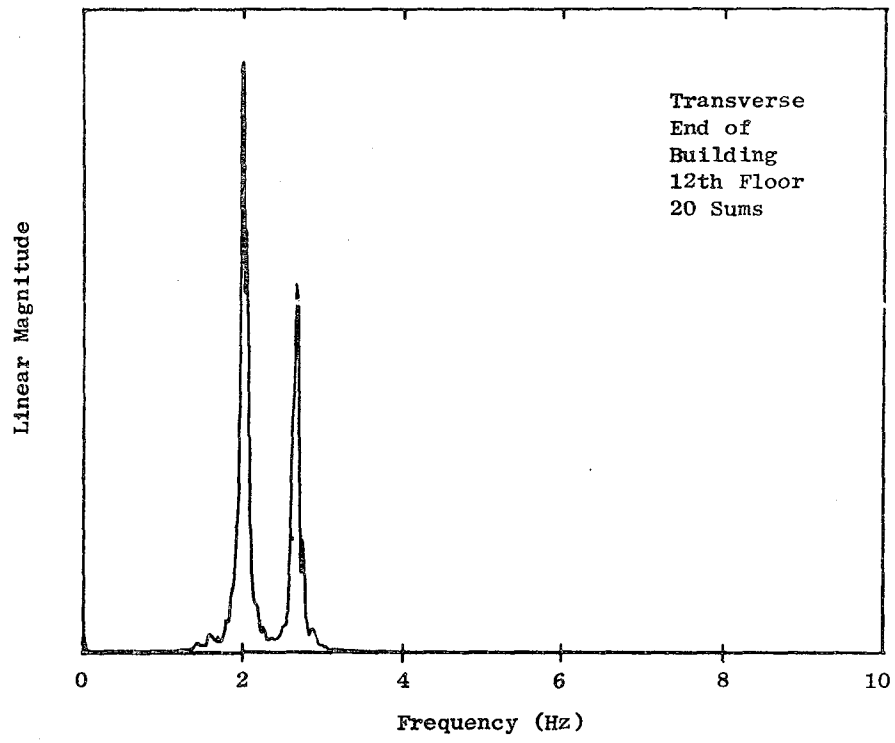

Fig. A.13. POWER SPECTRAL DENSITY PLOT, BLACKWELDER BUILDING.

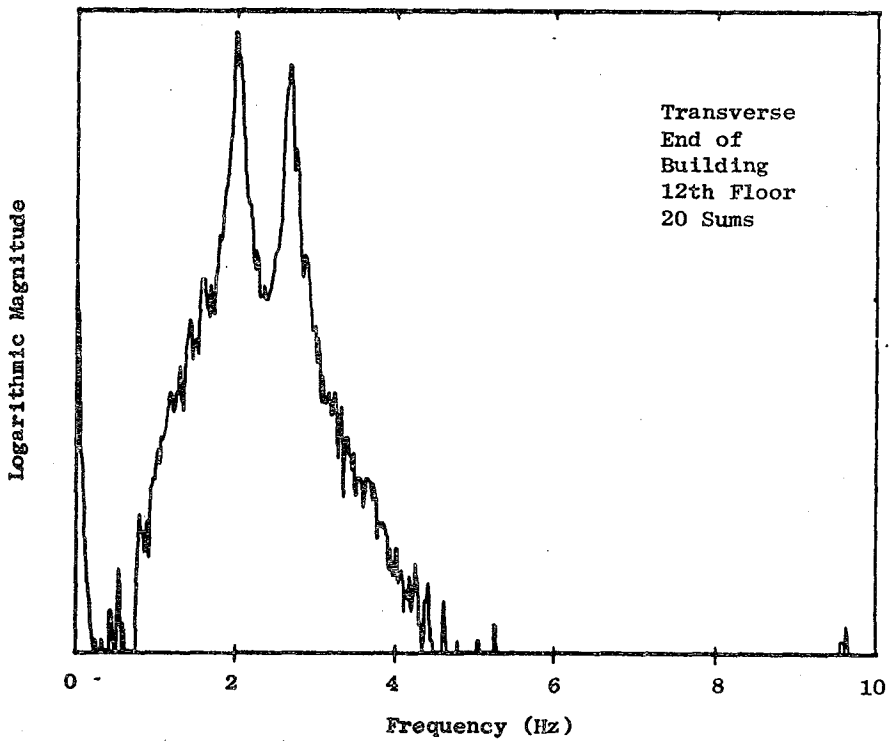

Fig. A.14. POWER SPECTRAL DENSITY PLOT, BLACKWELDER BUILDING.

Appendix B

POWER SPECTRAL DENSITY PLOTS FOR THE QUILLEN BUILDING AND A SUMMARY OF THE RESULTS

Table B.1

SUMMARY OF THE PREDOMINANT ENERGY TRANSFER POINTS FOR THE QUILLEN BUILDING

Figure	Accelerometer Orientation			Number of Spectrums Averaged	Natural Frequencies (Hz)		Other Points (Hz)
	Direction	Position in Building	Floor Level		1st	2nd	
B.1 B.2	transverse	center	12th	100	1.9	9.0	15.1
B.3 B.4	transverse	center	12th	200	1.9	9.0	15.1
B.5 B.6	longitudinal	center	12th	150	2.7	11.0	26.0
B.7 B.8	transverse	end	12th	75	1.9 2.5	8.8 9.7	15.0 17.9 22.8
B.9 B.10	transverse	end	12th	150	1.9 2.6	8.8 9.7	15.0 17.6 22.7
B.11 B.12	longitudinal	center	12th	50	2.74	---	---
B.13 B.14	transverse	end	12th	20	1.93 2.58	---	---

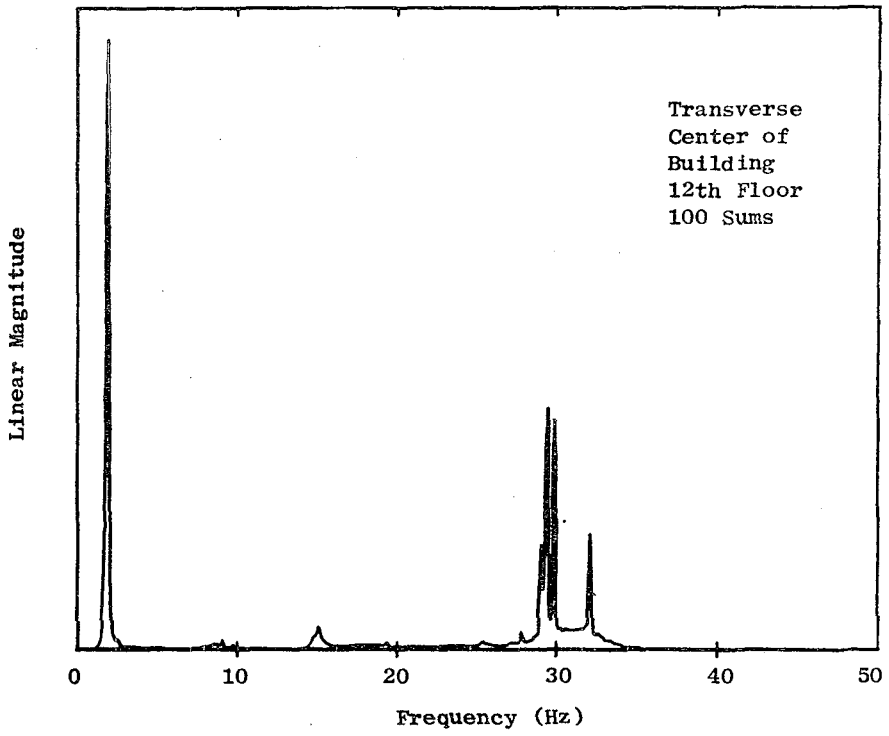

Fig. B.1. POWER SPECTRAL DENSITY PLOT, QUILLEN BUILDING.

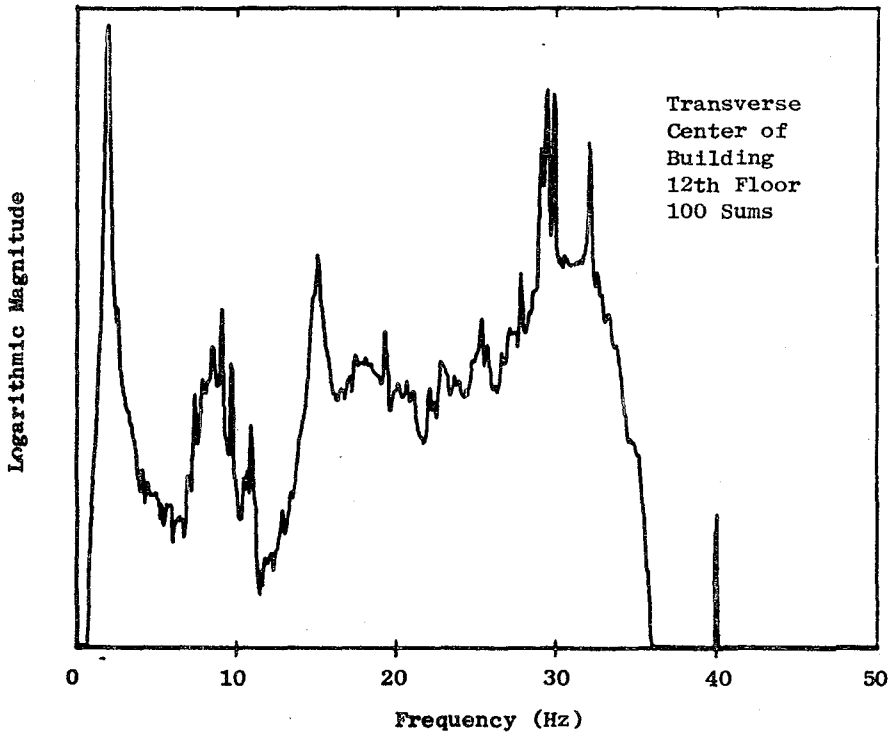

Fig. B.2. POWER SPECTRAL DENSITY PLOT, QUILLEN BUILDING.

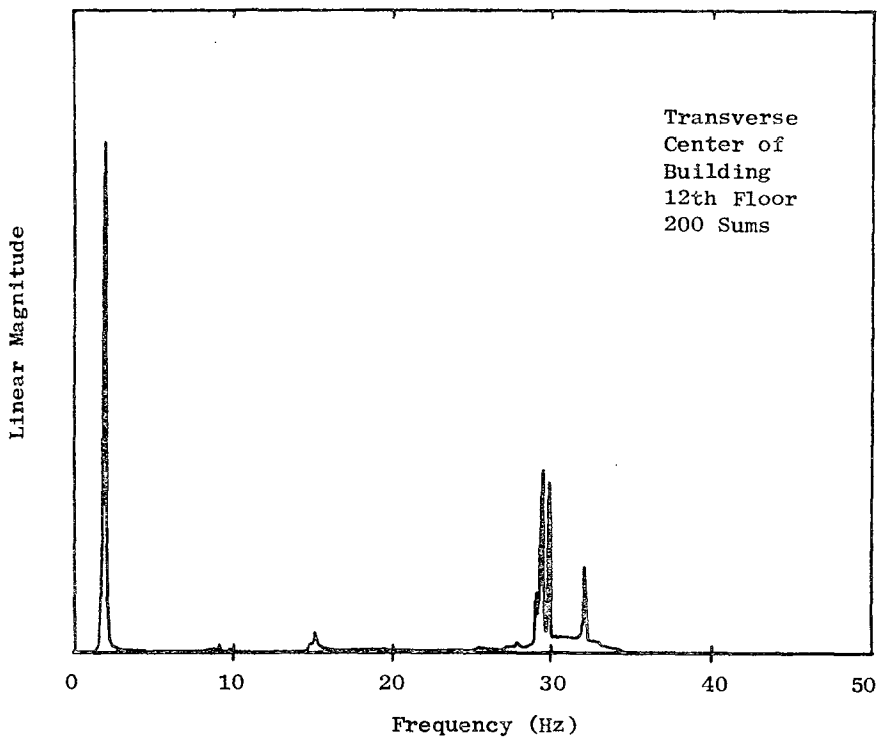

Fig. B.3. POWER SPECTRAL DENSITY PLOT, QUILLEN BUILDING.

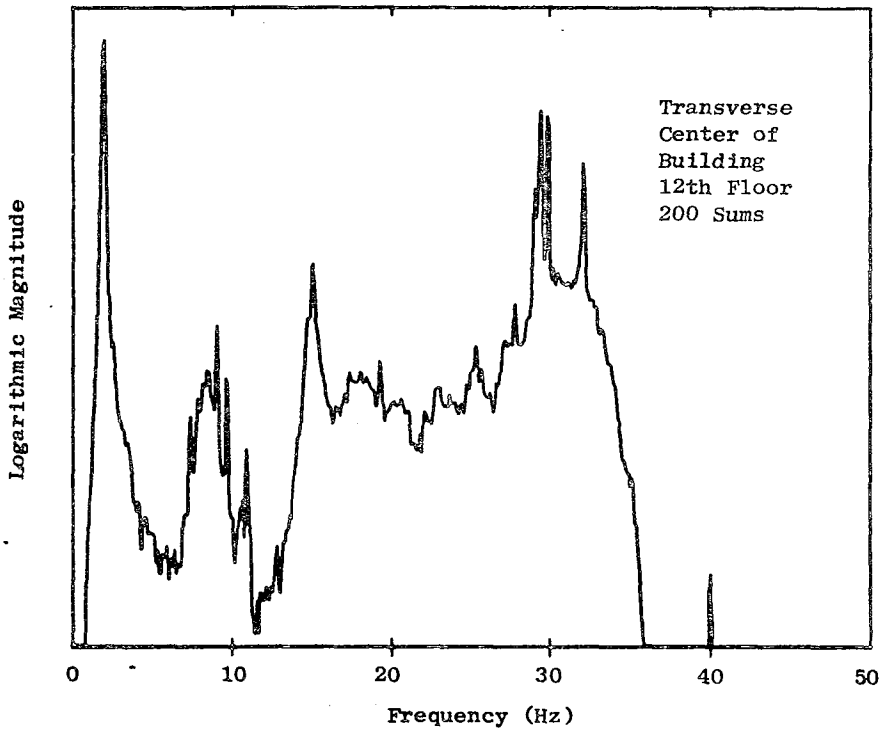

Fig. B.4. POWER SPECTRAL DENSITY PLOT, QUILLEN BUILDING.

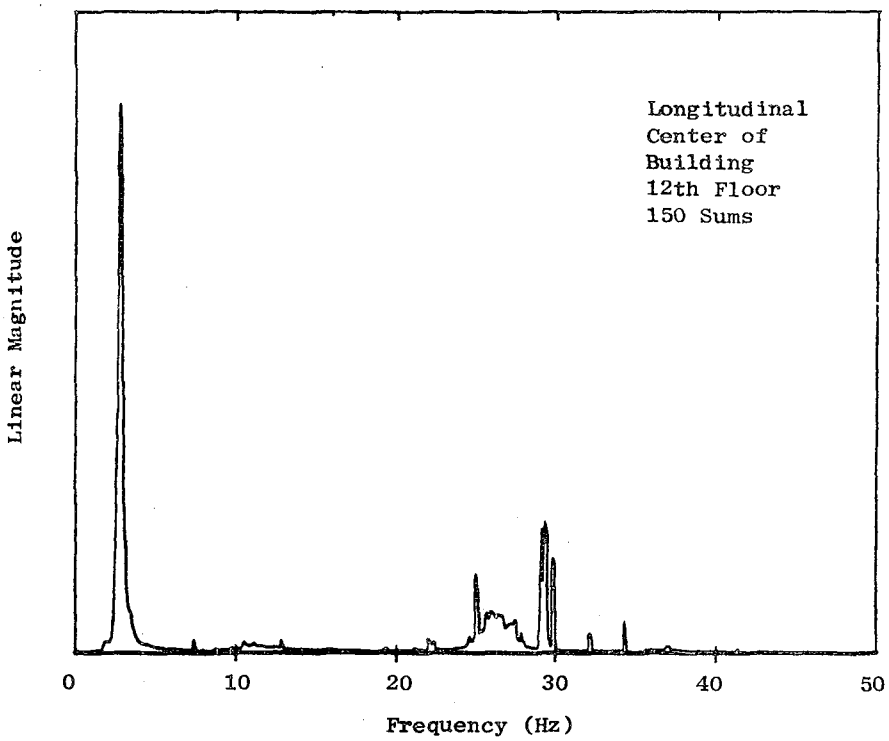

Fig. B.5. POWER SPECTRAL DENSITY PLOT, QUILLEN BUILDING.

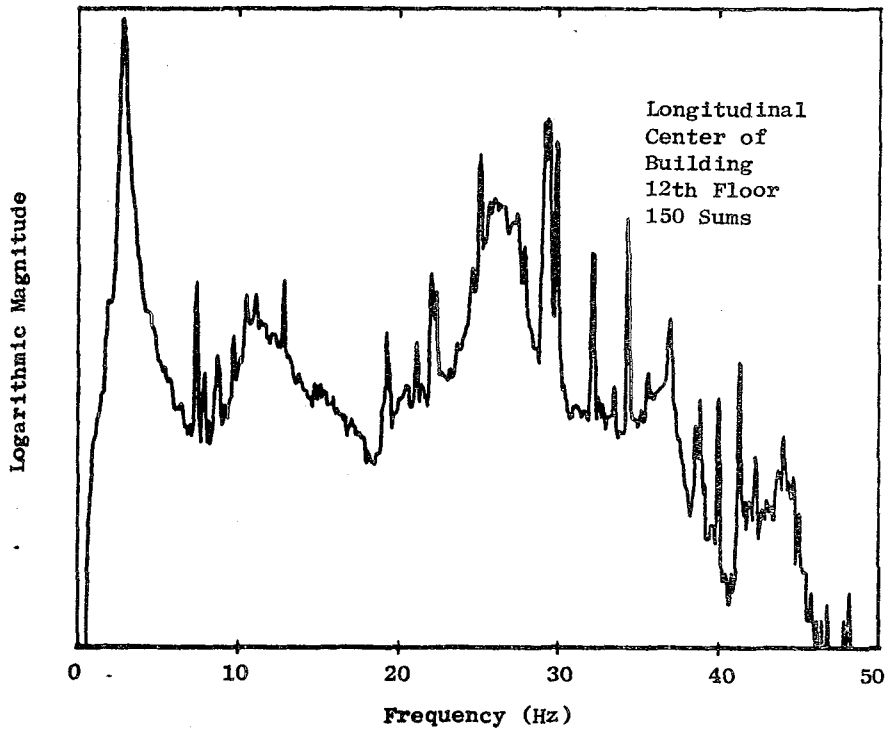

Fig. B.6. POWER SPECTRAL DENSITY PLOT, QUILLEN BUILDING.

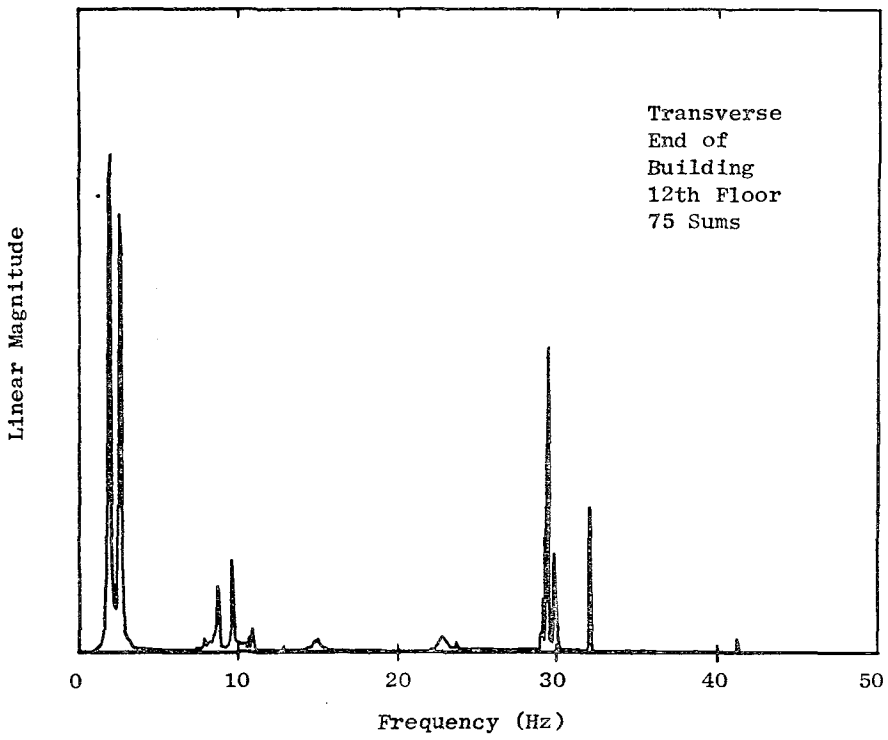

Fig. B.7. POWER SPECTRAL DENSITY PLOT, QUILLEN BUILDING.

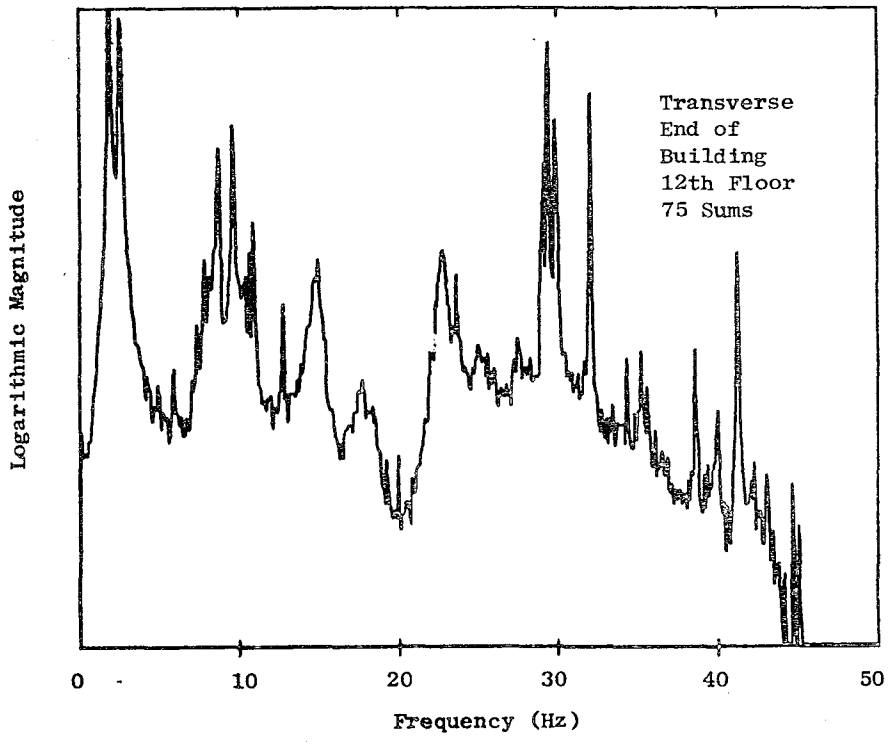

Fig. B.8. POWER SPECTRAL DENSITY PLOT, QUILLEN BUILDING.

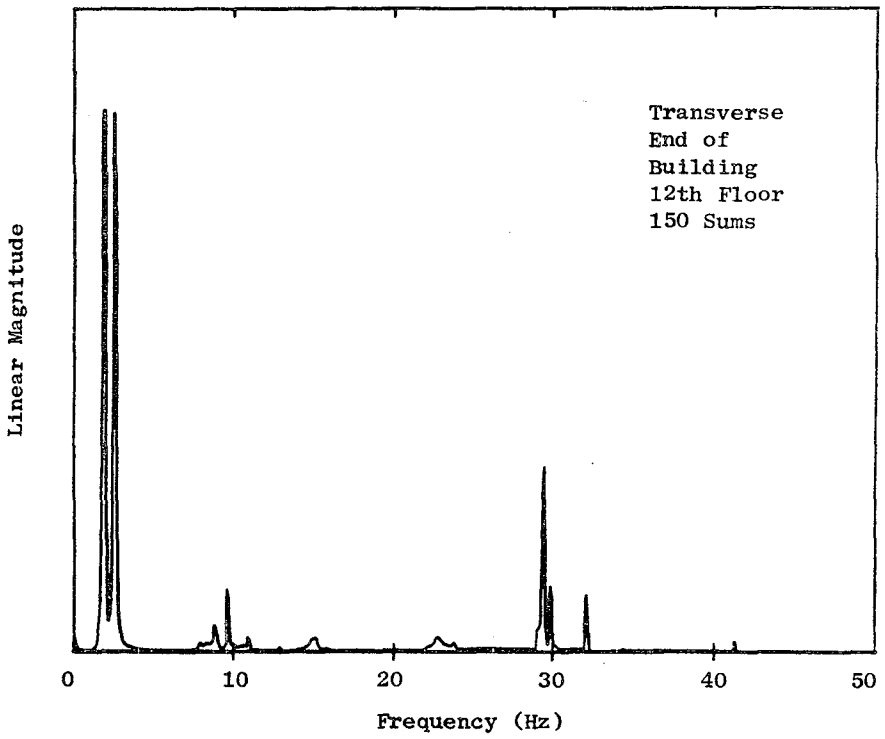

Fig. B.9. POWER SPECTRAL DENSITY PLOT, QUILLEN BUILDING.

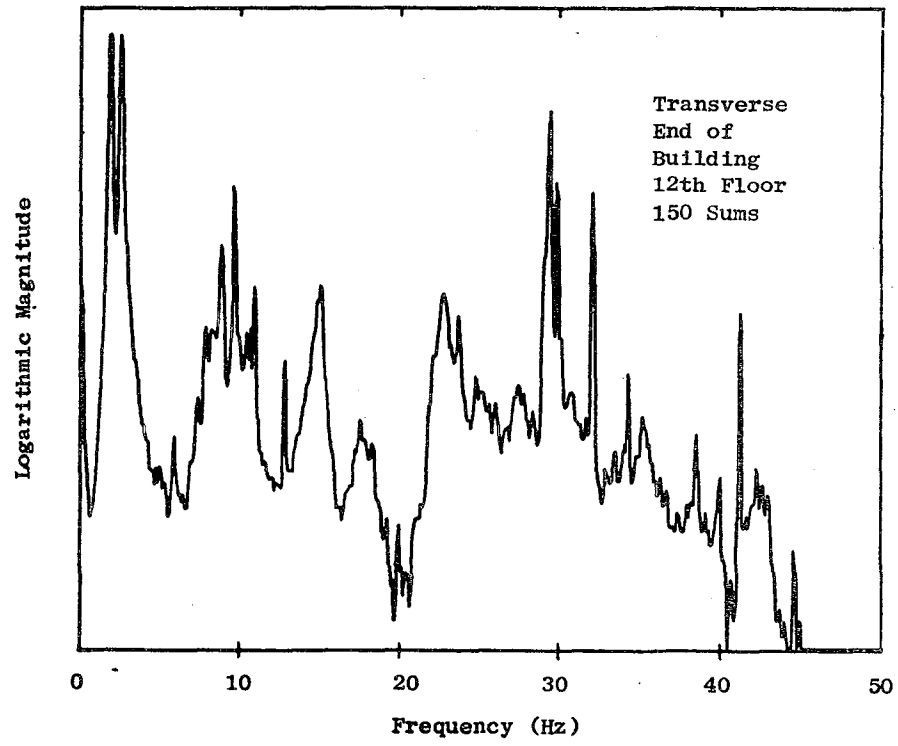

Fig. B.10. POWER SPECTRAL DENSITY PLOT, QUILLEN BUILDING.

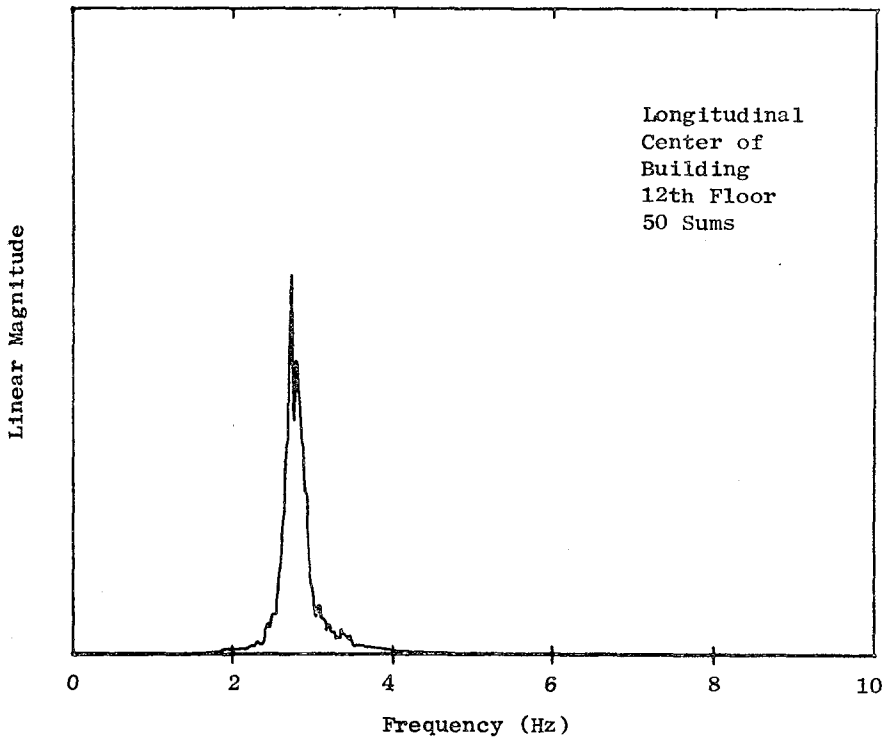

Fig. B.11. POWER SPECTRAL DENSITY PLOT, QUILLEN BUILDING.

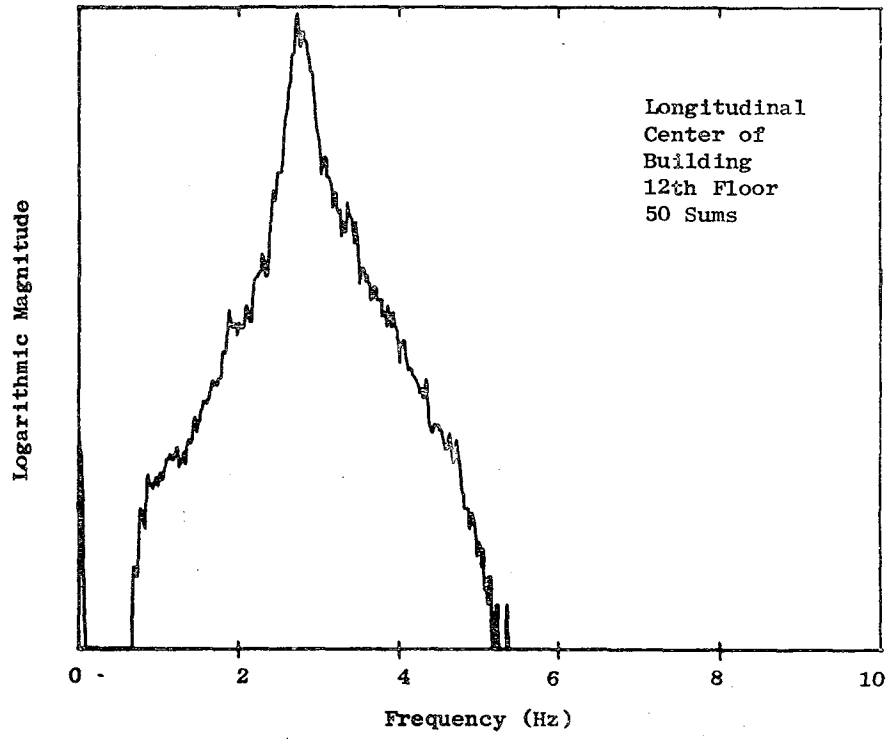

Fig. B.12. POWER SPECTRAL DENSITY PLOT, QUILLEN BUILDING.

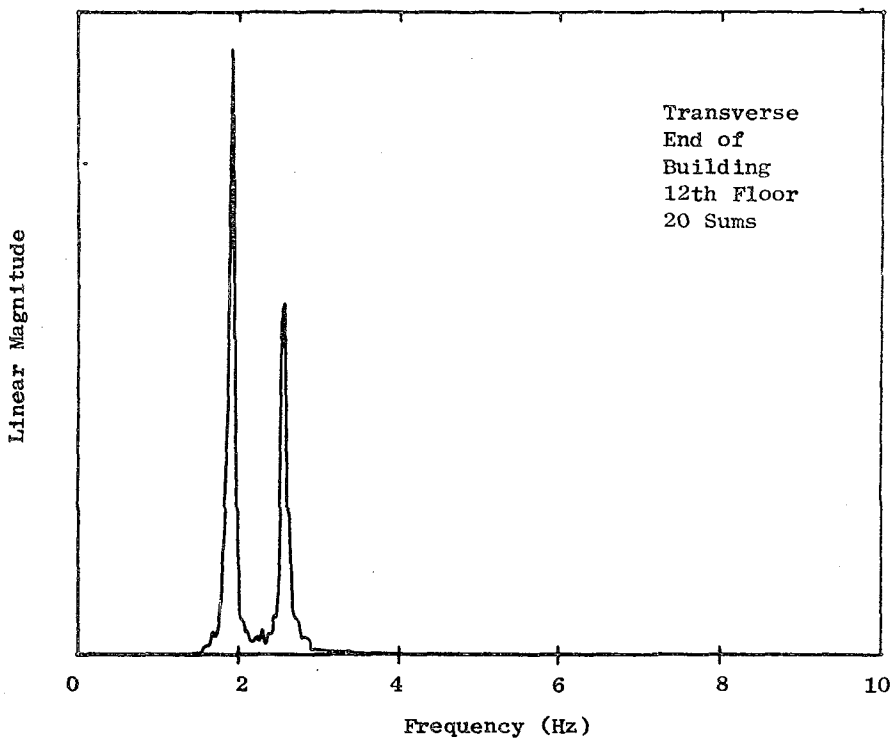

Fig. B.13. POWER SPECTRAL DENSITY PLOT, QUILLEN BUILDING.

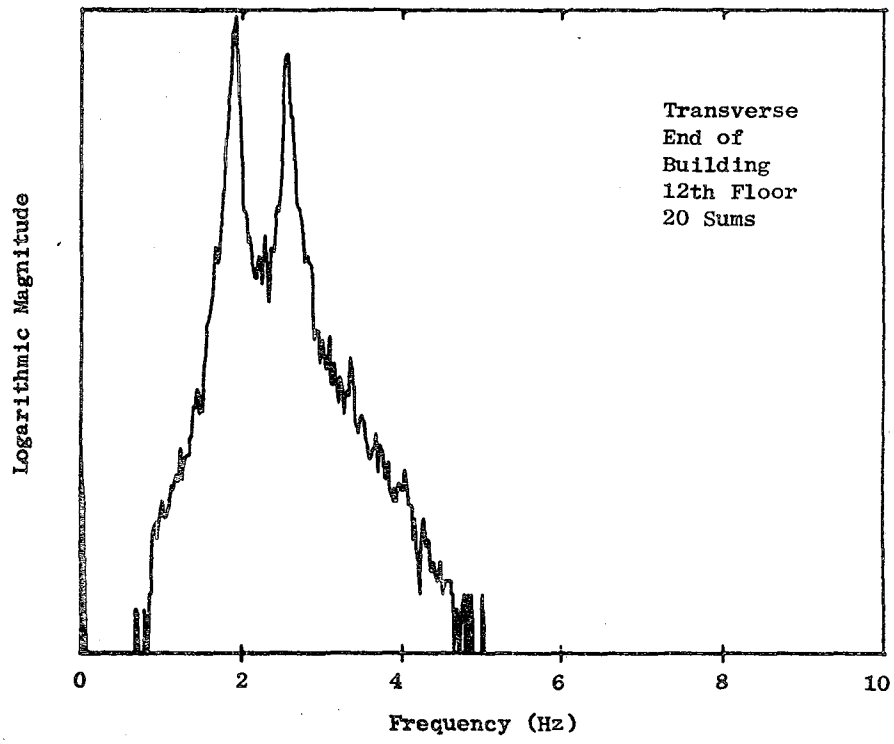

Fig. B.14. POWER SPECTRAL DENSITY PLOT, QUILLEN BUILDING.

Appendix C

POWER SPECTRAL DENSITY PLOTS FOR THE McFARLAND BUILDING AND A SUMMARY OF THE RESULTS

Table C.1

SUMMARY OF THE PREDOMINANT ENERGY TRANSFER POINTS FOR THE McFARLAND BUILDING

Figure	Accelerometer Orientation			Number of Spectrums Averaged	Natural Frequencies (Hz)		Other Points (Hz)	Percent of Critical Damping (1st mode)
	Direction	Position in Building	Floor Level		1st	2nd		
C.1 C.2	transverse	center	8th	100	2.6	9.8	20.2 29.5	---
C.3 C.4	longitudinal	center	8th	200	2.6	10.3	14.0 17.9 29.3	---
C.5 C.6	transverse	end	8th	200	2.6 3.8		18.1 20.3 29.3 29.7	---
C.7 C.8	transverse	center	8th	30	2.60	---	---	1.8
C.9 C.10	longitudinal	center	8th	30	2.54	---	---	1.8
C.11 C.12	transverse	end	8th	30	2.64 3.83	---	---	2.9 1.6

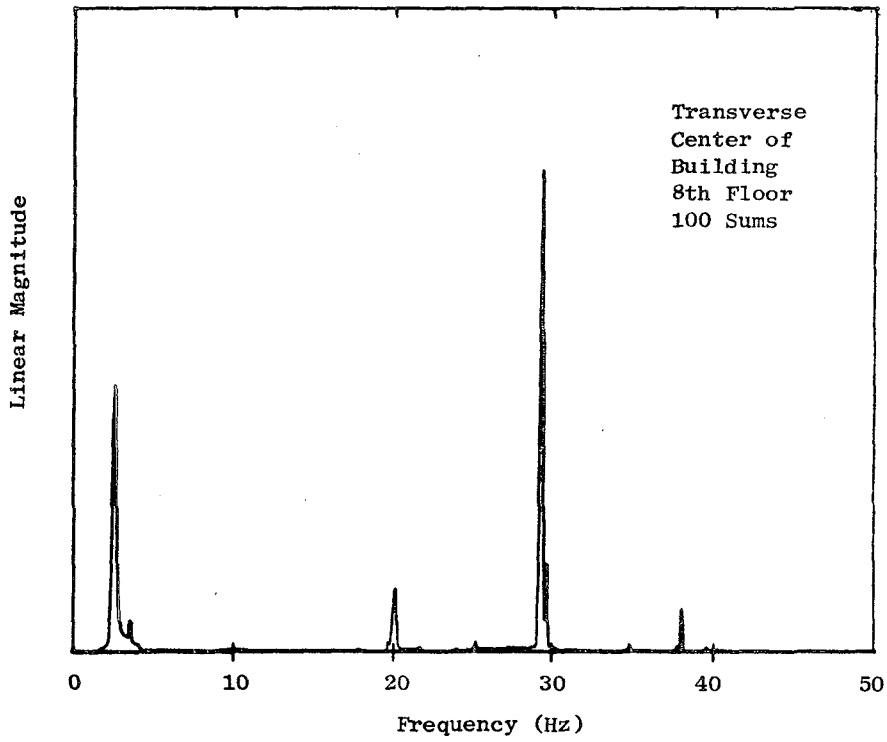

Fig. C.1. POWER SPECTRAL DENSITY PLOT, McFARLAND BUILDING.

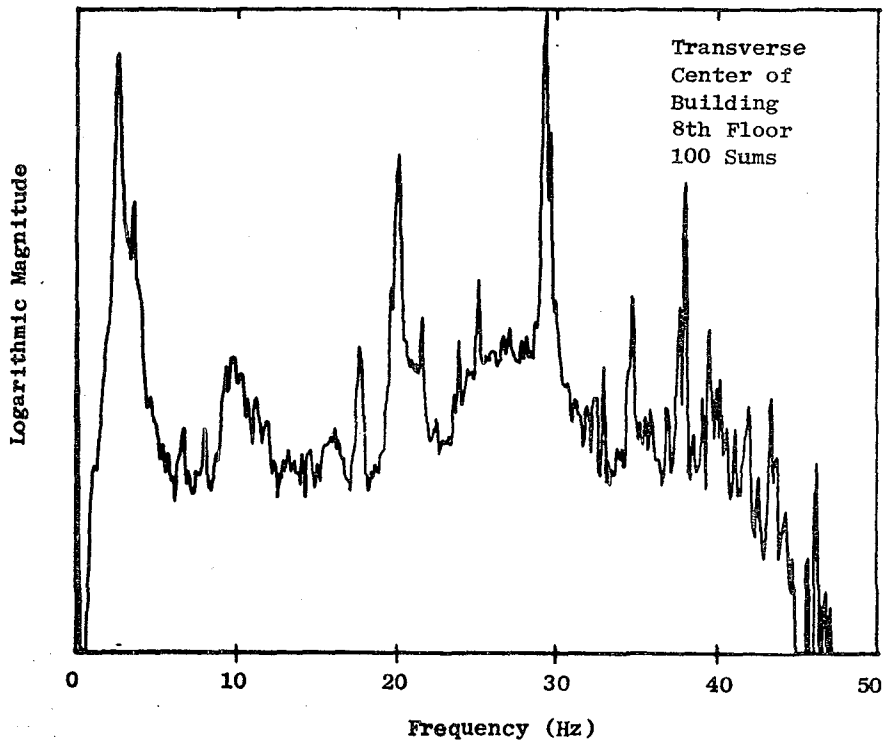

Fig. C.2. POWER SPECTRAL DENSITY PLOT, McFARLAND BUILDING.

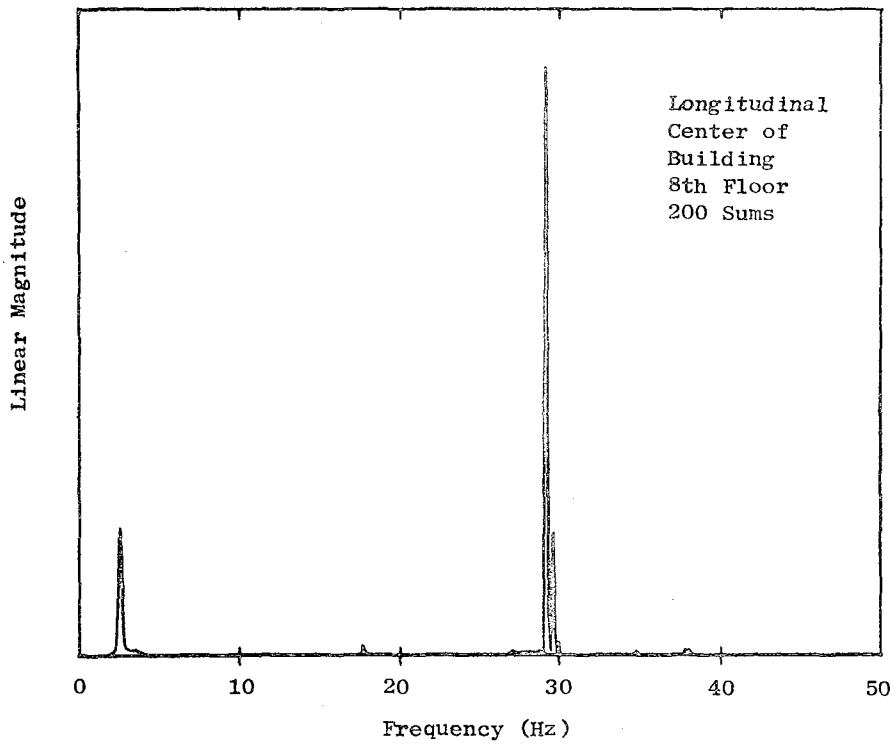

Fig. C.3. POWER SPECTRAL DENSITY PLOT, McFARLAND BUILDING.

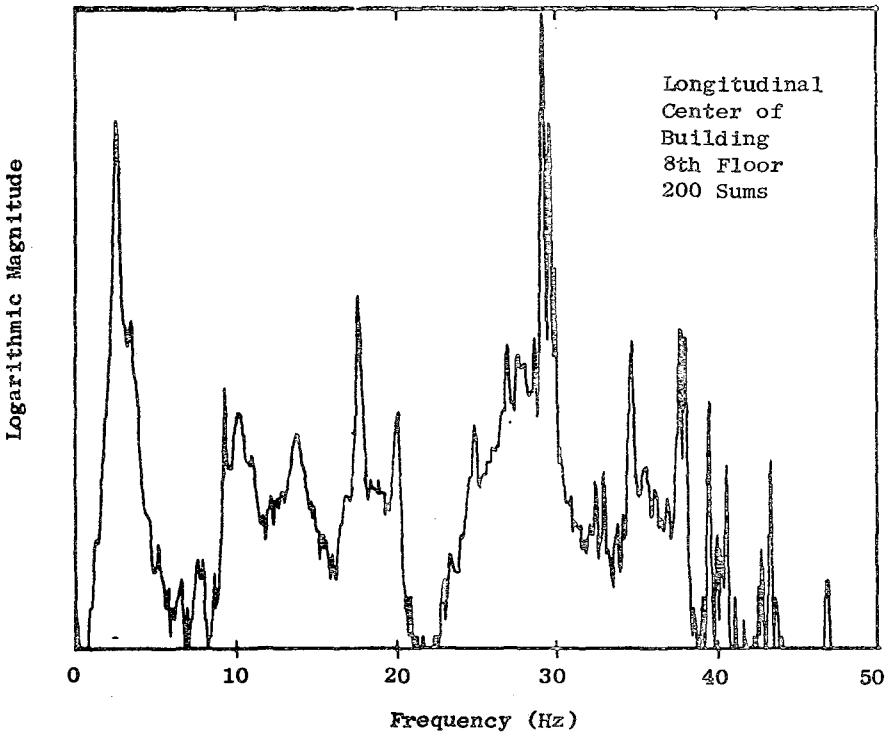

Fig. C.4. POWER SPECTRAL DENSITY PLOT, McFARLAND BUILDING.

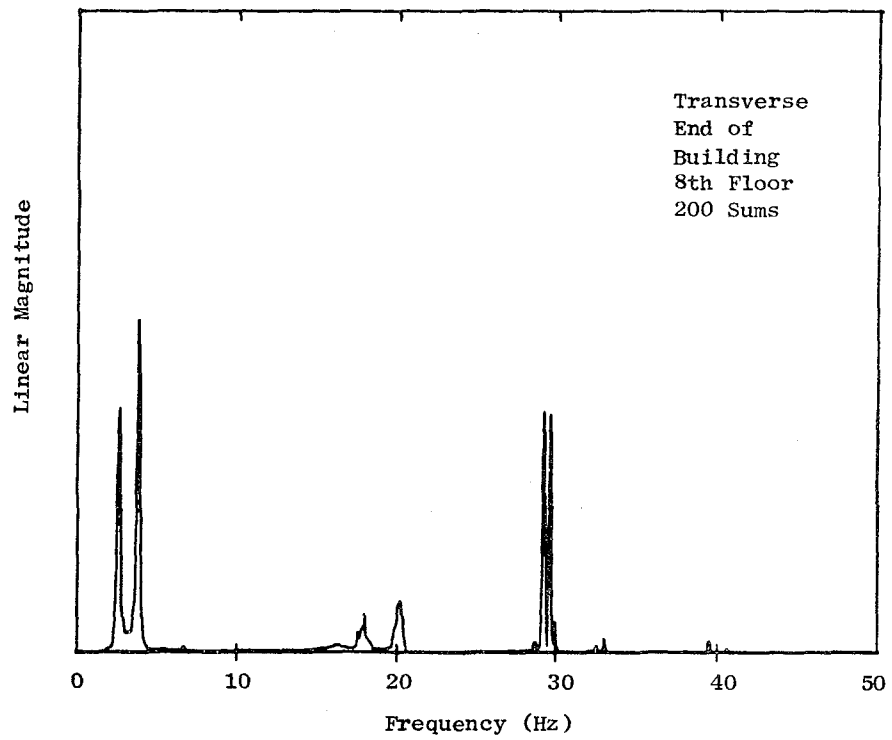

Fig. C.5. POWER SPECTRAL DENSITY PLOT, McFARLAND BUILDING.

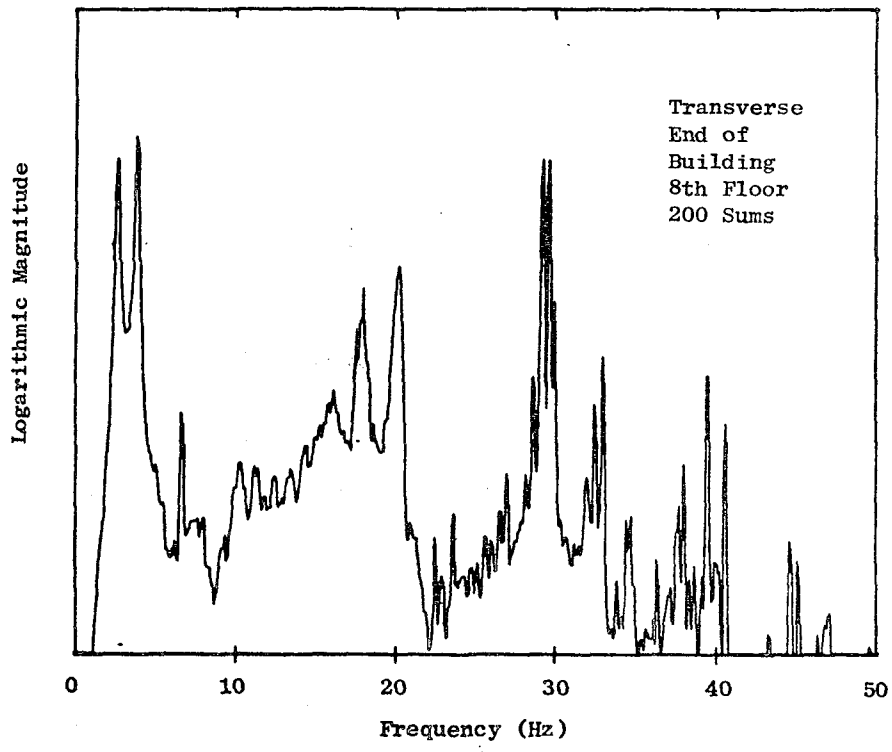

Fig. C.6. POWER SPECTRAL DENSITY PLOT, McFARLAND BUILDING.

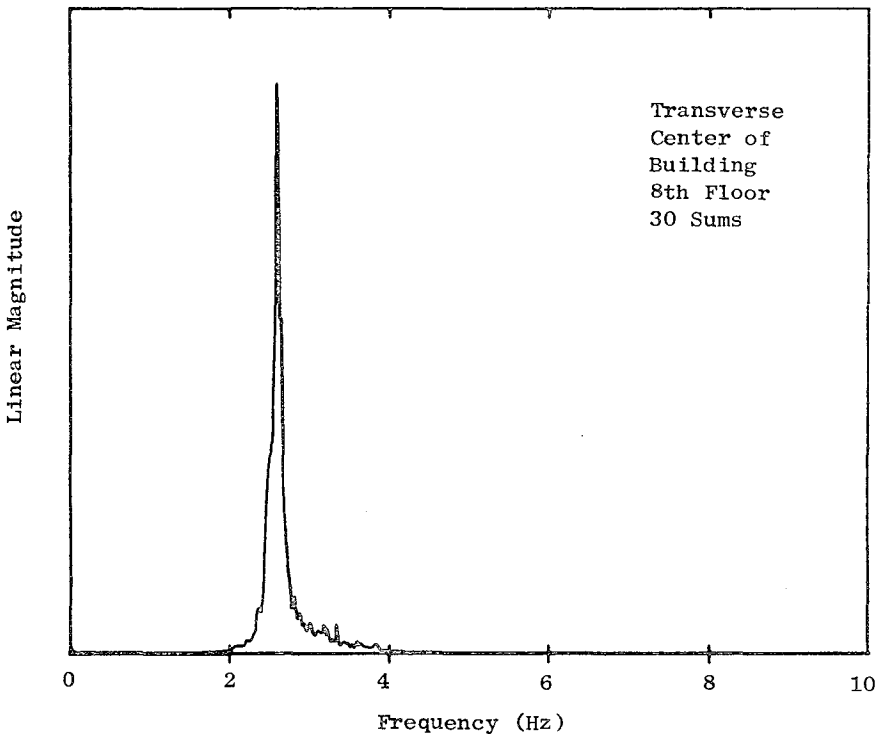

Fig. C.7. POWER SPECTRAL DENSITY PLOT, McFARLAND BUILDING.

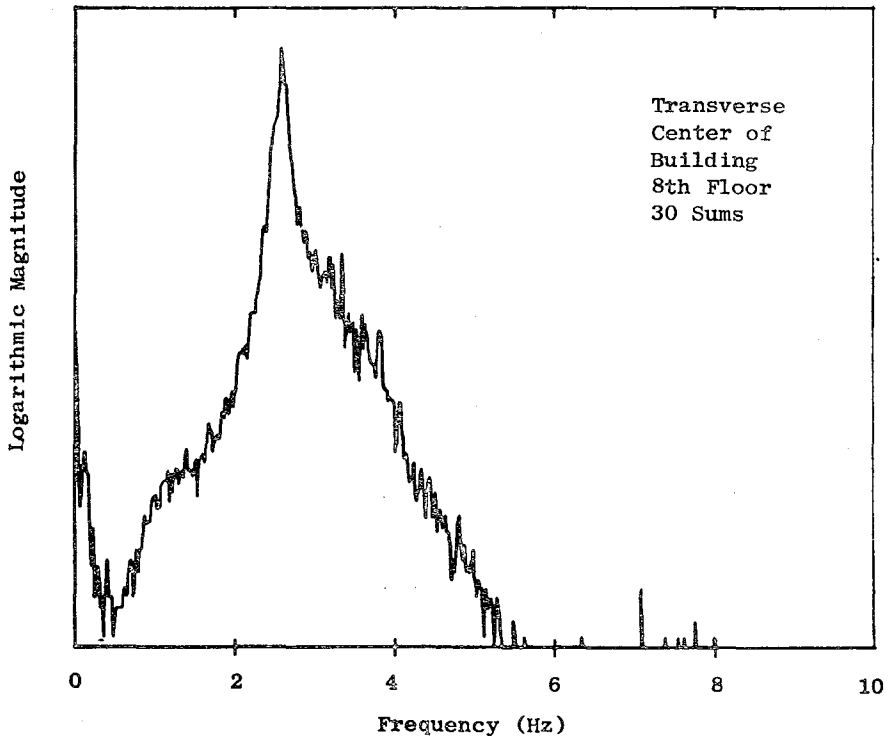

Fig. C.8. POWER SPECTRAL DENSITY PLOT, McFARLAND BUILDING.

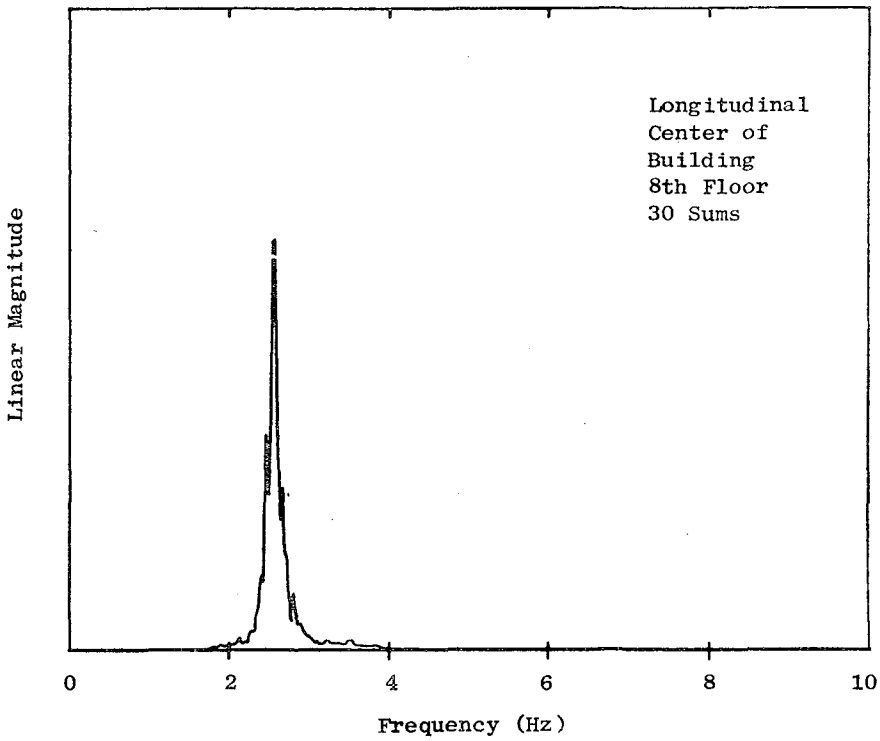

Fig. C.9. POWER SPECTRAL DENSITY PLOT, McFARLAND BUILDING.

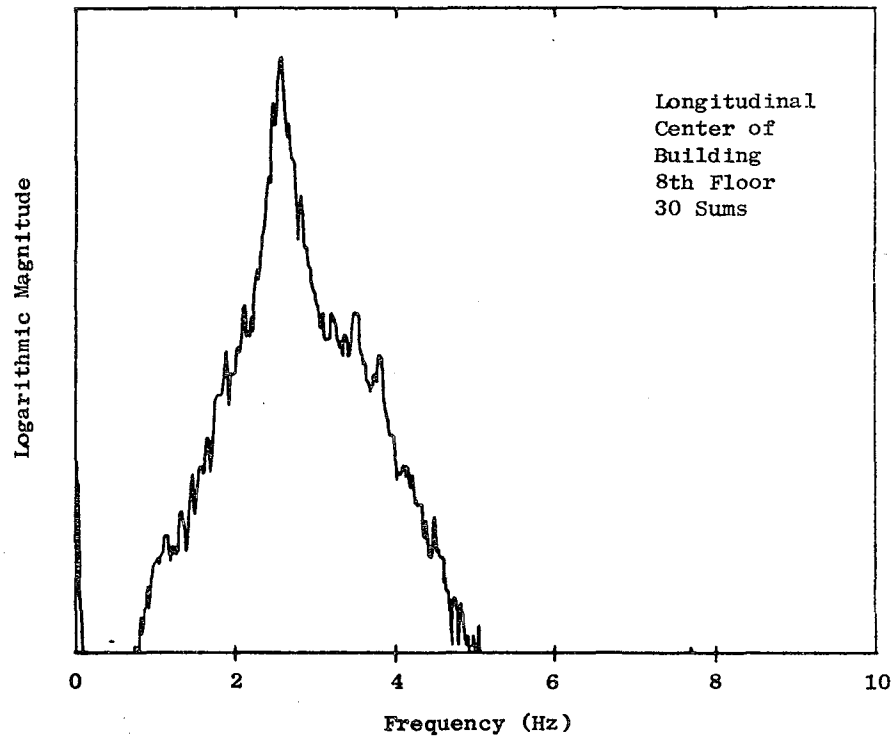

Fig. C.10. POWER SPECTRAL DENSITY PLOT, McFARLAND BUILDING.

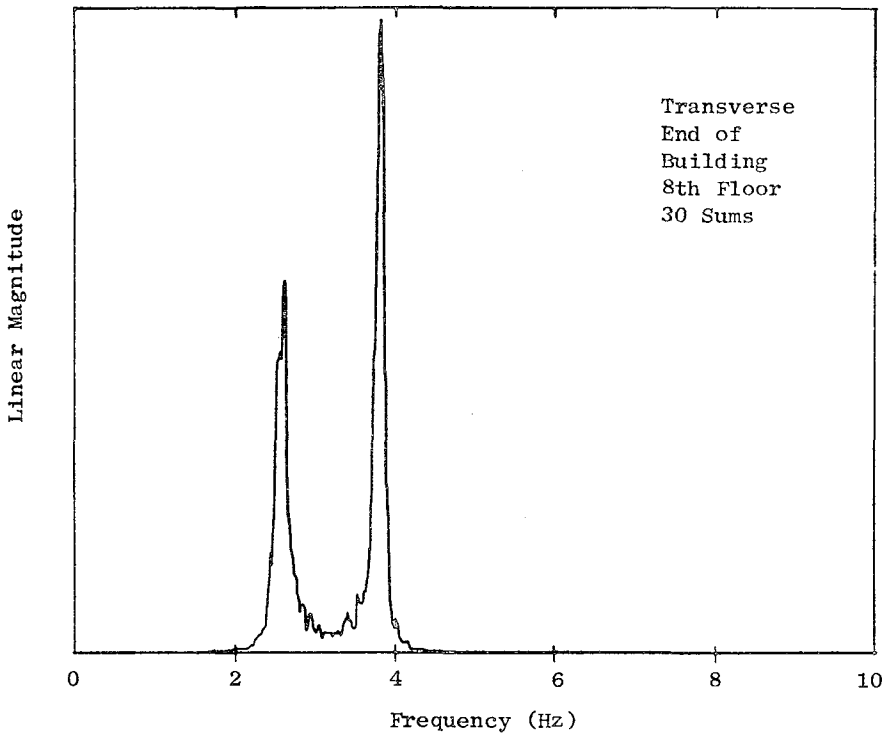

Fig. C.11. POWER SPECTRAL DENSITY PLOT, McFARLAND BUILDING.

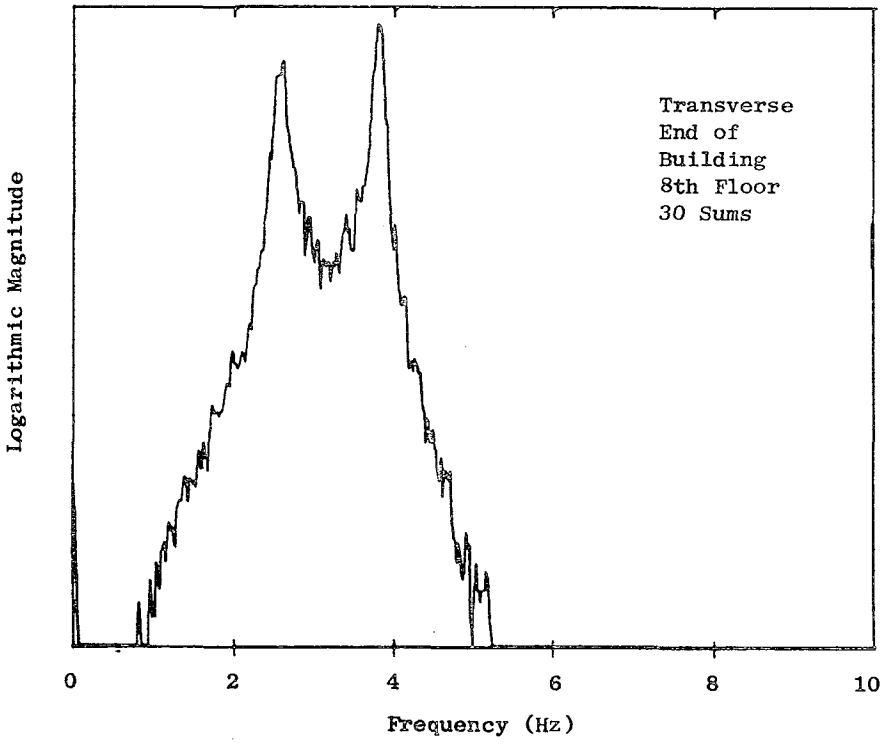

Fig. C.12. POWER SPECTRAL DENSITY PLOT, McFARLAND BUILDING.

Appendix D

POWER SPECTRAL DENSITY PLOTS FOR THE HOSKINS BUILDING AND A SUMMARY OF THE RESULTS

Table D.1

SUMMARY OF THE PREDOMINANT ENERGY TRANSFER POINTS FOR THE HOSKINS BUILDING

Figure	Accelerometer Orientation			Number of Spectrums Averaged	Natural Frequencies (Hz)		Other Points (Hz)	Percent of Critical Damping (1st mode)
	Direction	Position in Building	Floor Level		1st	2nd		
D.1 D.2	transverse	center	8th	200	2.6		17.5 20.0 29.3	---
D.3 D.4	longitudinal	center	8th	100	2.6		17.7 29.3	---
D.5 D.6	transverse	end	8th	200	2.6 3.8		7.9 17.4 29.3	---
D.7 D.8	transverse	center	8th	30	2.58	---	---	3.4
D.9 D.10	longitudinal	center	8th	30	2.54	---	---	1.9
D.11 D.12	transverse	end	8th	30	2.62 2.85	---	---	2.3 1.9

Preceding page blank

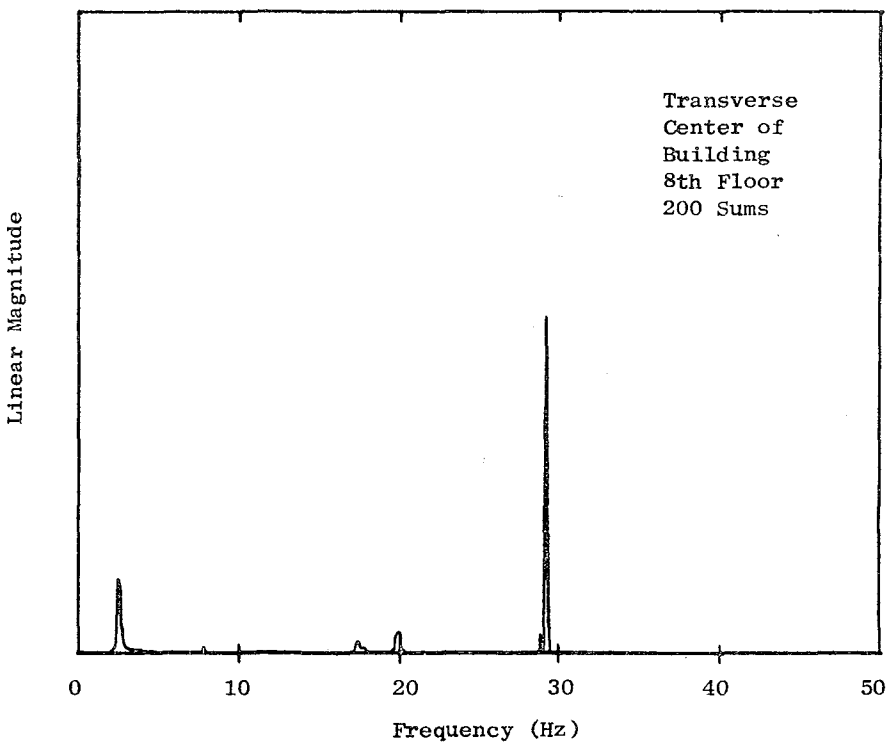

Fig. D.1. POWER SPECTRAL DENSITY PLOT, HOSKINS BUILDING.

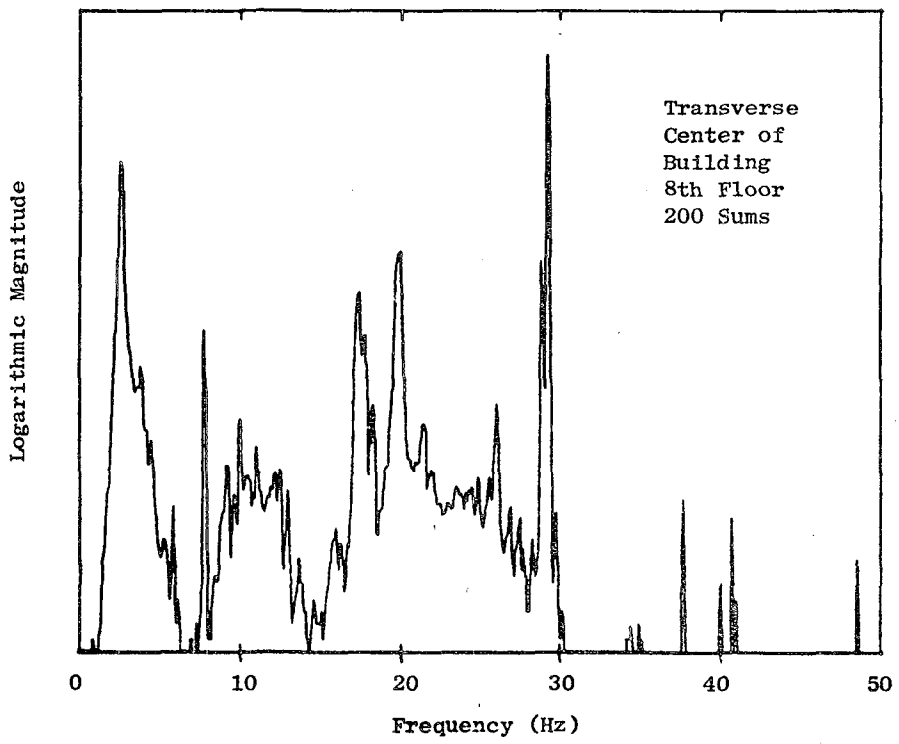

Fig. D.2. POWER SPECTRAL DENSITY PLOT, HOSKINS BUILDING.

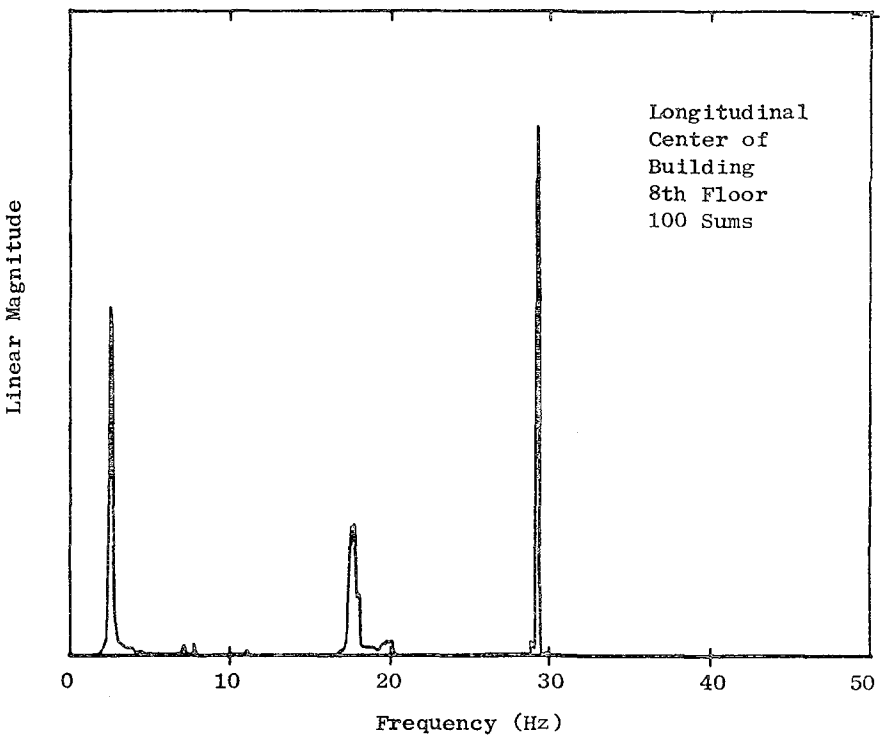

Fig. D.3. POWER SPECTRAL DENSITY PLOT, HOSKINS BUILDING.

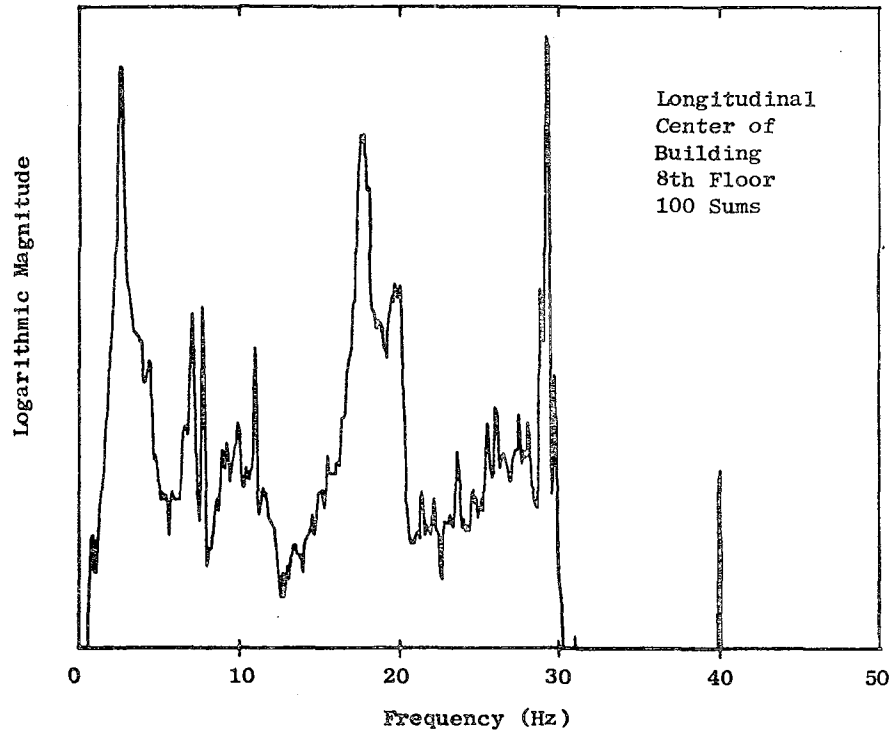

Fig. D.4. POWER SPECTRAL DENSITY PLOT, HOSKINS BUILDING.

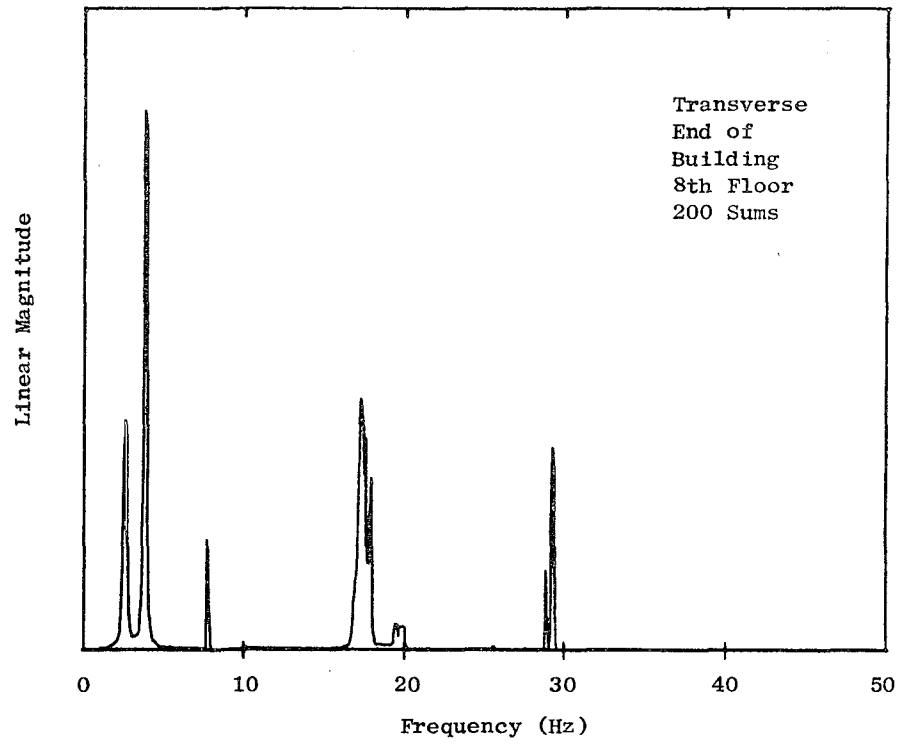

Fig. D.5. POWER SPECTRAL DENSITY PLOT, HOSKINS BUILDING.

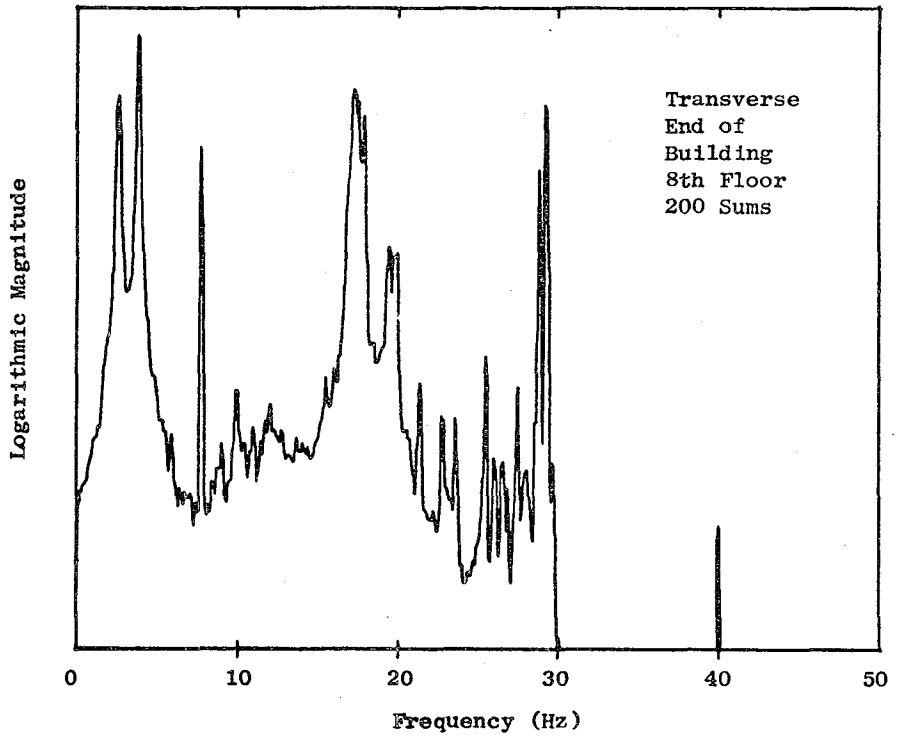

Fig. D.6. POWER SPECTRAL DENSITY PLOT, HOSKINS BUILDING.

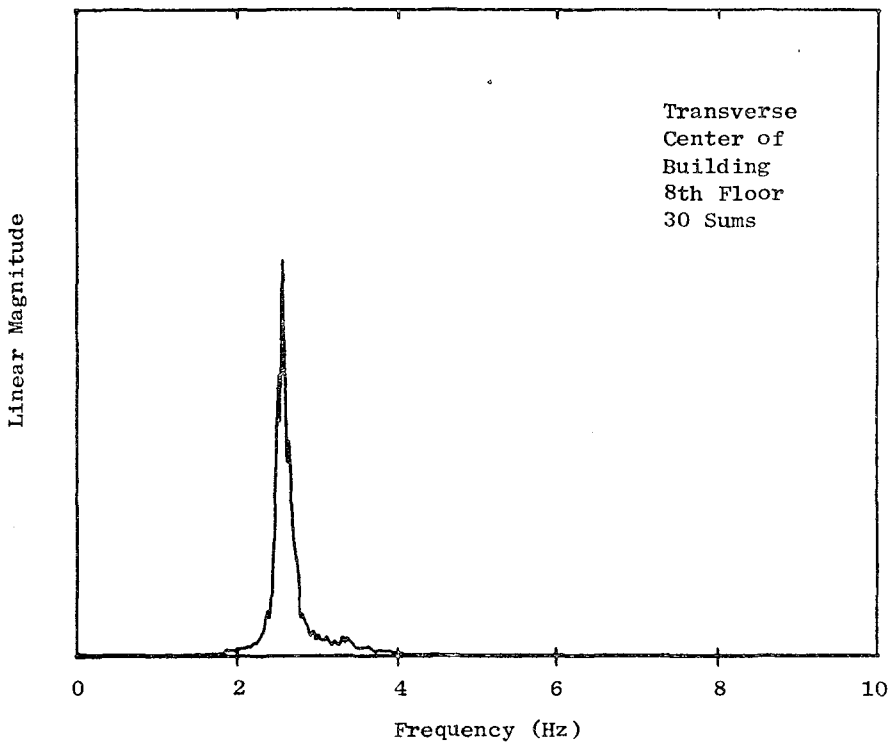

Fig. D.7. POWER SPECTRAL DENSITY PLOT, HOSKINS BUILDING.

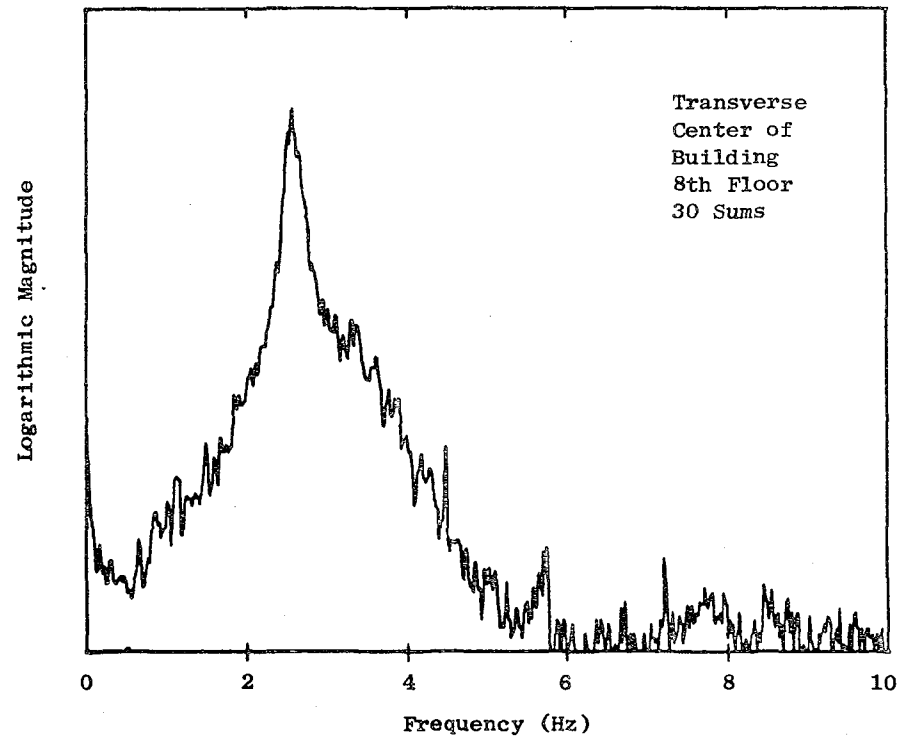

Fig. D.8. POWER SPECTRAL DENSITY PLOT, HOSKINS BUILDING.

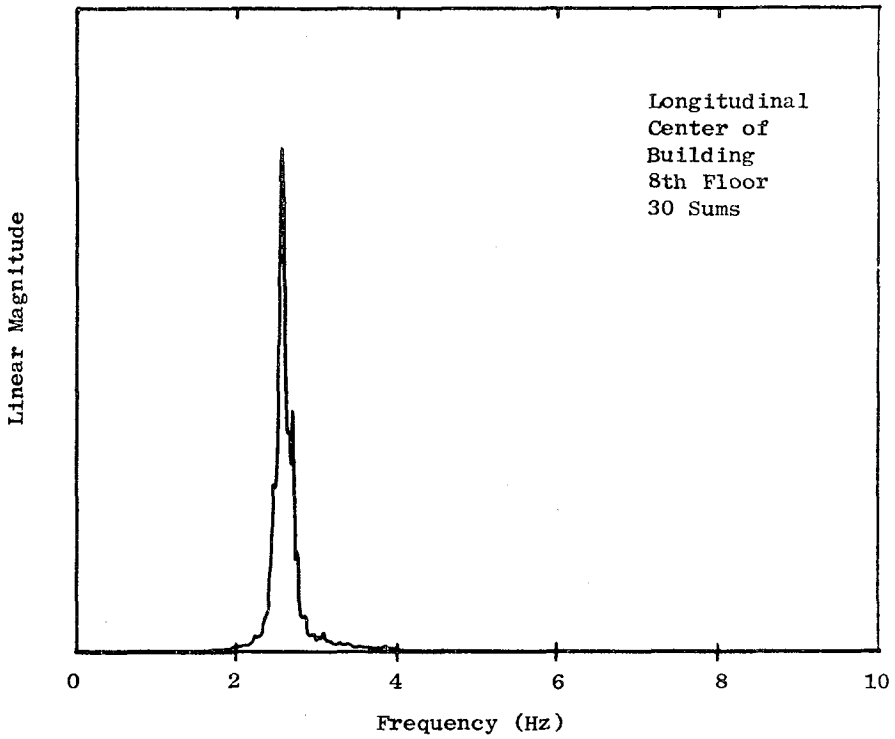

Fig. D.9. POWER SPECTRAL DENSITY PLOT, HOSKINS BUILDING.

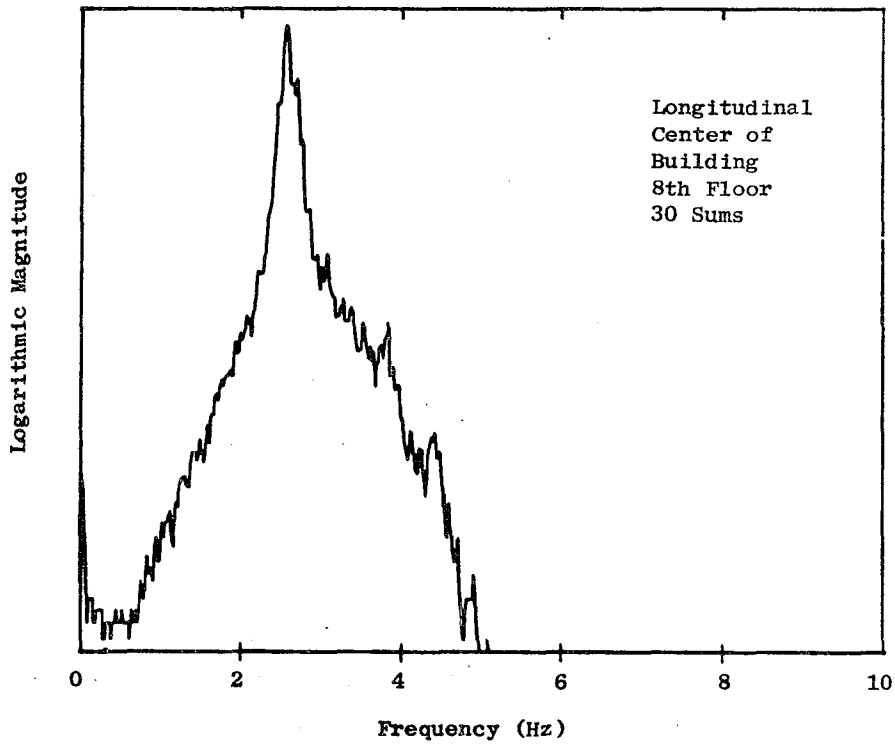

Fig. D.10. POWER SPECTRAL DENSITY PLOT, HOSKINS BUILDING.

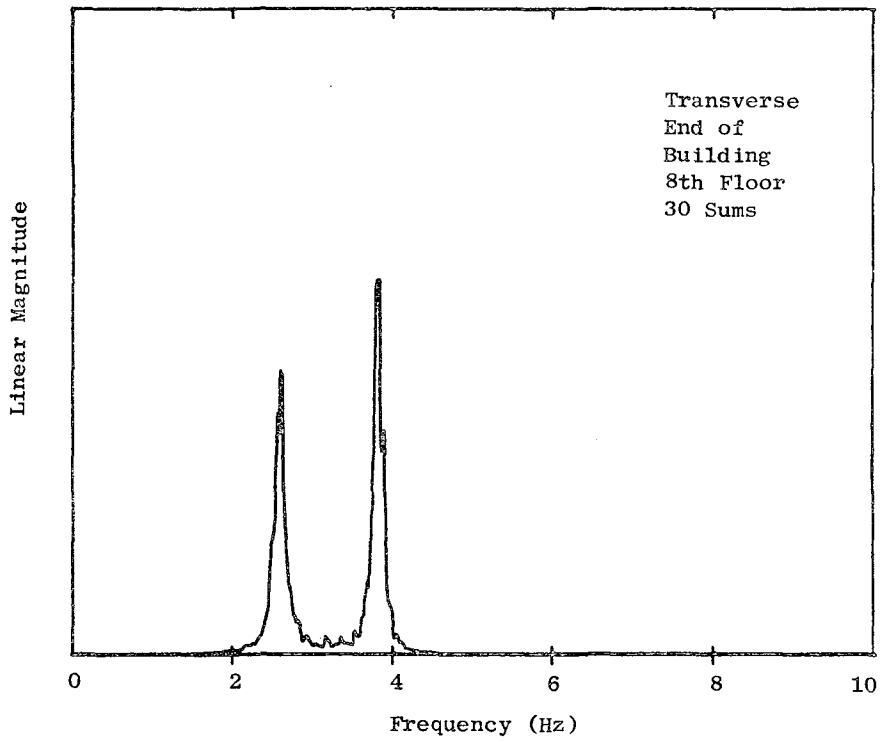

Fig. D.11. POWER SPECTRAL DENSITY PLOT, HOSKINS BUILDING.

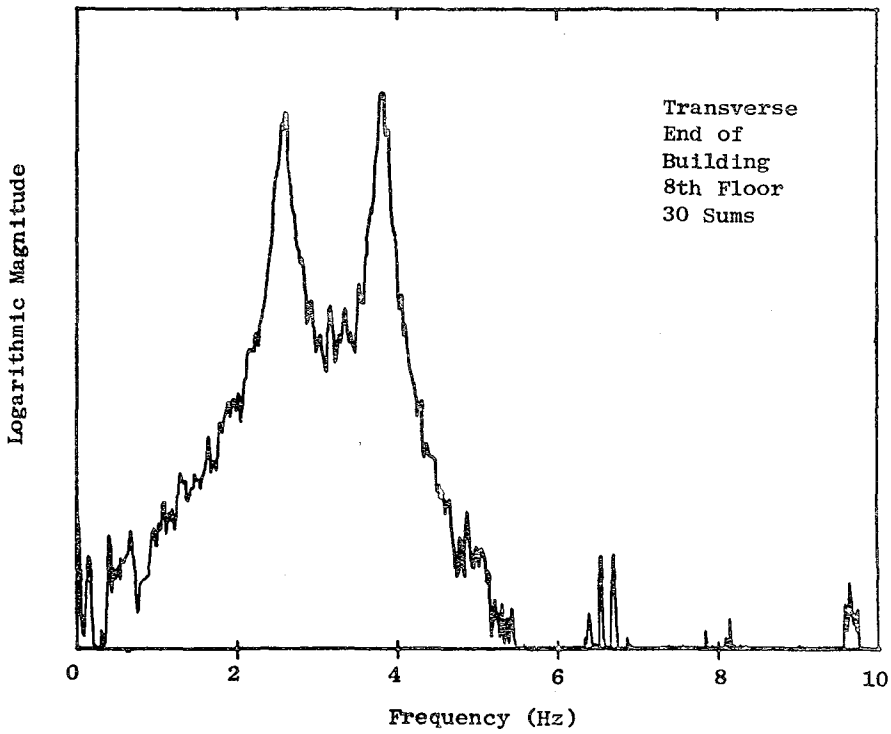

Fig. D.12. POWER SPECTRAL DENSITY PLOT, HOSKINS BUILDING.

Intentionally Blank

Appendix E

POWER SPECTRAL DENSITY PLOTS FOR THE HULME BUILDING AND A SUMMARY OF THE RESULTS

Table E.1

SUMMARY OF THE PREDOMINANT ENERGY TRANSFER POINTS FOR THE HULME BUILDING

Figure	Accelerometer Orientation			Number of Spectrums Averaged	Natural Frequencies (Hz)		Other Points (Hz)	Percent of Critical Damping (1st mode)
	Direction	Position in Building	Floor Level		1st	2nd		
E.1 E.2	transverse	center	8th	250	2.7		10.8 29.4 29.7	---
E.3 E.4	longitudinal	center	8th	250	2.6		10.8 14.0 29.4	---
E.5 E.6	transverse	end	8th	250	2.7 3.7		14.0 29.6	---
E.7 E.8	transverse	center	8th	50	2.72	---	---	2.9
E.9 E.10	longitudinal	center	8th	25	2.60	---	---	2.0
E.11 E.12	transverse	end	8th	40	2.66 3.69	---	---	2.7 1.7

Preceding page blank

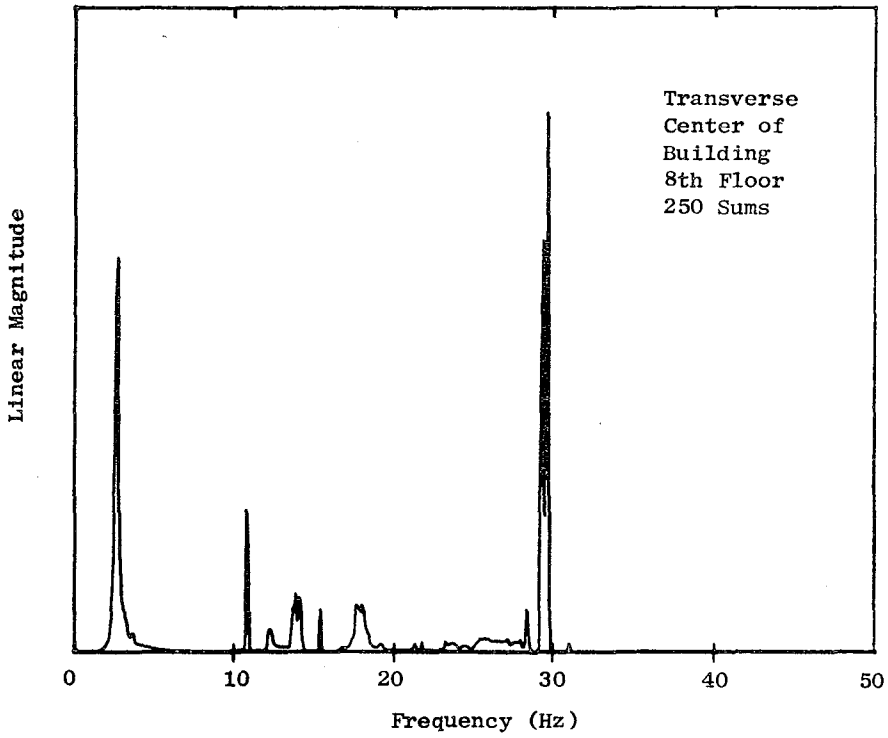

Fig. E.1. POWER SPECTRAL DENSITY PLOT, HULME BUILDING.

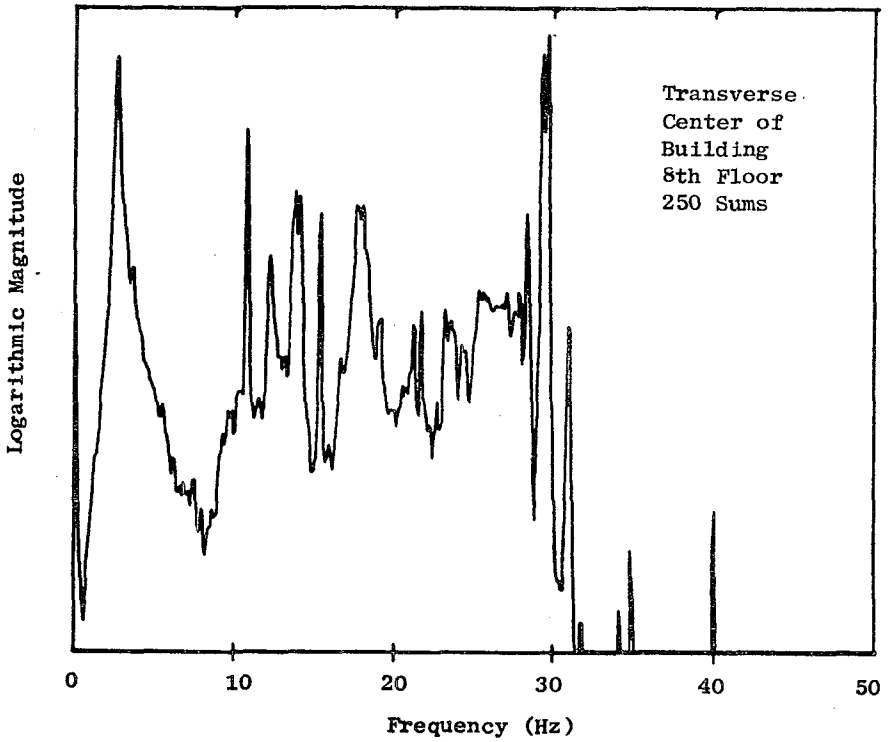

Fig. E.2. POWER SPECTRAL DENSITY PLOT, HULME BUILDING.

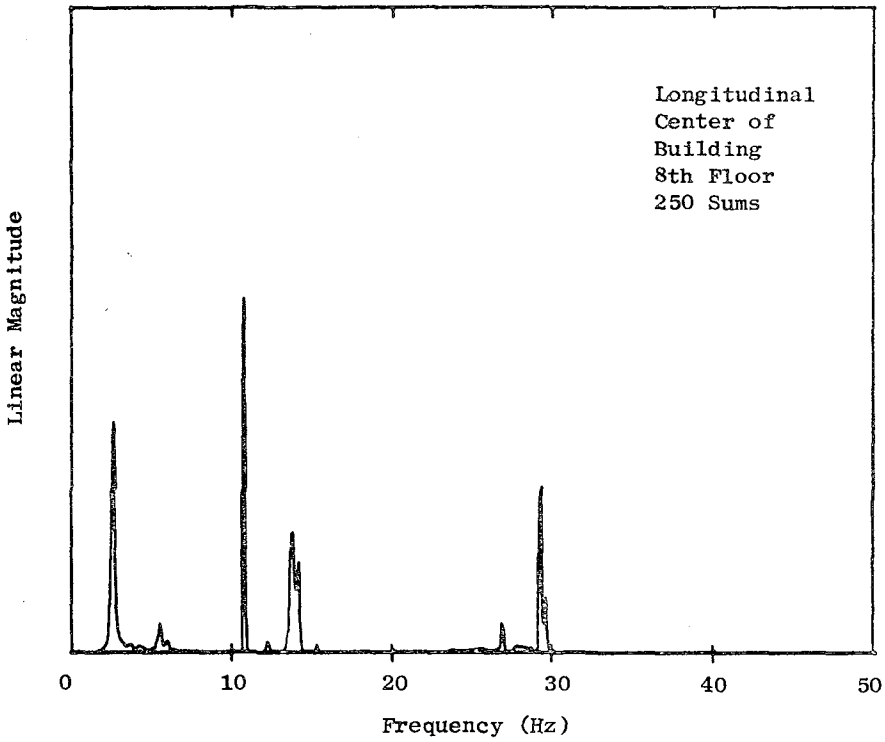

Fig. E.3. POWER SPECTRAL DENSITY PLOT, HULME BUILDING.

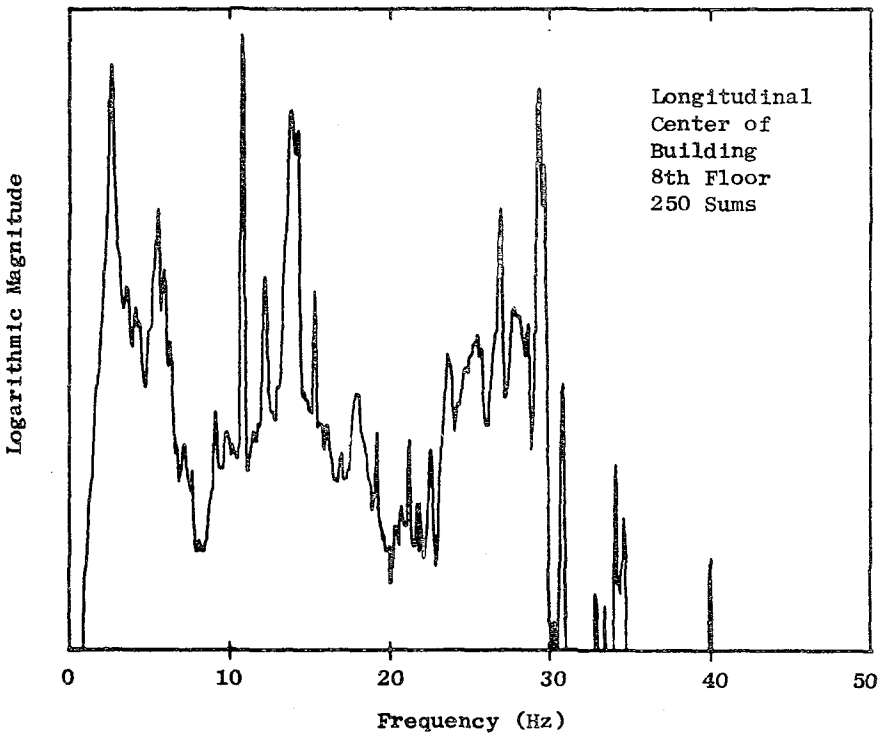

Fig. E.4. POWER SPECTRAL DENSITY PLOT, HULME BUILDING.

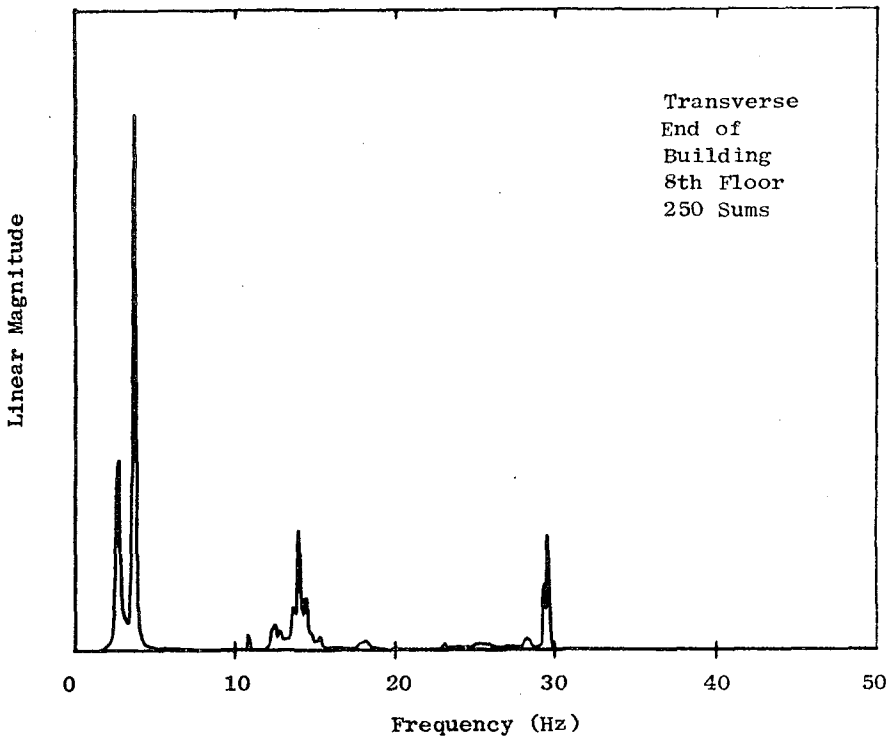

Fig. E.5. POWER SPECTRAL DENSITY PLOT, HULME BUILDING.

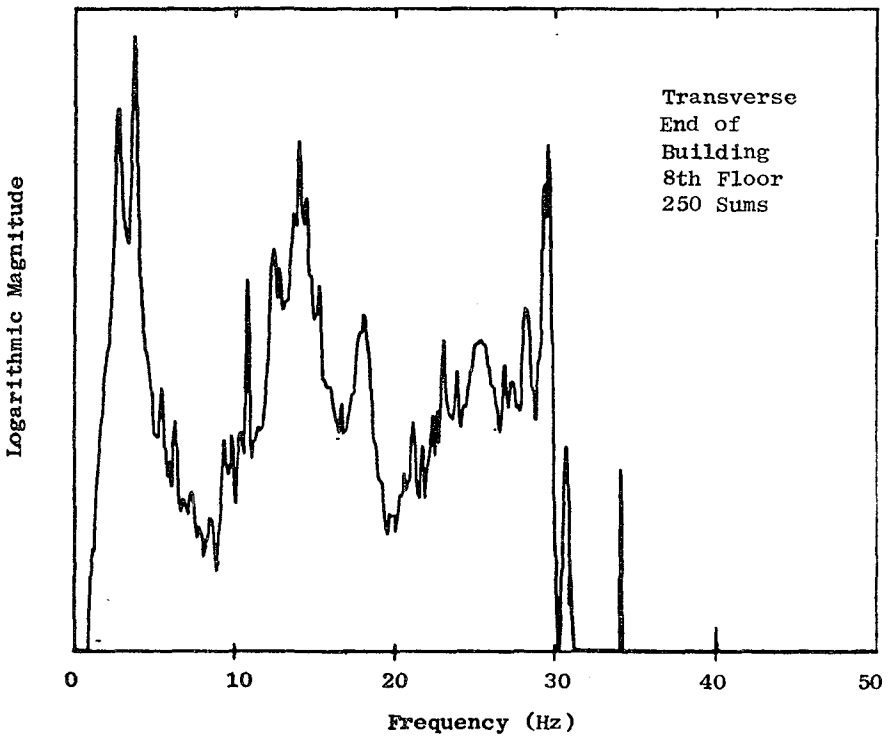

Fig. E.6. POWER SPECTRAL DENSITY PLOT, HULME BUILDING.

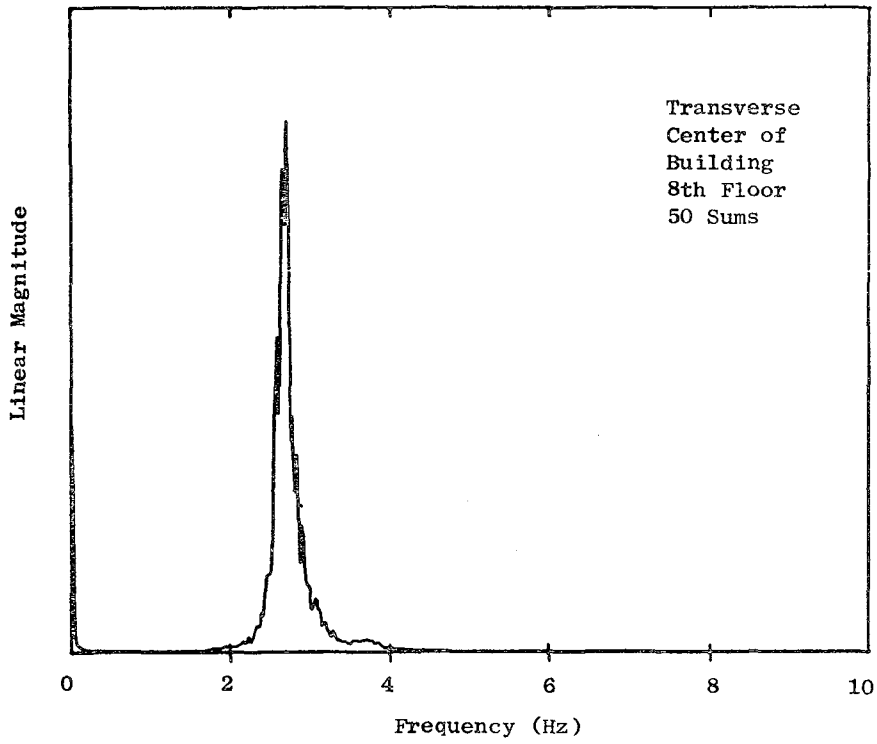

Fig. E.7. POWER SPECTRAL DENSITY PLOT, HULME BUILDING.

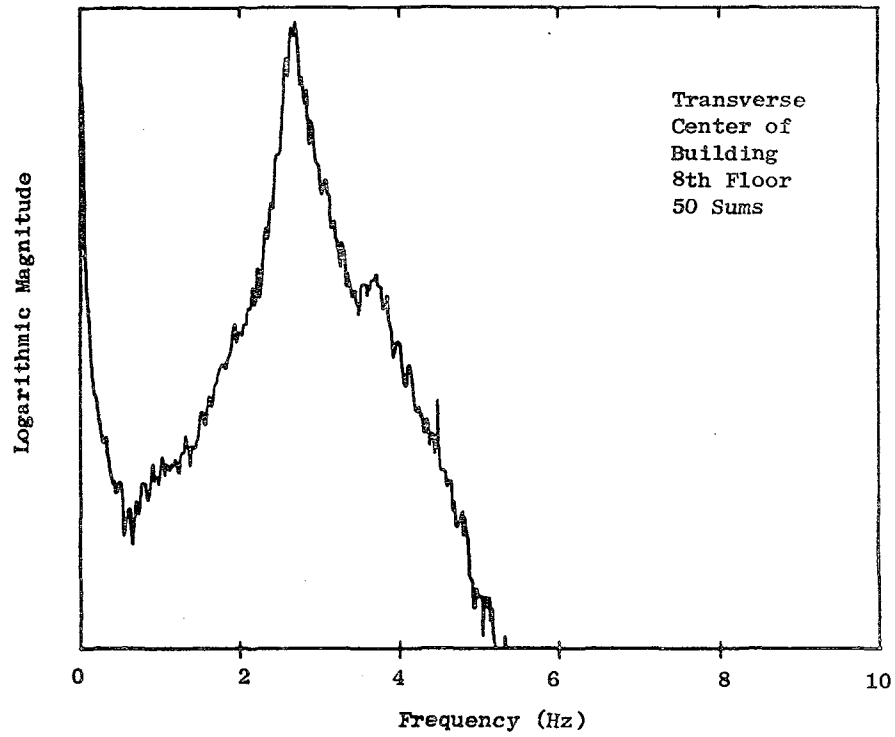

Fig. E.8. POWER SPECTRAL DENSITY PLOT, HULME BUILDING.

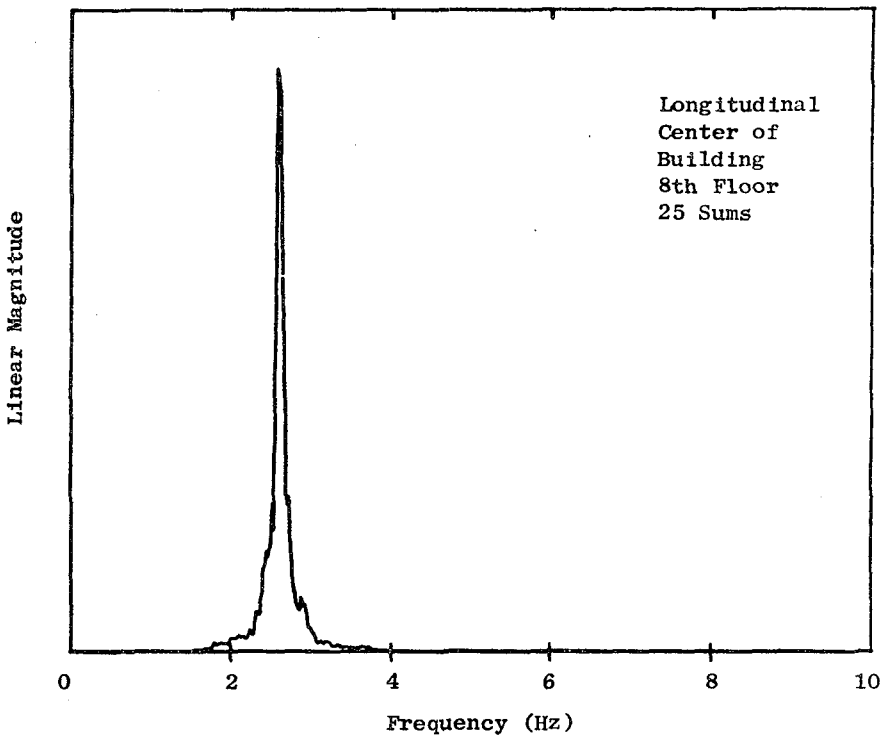

Fig. E.9. POWER SPECTRAL DENSITY PLOT, HULME BUILDING.

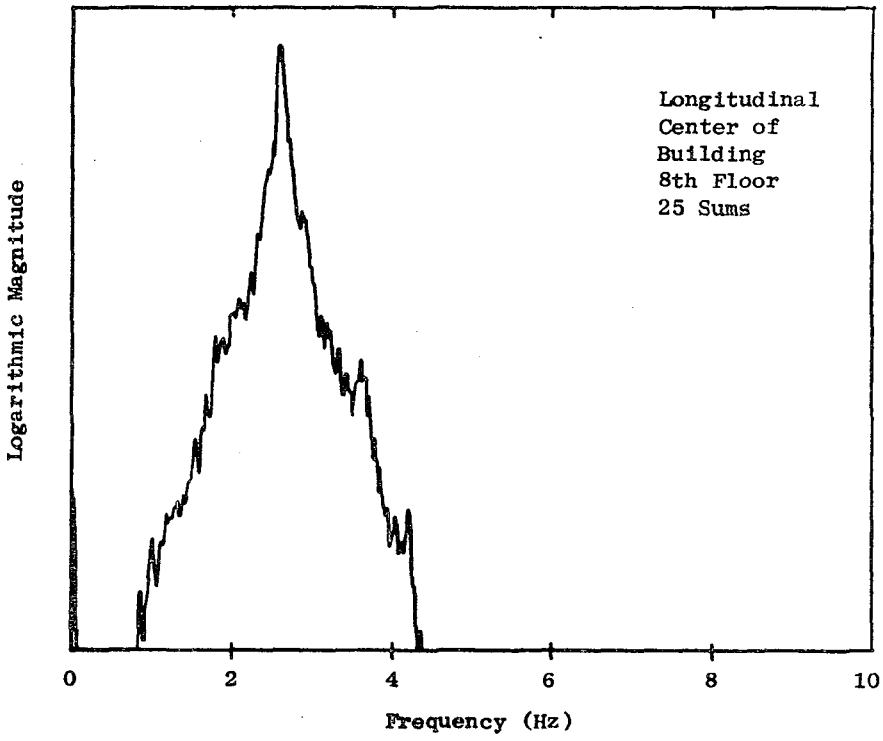

Fig. E.10. POWER SPECTRAL DENSITY PLOT, HULME BUILDING.

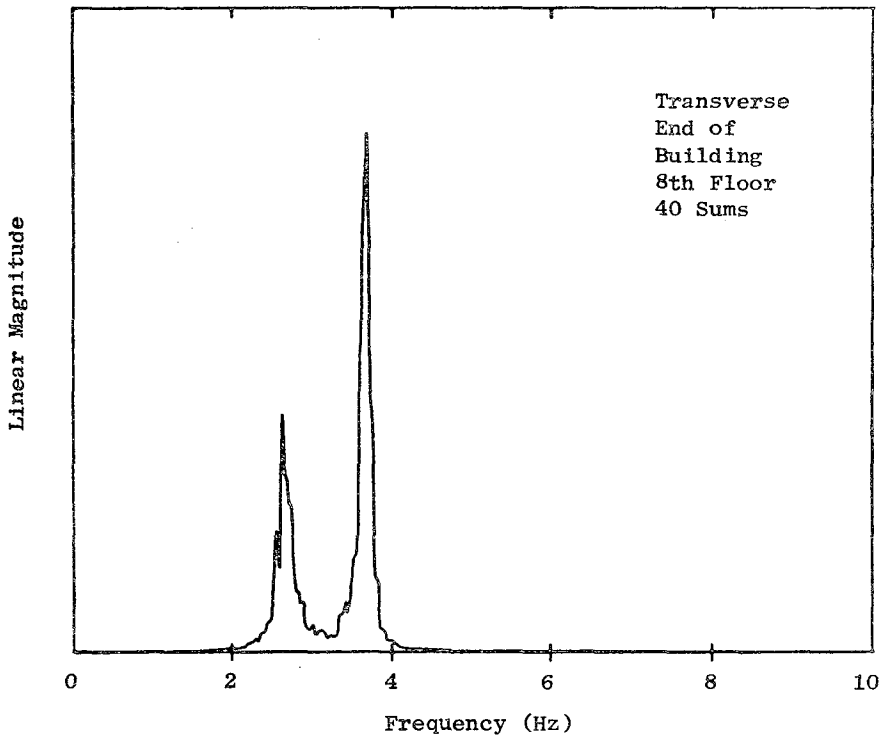

Fig. E.11. POWER SPECTRAL DENSITY PLOT, HULME BUILDING.

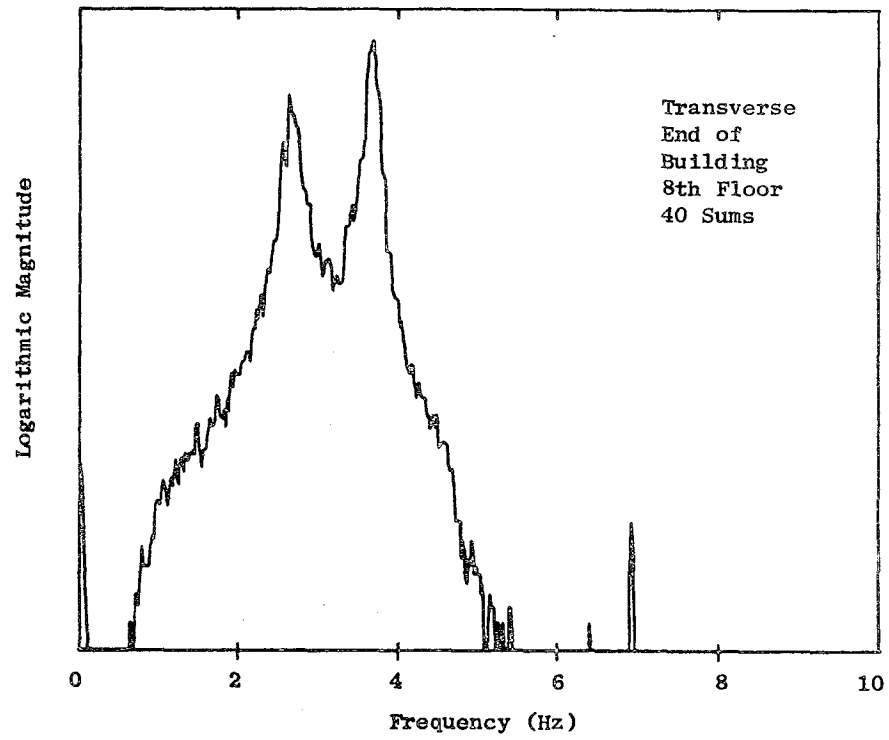

Fig. E.12. POWER SPECTRAL DENSITY PLOT, HULME BUILDING.

Intentionally Blank

76

Appendix F

POWER SPECTRAL DENSITY PLOTS FOR THE BARNES BUILDING AND A SUMMARY OF THE RESULTS

Table F.1

SUMMARY OF THE PREDOMINANT ENERGY TRANSFER POINTS FOR THE BARNES BUILDING

Figure	Accelerometer Orientation			Number of Spectrums Averaged	Natural Frequencies (Hz)		Other Points (Hz)	Percent of Critical Damping (1st mode)
	Direction	Position in Building	Floor Level		1st	2nd		
F.1 F.2	transverse	center	8th	300	2.6		15.7 18.1 29.6	---
F.3 F.4	longitudinal	center	8th	250	2.5		29.4	---
F.5 F.6	transverse	end	8th	150	2.5 3.6		18.1 29.4	---
F.7 F.8	transverse	center	8th	25	2.60	---	---	2.2
F.9 F.10	longitudinal	center	8th	50	2.58	---	---	2.1
F.11 F.12	transverse	end	8th	25	2.54 3.59	---	---	3.3 1.8

Preceding page blank

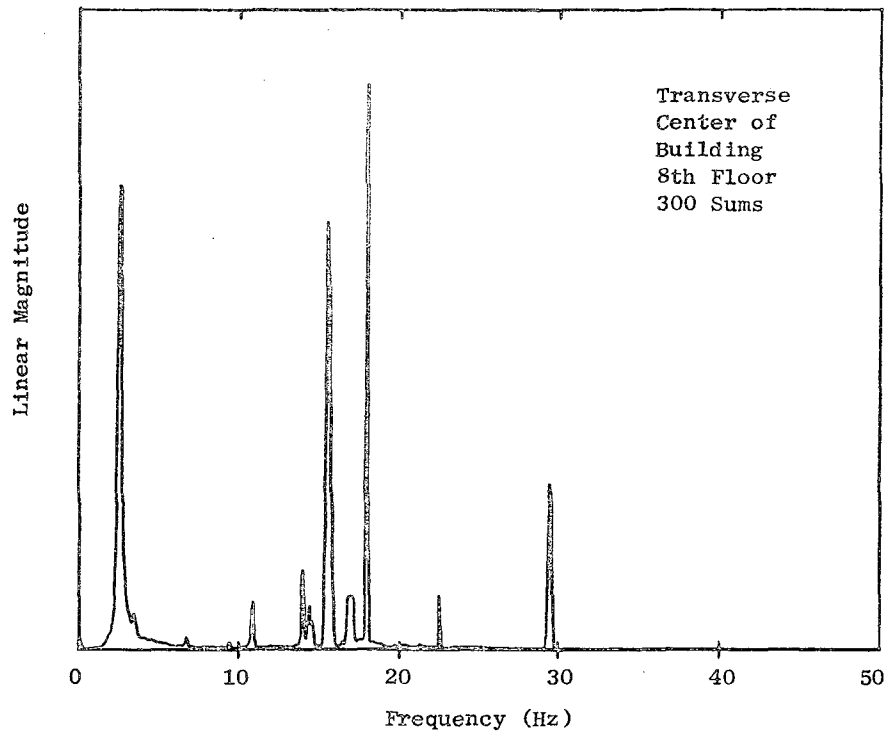

Fig. F.1. POWER SPECTRAL DENSITY PLOT, BARNES BUILDING.

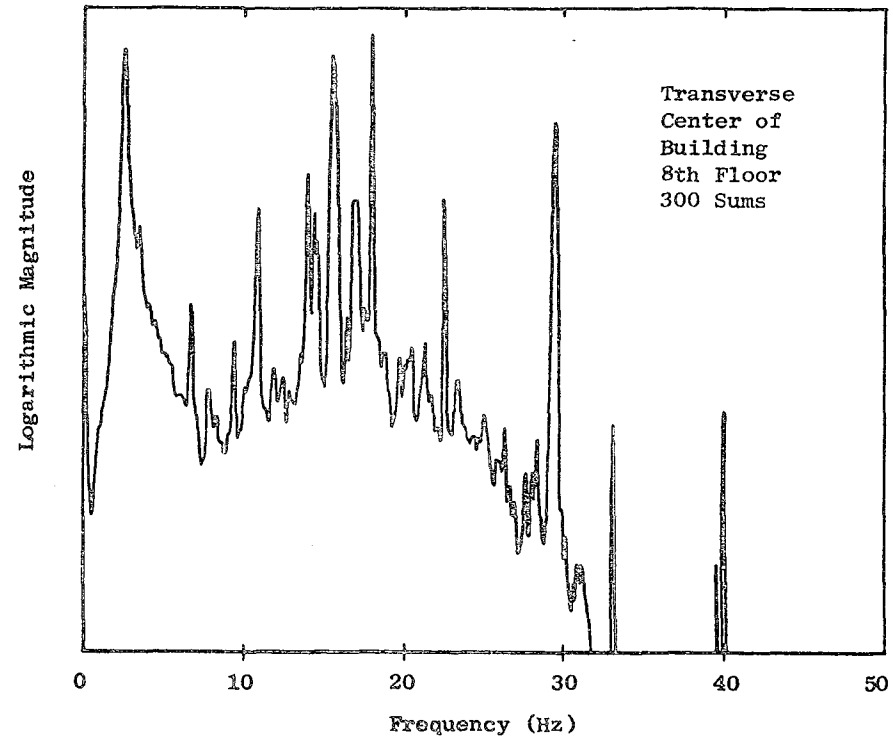

Fig. F.2. POWER SPECTRAL DENSITY PLOT, BARNES BUILDING.

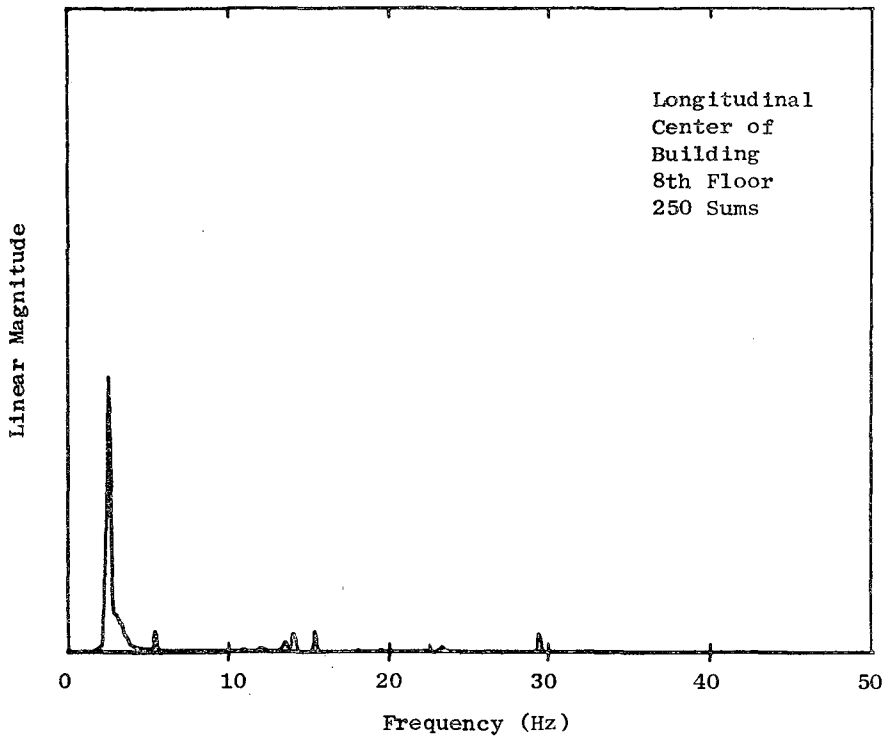

Fig. F.3. POWER SPECTRAL DENSITY PLOT, BARNES BUILDING.

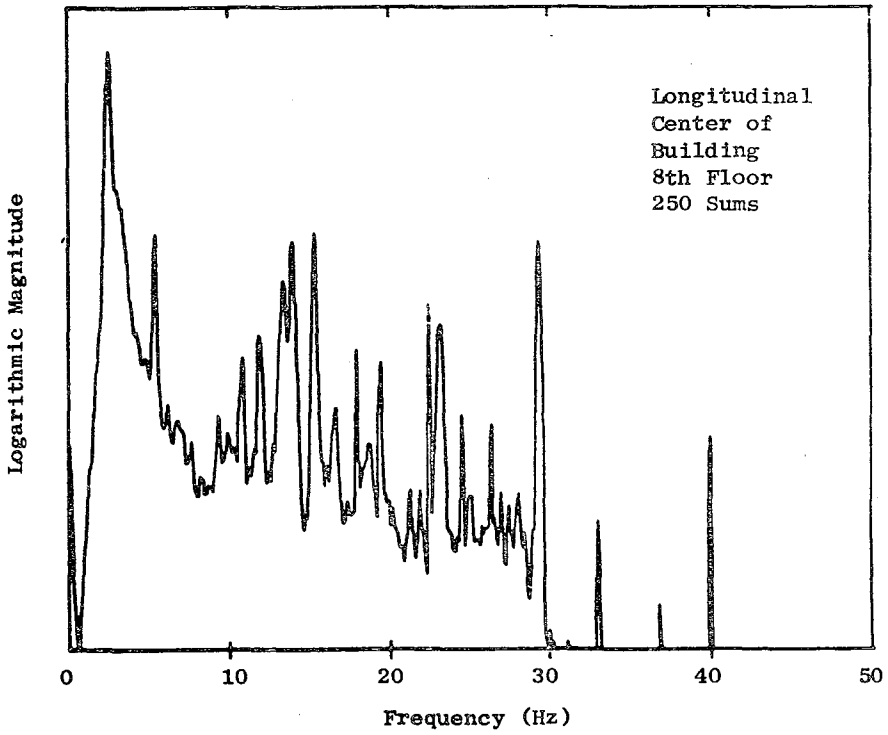

Fig. F.4. POWER SPECTRAL DENSITY PLOT, BARNES BUILDING.

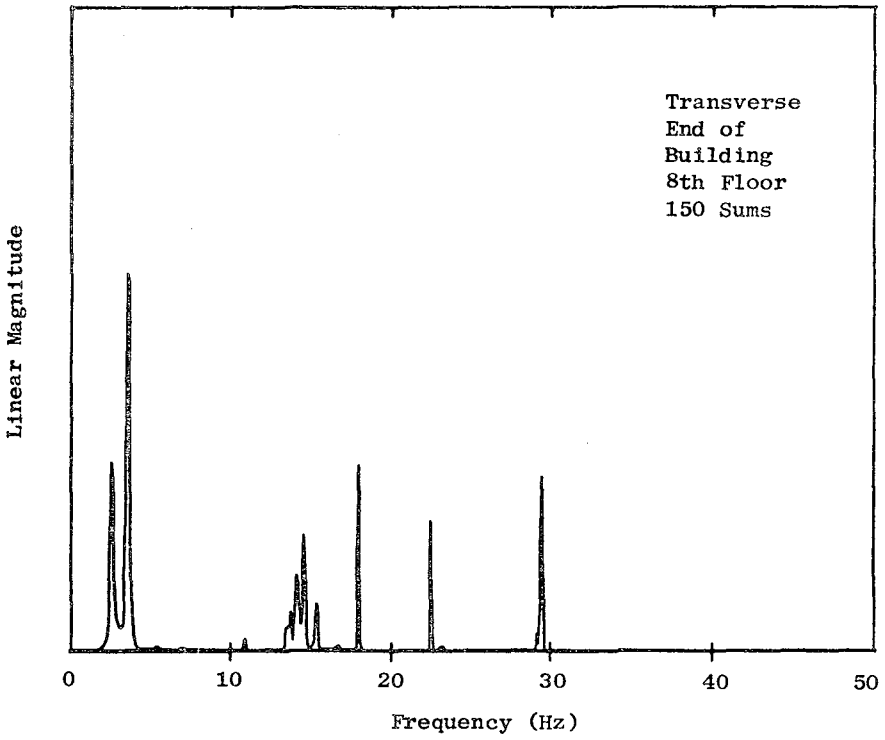

Fig. F.5. POWER SPECTRAL DENSITY PLOT, BARNES BUILDING.

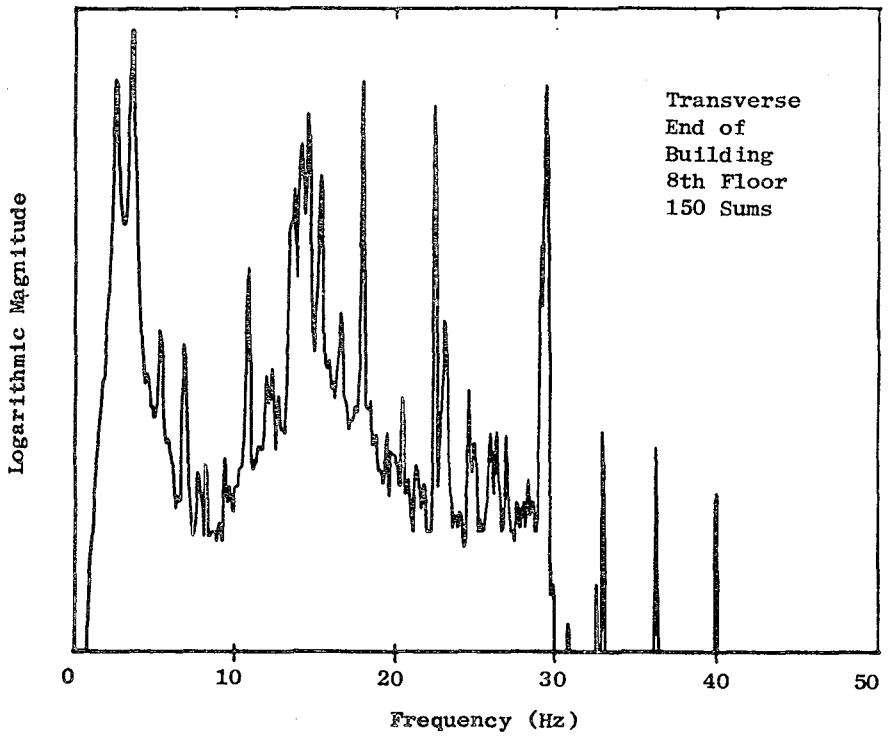

Fig. F.6. POWER SPECTRAL DENSITY PLOT, BARNES BUILDING.

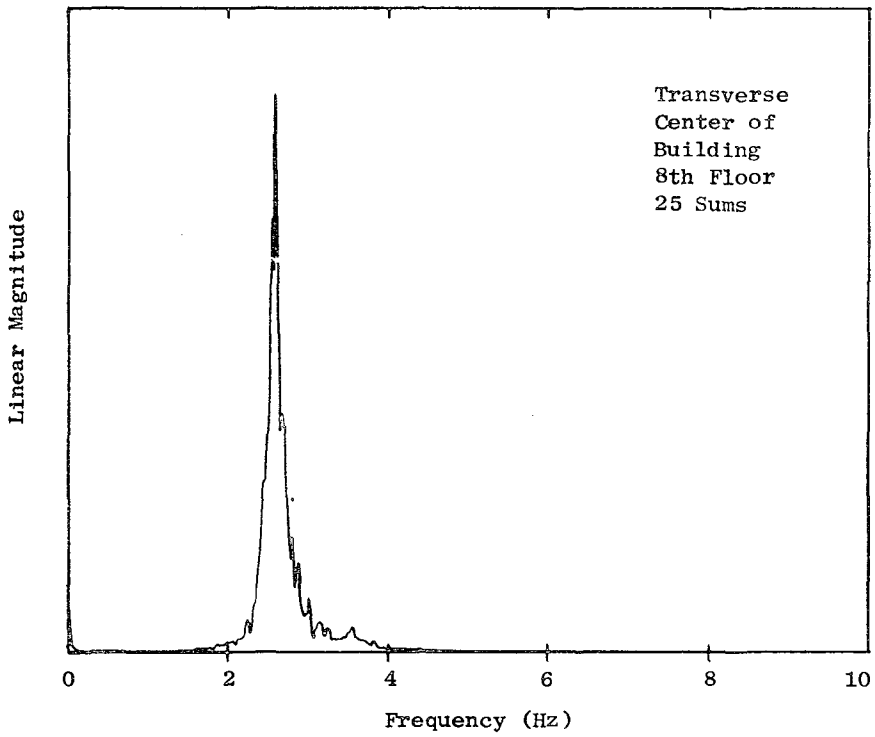

Fig. F.7. POWER SPECTRAL DENSITY PLOT, BARNES BUILDING.

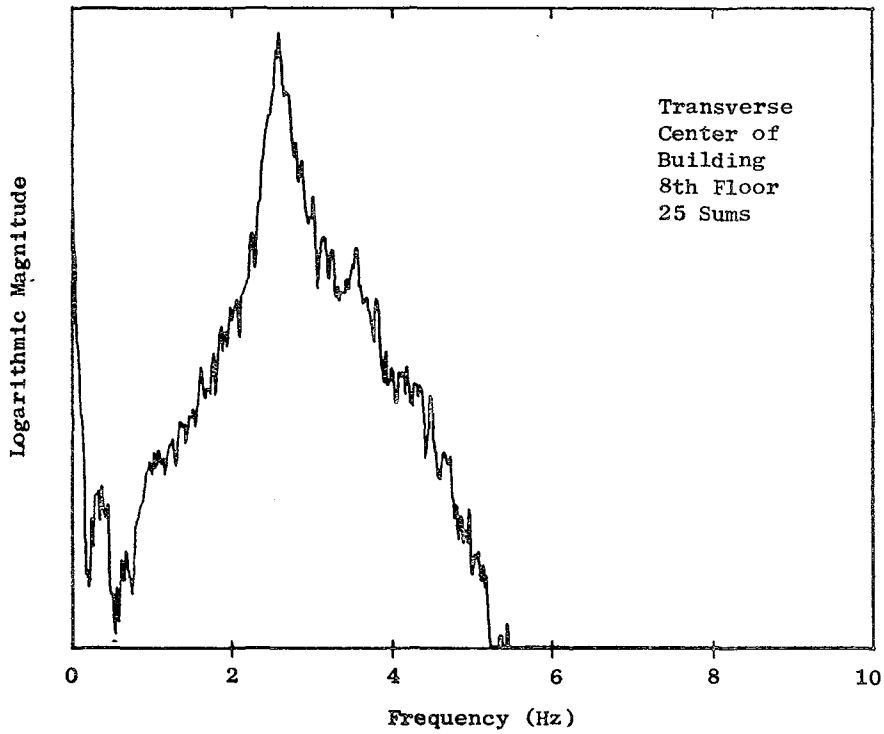

Fig. F.8. POWER SPECTRAL DENSITY PLOT, BARNES BUILDING.

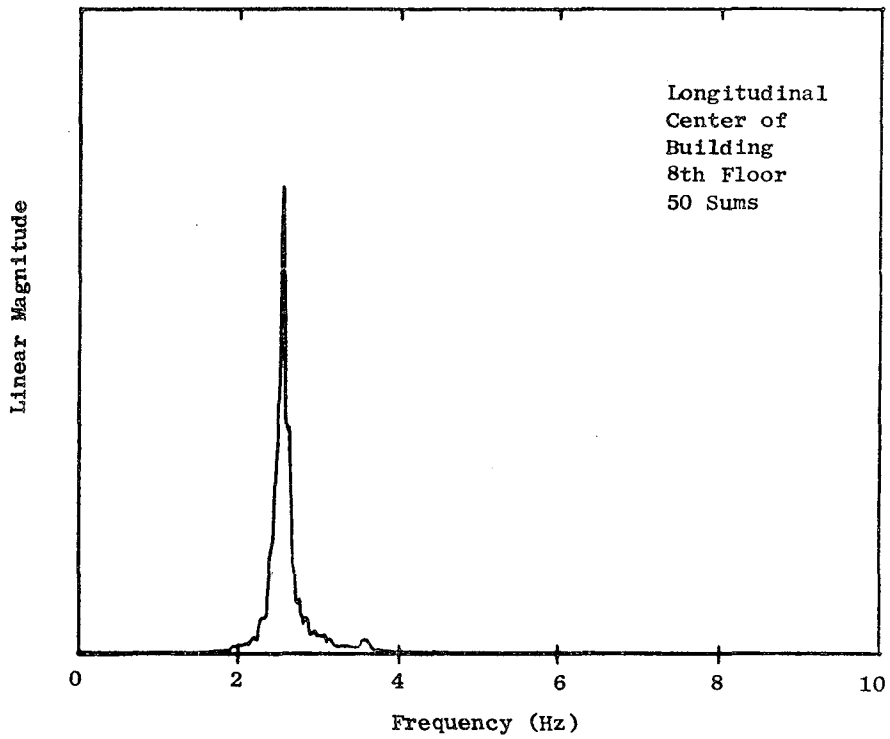

Fig. F.9. POWER SPECTRAL DENSITY PLOT, BARNES BUILDING.

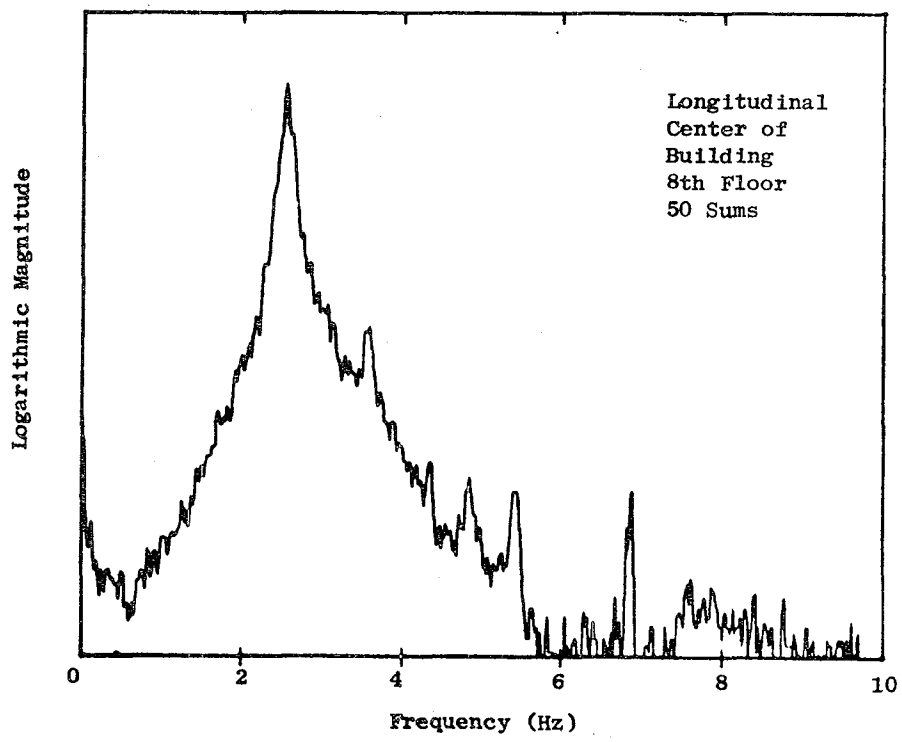

Fig. F.10. POWER SPECTRAL DENSITY PLOT, BARNES BUILDING.

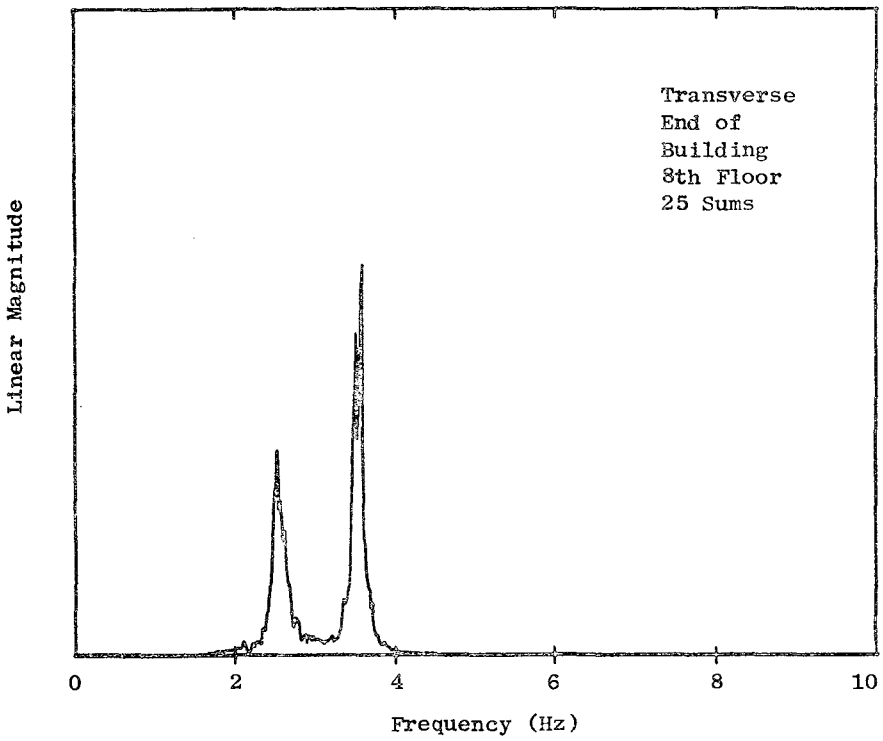

Fig. F.11. POWER SPECTRAL DENSITY PLOT, BARNES BUILDING.

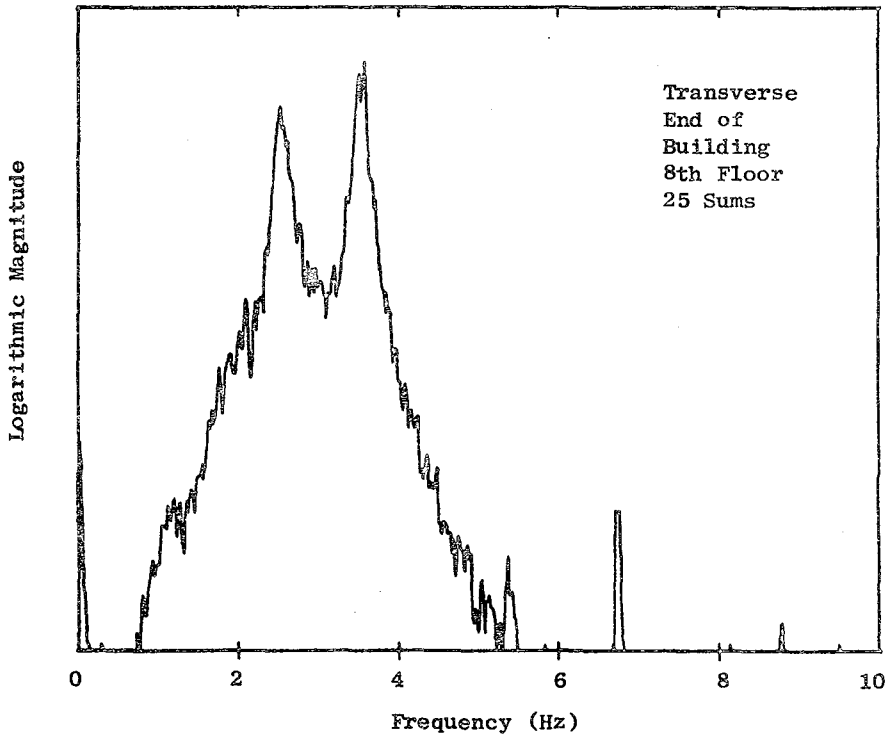

Fig. F.12. POWER SPECTRAL DENSITY PLOT, BARNES BUILDING.

Intentionally Blank

Appendix G

LIST OF EQUIPMENT USED ON SITE IN THE AMBIENT VIBRATION STUDY PERFORMED ON SIX HIGH-RISE APARTMENT HOUSES IN ESCONDIDO VILLAGE

1. Hewlett-Packard 5450A Fourier Analyzer Unit, including:

   a. HP 2115A Computer
   b. HP 5475A Control Unit
   c. HP 5465A Analog to Digital Converter
   d. HP H51-180A Oscilloscope
   e. HP 5460A Display Unit
   f. HP 2161A Power Supply
   g. HP 2748A Papertape Reader
   h. HP 7004B X-Y Recorder
   i. HP 2753A Papertape Punch

2. Hewlett-Packard 2752A Teleprinter

3. Kistler Model 305T Servo Accelerometer (2)

4. Kistler Model 515T Servo Amplifier (2)

5. Krohn-Hite 3323R Filter (2)

Preceding page blank

Appendix H

LIST OF EQUIPMENT, ADDITIONAL TO APPENDIX G, USED FOR AMBIENT AND NONAMBIENT VIBRATION STUDIES OF FULL-SCALE STRUCTURES

1. Hewlett-Packard Laser System, including:

   a. HP 5500A Laser Interferometer
   b. HP 5505A Laser Display
   c. HP 10550A Laser Reflector
   d. HP 6933B Digital to Analog Converter

2. Ling Electronics Portable Shaker System, including:

   a. Ling Model 370 Electromagnetic Shaker
   b. Ling Model PS-370D Dual Field Power Supply
   c. Ling Model TP 850 Power Amplifier

3. Hewlett-Packard 3722A Noise Generator

4. Hewlett-Packard 202B Low Frequency Oscillator

5. Hewlett-Packard 3960 Instrumentation Recorder

Preceding page blank

Appendix I

A COLLECTION OF SITES OF STRUCTURES WHICH HAVE BEEN USED IN AMBIENT AND NONAMBIENT VIBRATION STUDIES

List of Sites Tested	Date	Approximate Time
Embarcadero Trade Center Building San Francisco, California (45 stories)	May 1971	1 day
533 South Freemont Building Los Angeles, California (8 stories)	August 1971	1 day
5900 Wilshire Boulevard Building Los Angeles, California (32 stories)	August 1971	1 day
15250 Ventura Boulevard Building Sherman Oaks, California (13 stories)	August 1971	1 day
I.E.D. Systems Building Berkeley, California (12 stories)	October 1971	1 day
Guy West Suspension Bridge Sacramento, California	January 1972	1 day
Hoover Tower Stanford, California (275 feet)	May 1972	1 week
Devil's Canyon Power Plant California	July 1972	1 week
Pearblossom Pumping Plant California	July 1972	1 week
Oso Pumping Plant California	July 1972	1 week
Wheeler Ridge Pumping Plant California	August 1972	1 week
Edmonston Pumping Plant California	August 1972	1 week
Windgap Pumping Plant California	August 1972	1 week
975 California Avenue Building Palo Alto, California	September 1972	1 day

Preceding page blank

List of Sites Tested (continued)	Date	Approximate Time
Industrial Storage Racks, located at:		
3101 Kifer Rd., Santa Clara, Ca.	Spring 1973	1 day
579 Eccles Rd., S. San Francisco, Ca.	Spring 1973	1 day
Banco Central Building Managua, Nicaragua	May 1973	1 day
Banco de America Building Managua, Nicaragua	May 1973	1 day
Theatro National Building Managua, Nicaragua	May 1973	1 day
Enaluf Building Managua, Nicaragua	May 1973	1 day
Sherman Building San Jose, California	May 1974	2 days
I.E.D. Systems Building Mountain View, California	May 1974	2 days
Blackwelder Building Stanford, California (12 stories)	May 1974	2 days
Quillen Building Stanford, California (12 stories)	June 1974	2 days
McFarland Building Stanford, California (8 stories)	June 1974	1 day
Hoskins Building Stanford, California (8 stories)	June 1974	1 day
Hulme Building Stanford, California (8 stories)	June 1974	1 day
Barnes Building Stanford, California (8 stories)	June 1974	1 day
Abrahms Building Stanford, California (8 stories)	June 1974	1 day
Circuit Breakers (Air Blast Type BX2) located at A. D. Edmonston Pumping Plant, California	August 1974	1 week